Fall 2015

Near-field scanning study for radio frequency interference estimation

Jingnan Pan

Department: Electrical and Computer Engineering

NEAR-FIELD SCANNING STUDY FOR RADIO FREQUENCY INTERFERENCE ESTIMATION

by

JINGNAN PAN

A DISSERTATION

Presented to the Faculty of the Graduate School of the

MISSOURI UNIVERSITY OF SCIENCE AND TECHNOLOGY

In Partial Fulfillment of the Requirements for the Degree

DOCTOR OF PHILOSOPHY

in

ELECTRICAL ENGINEERING

2015

Approved
Jun Fan, Advisor
D. G. Beetner
J. Drewniak
D. J. Pommerenke
M. OKeefe

PUBLICATION DISSERTATION OPTION

This dissertation consists of the following three articles that have been submitted for publications as follows:

Pages 4-33 have been accepted in IEEE TRANSCTIONS ON ELECTROMAGNETIC COMPATIBILITY

Pages 34-65 have been submitted to in IEEE TRANSCTIONS ON ELECTROMAGNETIC COMPATIBILITY

Pages 66-91 will be submitted to IEEE TRANSCTIONS ON ELECTROMAGNETIC COMPATIBILITY

ABSTRACT

This dissertation discusses the novel techniques using near-fields scanning to do radio frequency interference (RFI) estimation. As the electronic products are becoming more and more complicated, the radio frequency (RF) receiver in the system is very likely interfered by multiple noise sources simultaneously. A method is proposed to identify the interference from different noise sources separately, even when they are radiating at the same time. This method is very helpful for engineers to identify the contribution of the coupling from different sources and further solve the electromagnetic interference issues efficiently. On the other hand, the equivalent dipole-moment models and a decomposition method based on reciprocity theory can also be used together to estimate the coupling from the noise source to the victim antennas. This proposed method provides convenience to estimate RFI issues in the early design stage and saves the time of RFI simulation and measurements. The finite element method and image theory can also predict the far fields of the radiation source, locating above a ground plane. This method applies the finite element method (FEM) to get the equivalent current sources from the tangential magnetic near fields. With the equivalent current sources, the far-field radiation can be calculated based on Huygens's Principle and image theory. By using only the magnetic near fields on the simplified Huygens's surface, the proposed method significantly saves measurement time and cost while also retaining good far-field prediction.

ACKNOWLEDGMENTS

I would like to express my sincere gratitude to my advisor, Dr. Jun Fan, for his teaching and advice during my Ph. D. program. I have learned both theoretical knowledge and engineering skills from him, from which I will benefit a lot in future life.

I would like to specially thank Dr. Daryl Beetner, Dr. David Pommerenke and Dr. James Drewniak for their valuable advice and teaching during my study. I would also like to thank Dr. Matt OKeefe for his advice and support on my dissertation.

I would also like to thank all other faculty members in the EMC Lab for their good teaching and help to me. I would like to express my appreciation to all the students in the EMC Lab for their teamwork. I am proud that I was a member of such an exceptional Lab in the EMC area.

Finally, I am deeply grateful to my parents, my husband, my families and friends for their constant support and encouragement.

This thesis is based upon work supported partially by the National Science Foundation under Grant No. IIP-1440110.

TABLE OF CONTENTS

LIST OF ILLUSTRATIONS

PAPER1 Page

PAPER2

PAPER3

1. INTRODUCTION

The first topic of this dissertation is far-field prediction using only magnetic near fields on a five-sided Huygens's surface. This Huygens's surface covers the ground plane and encloses the radiation source with the ground. Tangential magnetic fields on this Huygens's surface are used to calculate the electric fields based on the finite element method (FEM). For a typical PCB with a large ground plane, the five-sided Huygens's surface can be further simplified as one top near-field plane, very close to the DUT and the ground, with four side lines, shrunk from the four side walls of the five-sided surface. Because the side lines are also close to the ground, the vertical component of the magnetic fields can be approximately taken as zero. Thus, only the horizontal magnetic fields on the top plane and the side lines are needed in the proposed method. This allows all the measurements to be performed by only one probe so that both the consistency and the convenience of the measurements are greatly improved. By using only the magnetic fields, shrinking the four side walls into four lines, the proposed method saves a significant number of scanning points.

The second topic of this dissertation is using the equivalent dipole-moment models and the decomposition method based on reciprocity together to estimate the coupling from the noise source to the victim antennas. This method can improve the coupling estimation efficiency and is feasible for real products. The equivalent dipole-moment models were extracted to model the noise source from the tangential magnetic fields on one near-field plane, by the least square method. Employing only magnetic near fields, this method can save almost half of the measurement time compared to the traditional method, using both electric and magnetic near fields. Since there are close

equations to calculate the dipole radiation, the tangential electromagnetic fields on the Huygens's box can be obtained quickly in MATLAB rather than doing a full-wave simulation. Thus, the first step of the decomposition method was fulfilled. Then, similarly with, the victim antenna was modeled and excited in simulation software to export the tangential fields on the same Huygens's box. Finally, the coupling from the noise source to the victim antenna was estimated by reciprocity theory.

The proposed method prevents using complex models and time-consuming simulations for the source. Using only magnetic near fields for dipole extraction, the scanning consistency can be kept and the scanning time is also saved significantly. With the equivalent dipole-moment models and the tangential fields from the antenna on the Huygens's box, the source and antenna can be placed in arbitrary locations. The proposed method can estimate the interference quickly and accurately for each location combination in the early design phase. The measurement validation for this kind of problem is demonstrated for the first time.

In the third part, the Huygens's surfaces are proposed to move to the locations of the sources. By doing this, the fundamental theory still works and the coupling from different sources to the same antenna can be obtained. It not only makes it possible to discriminate the coupling contribution from each source at the same frequency, but also overcomes the difficulty when the setup of the antenna is not suitable to place the Huygens's surface. And also, in this method, the corresponding electric fields will be converted from scanned magnetic fields by finite element method (FEM) on the Huygens's surface. The processing approach in the first part of this dissertation is suitable to convert the magnetic fields to electric fields in the "Forward Problem". A novel and

creative FEM processing procedure is proposed for the first time to solve the electric fields from the magnetic fields in the “Reverse Problem”. Thus, the decomposition method can be fulfilled by only the magnetic fields from measurements. This approach prevents using electric probe, which usually performed worse in accuracy compared to magnetic probe, and also saves half of the scanning time and the cost of related resources.

PAPER

I. FAR-FIELD PREDICTION BY ONLY MAGNETIC NEAR FIELDS ON A SIMPLIFIED HUYGENS'S SURFACE

Jingnan Pan, Xu Gao, Jun Fan, *Senior Member, IEEE*
Electrical Engineering
Missouri University of Science and Technology, Missouri, U. S. A. 65409
Email: jpfz6@mst.edu, jfan@mst.edu

Abstract

For radiation source locating above a ground plane, its far-field can be predicted by only the magnetic near-field through the method proposed in this paper. This method applies the finite element method (FEM) to get the equivalent current sources from the tangential magnetic near fields. With the equivalent current sources, the far-field radiation can be calculated based on Huygens's Principle and image theory. The magnetic near-field is scanned on a Huygens's surface that encloses the source with its ground. In this paper, this Huygens's surface was first proposed as a five-surface cube on the ground. Then, the Huygens's surface was further simplified by using four lines instead of four side walls to make the proposed method easier in regards to practical near-field scanning. Several numerical examples were tested to validate the proposed method. In addition, the proposed method was validated experimentally by using a patch antenna. The performance of using only the top plane near fields was also investigated and discussed. By using only the magnetic near fields on the simplified Huygens's surface, the proposed method significantly saves measurement time and cost while also retaining good far-field prediction.

Index Terms

Near-field to far-field transformation, Finite element method, Huygens's principle, Image theory, Near-field scanning.

I. INTRODUCTION

Electromagnetic Interference (EMI) is one of the important issues to consider when evaluating modern electronic products. Because of the lack of expertise in noise reduction and immunity improvement, the EMI issue has become one of the primary reasons for the integrated circuit (IC) redesign [1]. Several international standards have been established to quantify EMI performance. IEC 61967 and IEC 62132 have given multiple measurement approaches for emission and susceptibility characterization [2]. Far-field radiation, one of these significant standards, has attracted a large amount of research interest. Traditionally, the device under test (DUT) is placed in a semi-anechoic chamber for the far-field radiation measurements. However, the cost of the chamber build-up is high. Papers [3]-[5] proposed the far-field estimation method by transverse electromagnetic (TEM) cell measurements. The dipole-moments model or voltages are determined from the measured data to predict the far-field radiation of the DUT. These methods work well at low frequency, but are limited by the working frequency band of the TEM cell. In addition, the size of the DUT has to meet certain requirements. Some other interests focus on the near-field to far-field (NF-FF) transformation technique, which was first introduced in the antenna field in the 1950s. The author of [6] carefully expatiated the evolution of this technique. NF-FF transformations have also recently been performed for the radiation estimation of electronic products. In [7]-[9], equivalent electric and/or magnetic current sources are extracted at a source reconstruction plane to represent the real source. The far-field radiation is calculated from these equivalent sources. A popular alternative approach is to establish the dipole-moment models at the real source location. Many relevant studies are reported in [10]-[19]. Articles [10]-[14]

provide various dipole-moment model determination algorithms and their corresponding validations. Furthermore, in [12] and [15]-[17], the methods to import the dipole-moment models in commercial full-wave simulation tools are developed. In this instance, the dipole models replace the real sources and are simulated with other structures to evaluate the entire system. This will benefit the overall design of the products in the early stage. Various optimizing algorithms for the dipole moments determination are discussed in [18]-[20]. They take the perspective of improving the solutions of the inverse problem to enhance the accuracy of the dipole-moment models.

The above-mentioned NF-FF transformation methods employ the scanned electric near fields, either by themselves or together with the magnetic near fields. However, designing tangential electric field probes is more difficult than designing magnetic probes. To extend the application of the NF-FF transformation, the far-field prediction algorithm using only measured magnetic near fields is preferred. Additionally, it will save half of the measurement time.

The authors of [21] have proposed a method to extract the electric fields from the tangential magnetic fields on a Huygens's surface. For the EMC application of the maximum far-field prediction, this method has shown good robustness against input data errors. However, the Huygens's surface in [21] is a six-sided closed surface. It is no longer available when the DUT is located close to a ground plane, which is the common situation for PCBs. In addition, the measurement of this Huygens's surface is limited by the 3-D near field scanning technique.

This paper proposes a method for far-field prediction using only magnetic near fields on a five-sided Huygens's surface. This Huygens's surface covers the ground plane

and encloses the radiation source with the ground. Tangential magnetic fields on this Huygens's surface are used to calculate the electric fields based on the finite element method (FEM). For a typical PCB with a large ground plane, the five-sided Huygens's surface can be further simplified as one top near-field plane, very close to the DUT and the ground, with four side lines, shrunk from the four side walls of the five-sided surface. Because the side lines are also close to the ground, the vertical component of the magnetic fields can be approximately taken as zero. Thus, only the horizontal magnetic fields on the top plane and the side lines are needed in the proposed method. This allows all the measurements to be performed by only one probe so that both the consistency and the convenience of the measurements are greatly improved. By using only the magnetic fields, shrinking the four side walls into four lines, the proposed method saves a significant number of scanning points.

This paper is composed of seven sections. Section II and Section III describe the algorithm of the far-field prediction by 5-sided Huygens's surface and its numerical validation. Section IV explains the procedure of the Huygens's surface simplification for PCBs and the improved method. Several numerical examples are given to verify the improved method in Section V. In Section VI, a PCB with an antenna is scanned, and the improved method is validated with measurements. Finally, discussions and conclusions are given in Section VII.

II. THEORY AND ALGORITHM

A. Huygens's Principle

Huygens's principle is also widely known as the surface equivalent theorem. It places suitable current densities over an imaginary closed surface to represent the actual radiating source. The current densities produce the same fields as the actual source outside the closed surface [22], as shown in Fig. 1.

The actual sources are $J1$ and $M1$, which are enclosed by the closed surface S, as illustrated in Fig. 1(a). In Fig. 1(b), the tangential electric and magnetic fields on S are taken to calculate the equivalent current densities J_s and M_s by (1) and (2). Thus, the original problem in Fig. 1(a) is represented by the problem in Fig. 1(b). The fields outside the surface S are the same in the two problems, and they can be obtained by (3-6).

$$\bar{J}_s = \hat{n} \times \bar{H}_2 \tag{1}$$

$$\bar{M}_s = -\hat{n} \times \bar{E}_2 \tag{2}$$

$$\bar{A} = \frac{\mu}{4\pi} \iint_S \bar{J}_s \frac{e^{-j\beta R}}{R} ds \tag{3}$$

$$\bar{F} = \frac{\varepsilon}{4\pi} \iint_S \bar{M}_s \frac{e^{-j\beta R}}{R} ds \tag{4}$$

$$\bar{E} = -j\omega\bar{A} - j\frac{1}{\omega\mu\varepsilon}\nabla\left(\nabla \cdot \bar{A}\right) - \frac{1}{\varepsilon}\nabla \times \bar{F} \tag{5}$$

$$\bar{H} = -j\omega\bar{F} - j\frac{1}{\omega\mu\varepsilon}\nabla\left(\nabla \cdot \bar{F}\right) + \frac{1}{\mu}\nabla \times \bar{A} \tag{6}$$

where $R = \left|\bar{r} - \bar{r}'\right|$, $\bar{r}$ is the observation point, and $\bar{r}'$ is the source point.

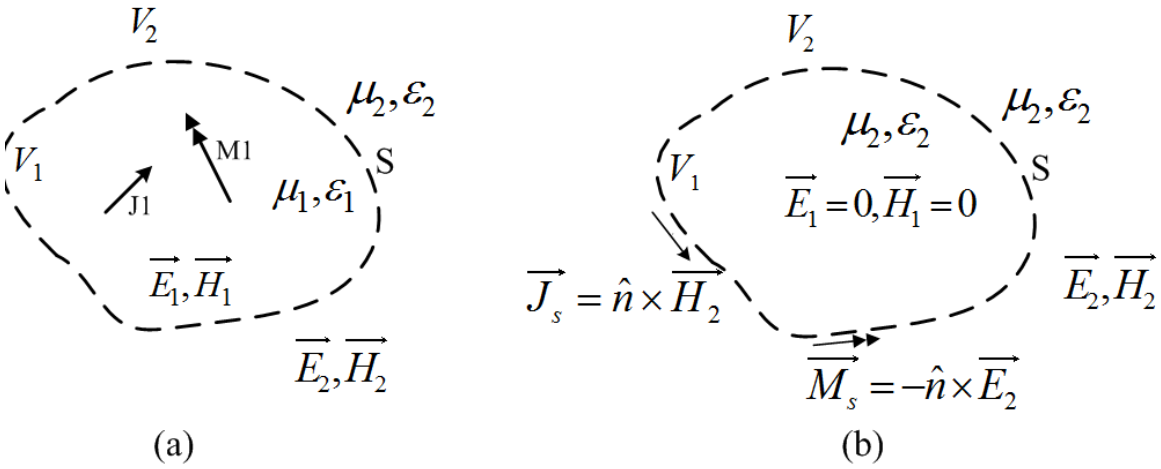

Fig. 1. Huygens's principle. (a) Original problem. (b) Equivalent problem.

B. Image Theory

Image theory introduces virtual sources (images) that account for the reflections to analyze the performance of a radiating element near an infinite plane conductor. The imaginary sources, in combination with the real ones, form an equivalent system that replaces the actual system for analysis purposes only and gives the same radiated field above the conductor [22]. Fig. 2 sketches the current densities and their images over a perfect electric conductor (PEC) and a perfect magnetic conductor (PMC).

In Fig. 2, when the sources are very close to the conductors, tangential electric and vertical magnetic sources will not radiate near the PEC, while vertical electric and tangential magnetic sources will not radiate near the PMC.

C. Far-field Prediction Algorithm

Fig. 3 demonstrates the steps of the proposed algorithm for far-field prediction by only the magnetic near-field. In Fig. 3(a), the original radiation problem is described. Assuming the radiation source is located above an infinitely large PEC plane, a Huygens's surface can be selected as shown in Fig. 3(b) and Fig. 3 (c).

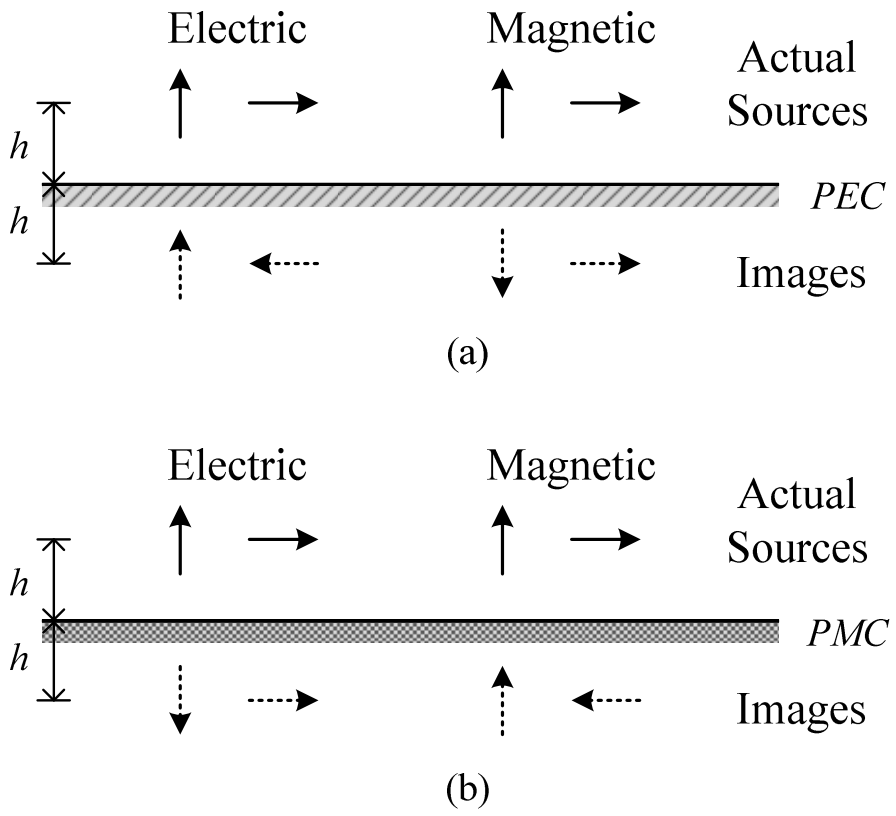

Fig. 2. Electric and magnetic sources and their images near (a) electric and (b) magnetic conductors.

This Huygens's surface consists of five sides of a box and the infinite ground (PEC) plane outside of the box. The Huygens's surface is selected in this way so that the entire radiating structure (the whole PCB) is underneath the Huygens's surface. According to Huygens's principle, the field above the Huygens's surface can be calculated by using the equivalent electric current and equivalent magnetic current on the Huygens's surface, as shown in Fig. 3(c). As a result of the ground (PEC) plane, the equivalent magnetic current on the bottom surface of the Huygens's surface is zero. The equivalent problem in Fig. 3(c) can be further simplified by filling the PEC and PMC boundary condition inside the Huygens's surface in the manner shown in Fig. 3(d).

Because the electric current placed on the PEC and the magnetic current placed on the PMC do not radiate [22], the equivalent electric currents on the five sides of the box are needed to calculate the fields above the Huygens's surface. These electric currents are induced currents converted from the magnetic fields on the Huygens's surface. They are used to compensate the discontinuity of the magnetic fields on the Huygens's surface so that the electromagnetic fields outside it in this equivalent problem are the same with the original problem. Thus, only the tangential magnetic field on the five-sided Huygens's surface needs to be known to predict the far-field in the equivalence in Fig. 3(d). By using the equivalence in Fig. 3(d), however, the effect of the PEC and PMC boundaries need to be considered. Therefore, the free space Green function is not working in this case, which means equations (3)-(6) cannot be used. To solve this problem, the finite element method (FEM) is applied. The FEM setup is shown in Fig. 4(a). The calculation region is truncated by a large box on which the absorbing boundary condition (ABC) [21] is applied. With equivalent electric currents and the boundary setup, the radiation fields can be solved by FEM. The volume between S_2 and the five-sided Huygens's surface is the FEM operation region and should be meshed based on the wavelength of interest [21]. Then, the tangential electric fields on S_2 can be numerically obtained by the wave equation in (7) using FEM. The tangential magnetic fields on S_2 are given by equation (8).

$$\nabla\times\left(\frac{1}{\mu_r}\nabla\times\bar{E}\right)-k_0^2\varepsilon_r\bar{E}=-jk_0Z_0\bar{J} \tag{7}$$

$$\bar{H}=\frac{j}{\omega\mu}\nabla\times\bar{E} \tag{8}$$

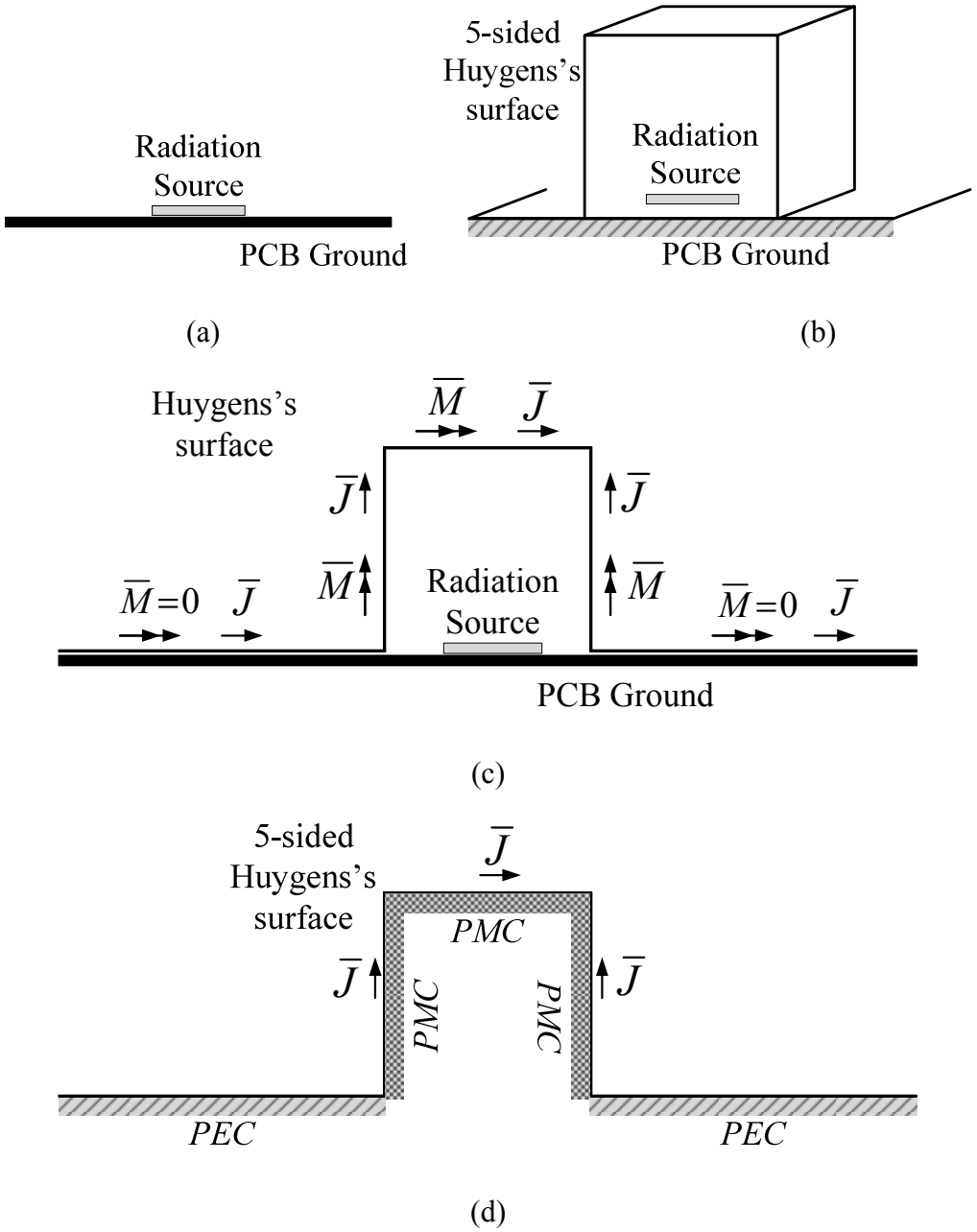

Fig. 3. The proposed far-field prediction algorithm. (a) Original problem. (b) Setup of the 5-sided Huygens's surface. (c) Huygens's surface, 2D view. (d) Equivalent problem of the original problem.

After solving the equivalent problem in Fig. 4(a), both the E and H fields on the boundary S_2 can be obtained. To predict the far-field, it is straightforward to use the outer box as a new Huygens's surface, as shown in Fig. 4(b). Because both the magnetic

current and electric current on S_2 are known, image theory can be applied based on Section II Part B. By using image theory, the PEC boundary is removed, and the free space radiation equations (3)-(6) are used for the equivalent currents and their images to calculate the far fields [24]. This approach prevents the mesh and calculation in the entire region from the source to the far-field domain so that the overall computation time is significantly condensed.

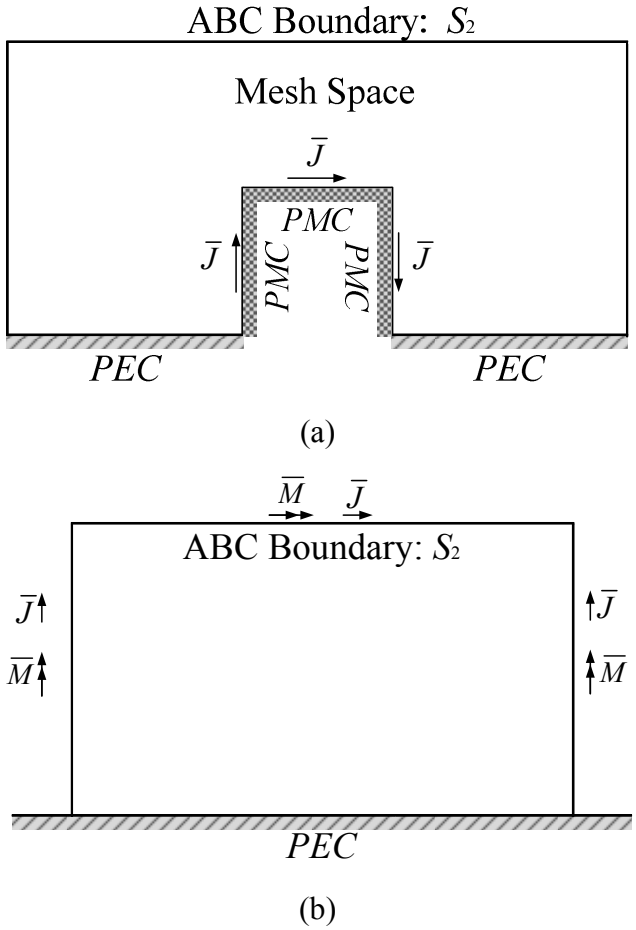

Fig. 4. The proposed far-field prediction algorithm. (a) FEM implementation to determine the electromagnetic fields on S2. (b) Far-field calculation based on image theory and Huygens's principle.

III. FAR-FIELD PREDICTION ALGORITHM VALIDATION

This section gives numerical examples to verify the far-field prediction algorithm proposed in Section II Part C.

A. An Infinitesimal Electric Dipole

The first example is an infinitesimal electric dipole, which is located above an infinitely large PEC. Fig. 5 shows the setup of the Huygens's surface S_1 and outer box S_2.

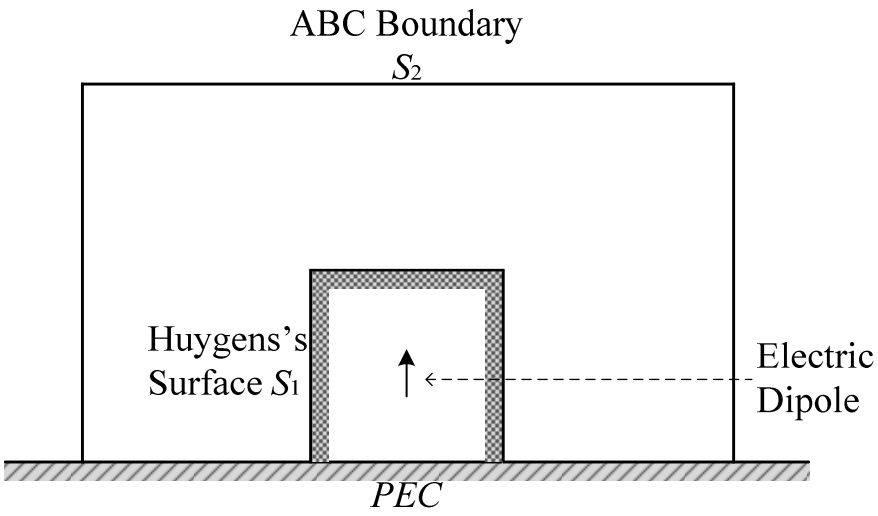

Fig. 5. Example of an infinitesimal electric dipole. The dipole is in the center of the five-sided Huygens's surface, which is a 60 mm × 60 mm × 60mm cube. The outer box is set with a length of 210 mm, a width of 210 mm and a height of 135 mm.

An HFSS model is established following Fig. 5. The five-sided Huygens's surface is a 60 mm × 60 mm × 60 mm cube. The dipole, with the magnitude of 1e-6 A·m, is located in the center of the cube. The outer box has a length of 210 mm, a width of 210 mm and a height of 135 mm. The tangential magnetic fields are exported and applied in the proposed far-field prediction algorithm. Fig. 6 compares the FEM-solved tangential electromagnetic fields to the simulated fields on the top plane of the outer box. The

algorithm has similar performance for the other four surfaces. The calculated results agree with the simulation results.

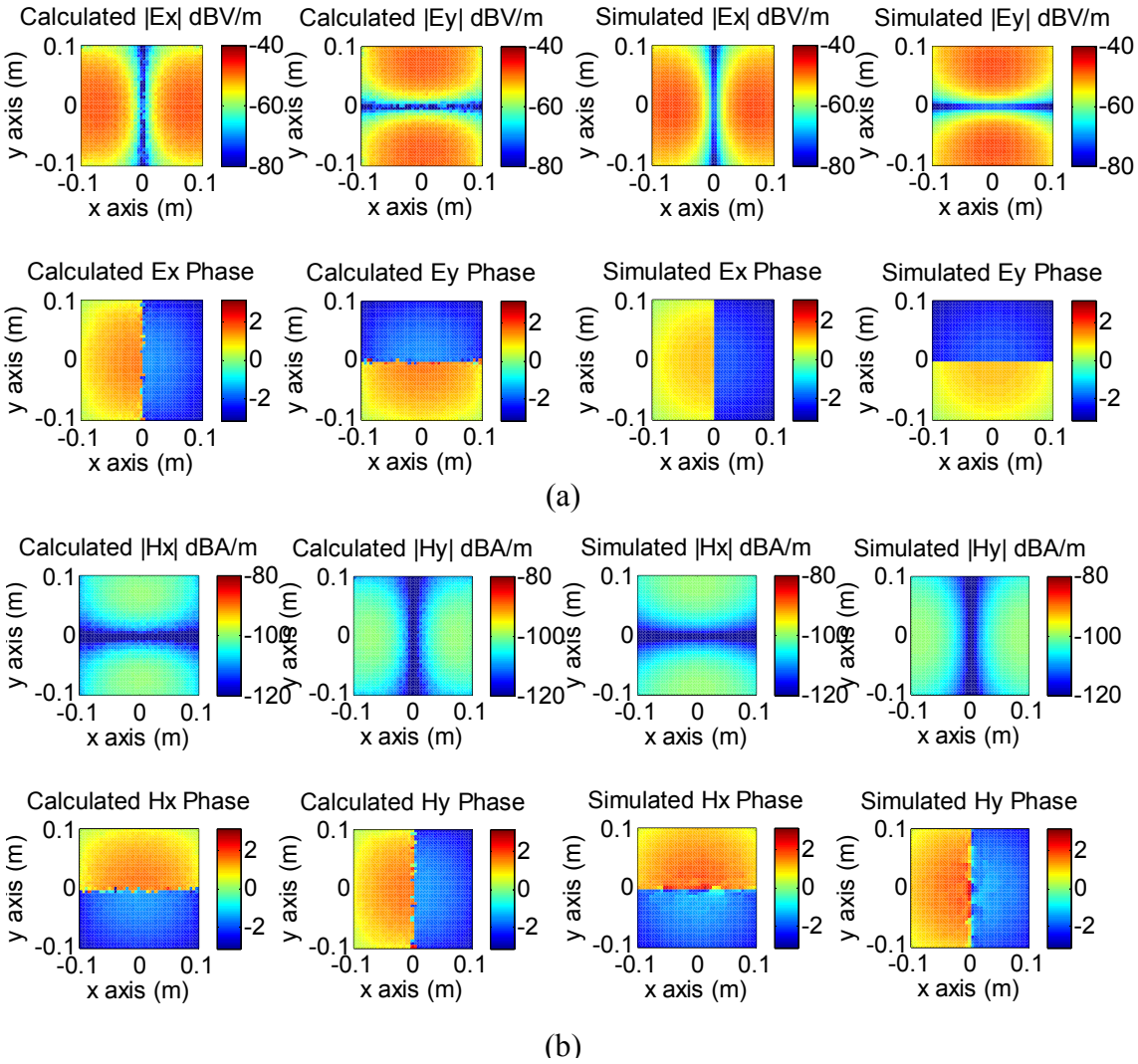

Fig. 6. Comparison between the FEM-solved tangential electromagnetic fields and the simulated fields on the top plane of the outer box. (a) Comparison of the electric fields. (b) Comparison of the magnetic fields.

Fig. 7 presents the far-field prediction by the algorithm in Section II Part C. The estimated vertical electric far fields are compared to the far-field simulation at three circular curves whose locations in spherical coordinates are $r = 3$ m, and $\theta = 20°$, 50°, 70°. The predicted E_z patterns at these three circles match the simulation results.

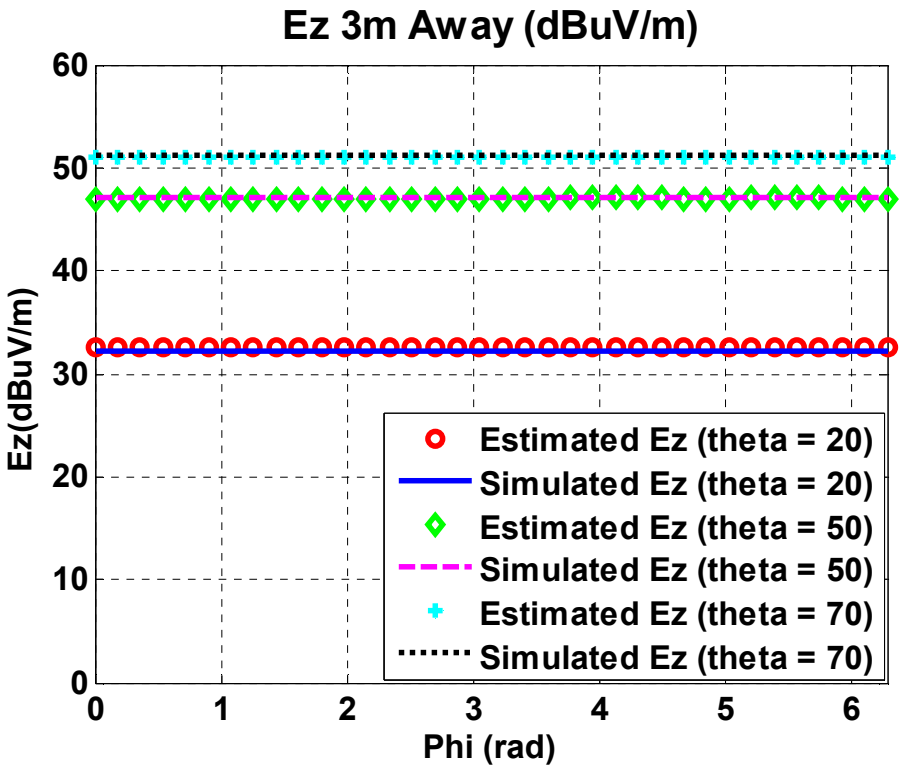

Fig. 7. Far-field prediction of one vertical electric dipole compared to direct simulation.

B. Three Arbitrary Dipoles

The other example is three arbitrarily placed dipoles. With the center of the bottom plane of the Huygens's surface as the coordinate origin, the three dipoles are one z-direction electric dipole at (-5mm, 0mm, 5mm) with a magnitude of 1e-7 A×m, one x-direction magnetic dipole at (0mm, 8mm, 3mm) with a magnitude of 8e-5 V/m, one y-direction magnetic dipole at (3mm, -3mm, 4mm) with a magnitude of 5e-5 V/m. The vertical and horizontal far-field electric field patterns are predicted at the circle defined by $r = 3$ m, $\theta = 60°$. The comparison with direct simulation is shown in Fig. 8. Both the vertical components and the horizontal components of the far-field prediction agree well with the simulation.

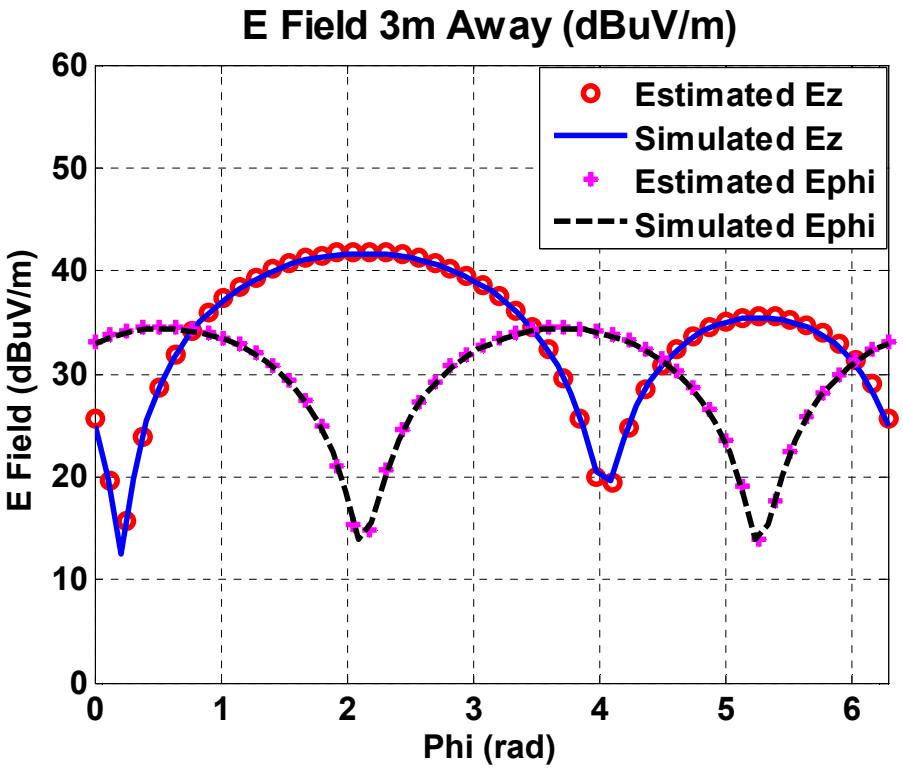

Fig. 8. Far-field prediction of three arbitrary dipoles compared to direct simulation.

IV. IMPROVED METHOD WITH SIMPLIFIED HUYGENS'S SURFACE

Although the tangential fields on a five-sided Huygens's surface are quite easy to export, the measurements for 3-D near-field scanning are very difficult to implement in practice. The aforementioned method is further improved for a radiation source located close to its ground by simplifying the Huygens's surface. It is one top near-field plane, very close to the DUT, with four side lines, shrunk from the four side walls of the five-sided box. Thus, only the horizontal magnetic fields on the top plane and the side lines are needed in the improved method, because the vertical magnetic fields near the PEC boundary are close to zero. Fig. 9 shows the setup of the simplified Huygens's surface.

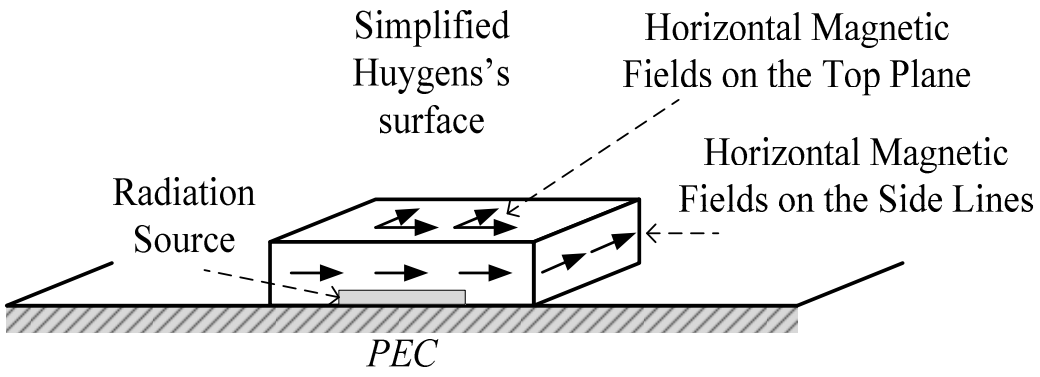

Fig. 9. Setup of the simplified Huygens's surface.

In the improved method, only the horizontal magnetic fields on the top plane and four side lines are simulated or measured; the vertical components on the side lines are set to zero when applied in FEM to solve the tangential electromagnetic fields on the outer box. Thus, much fewer scanning points are needed compared to the five-sided surface. With the calculated fields on the outer box, the same approach based on image theory and Huygens's principle will give the far-field estimation.

V. NUMERICAL VALIDATION OF THE IMPROVED METHOD

For the validation of the improved method, more practical numerical models are employed. The horizontal magnetic fields on the simplified Huygens's surface are exported and applied in the improved method.

A. Microtrip Trace

A PCB with a 50 Ohm microstrip trace is modeled in HFSS, shown in Fig. 10. The PCB size is 10 cm × 10 cm with a dielectric of FR4. The trace is 70 mm long copper, and the bottom of the PCB is the ground. One end of the trace is excited by the lumped

port with 0 dBm power at 1 GHz. The other end of the trace can be terminated by a 50 Ohm load, open or short.

The simplified Huygens's surface is composed by a 12 cm long, 12 cm wide, 5 mm high top plane and four side lines with a height of 3 mm. The magnetic near fields on this box are applied in the improved method. The predicted far-field electric fields, at r = 3 m, $\theta = 60°$, are compared to the simulation for the trace matched, open and short cases in Fig. 11, 12, and 13. All three comparisons illustrate good agreement.

The near fields of the open and short traces are dominated by electric fields and magnetic fields, separately. Good estimation in both cases indicates that the method works for general radiation sources.

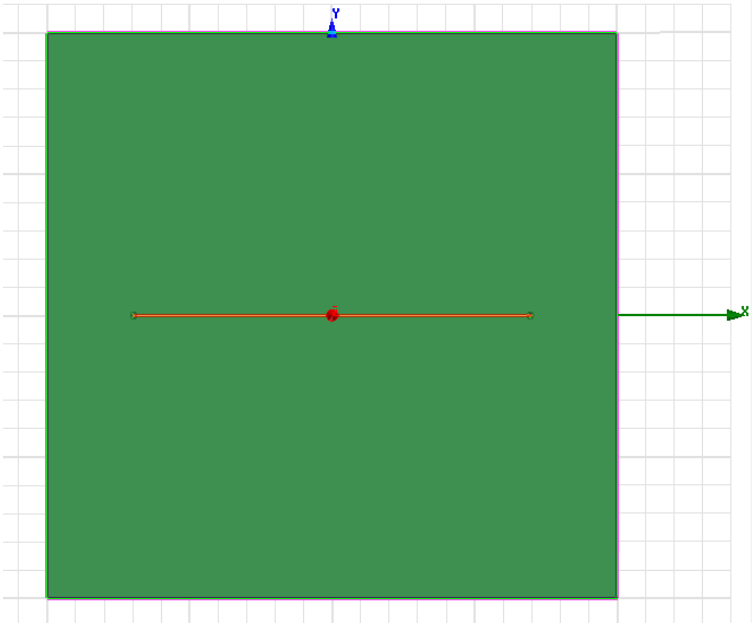

Fig. 10. The numerical model for the trace in HFSS.

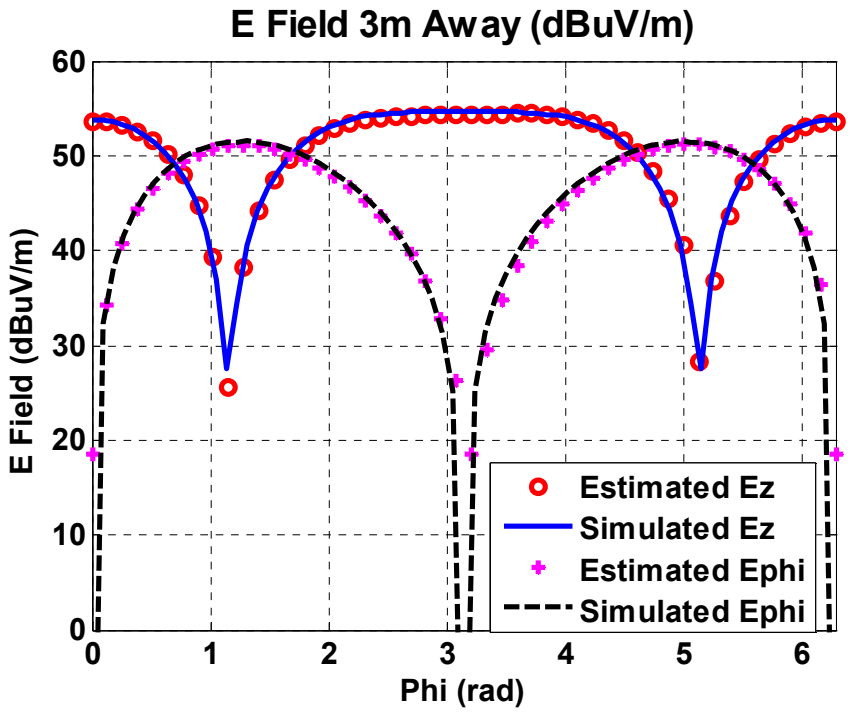

Fig. 11. Vertical and horizontal electric far-field prediction by the improved method compared to the simulation for the matched trace.

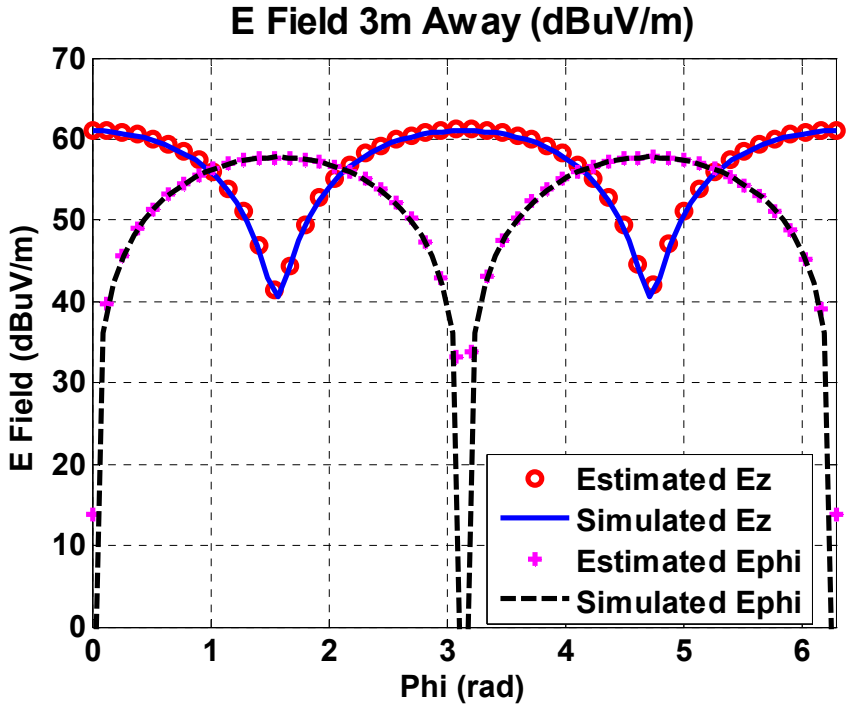

Fig. 12. Vertical and horizontal electric far-field prediction by the improved method compared to the simulation for the open trace.

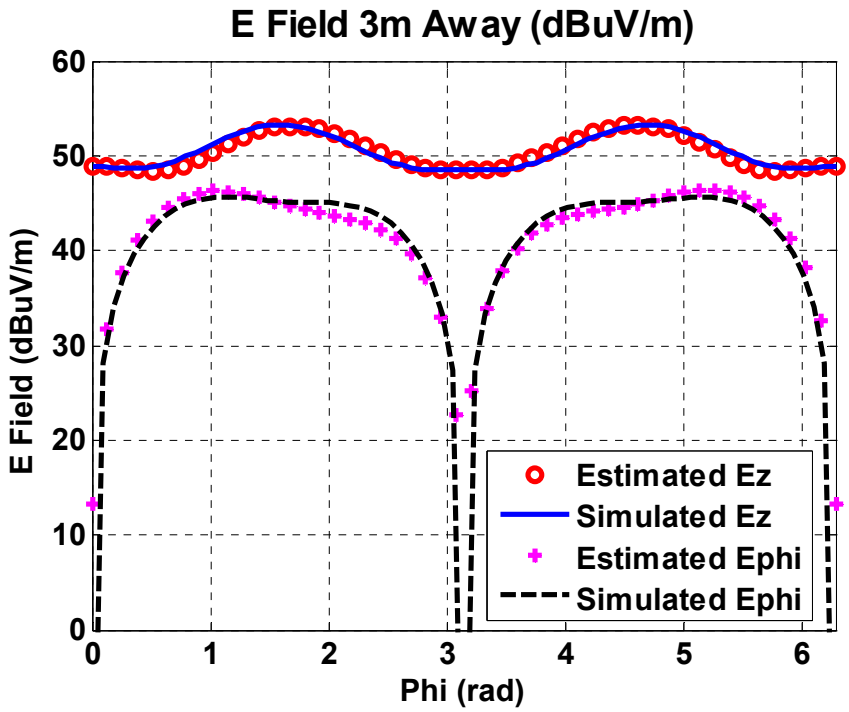

Fig. 13. Vertical and horizontal electric far-field prediction by the improved method compared to the simulation for the short trace.

B. Patch Antenna

Antenna is one of the good radiators [25], [26]. Another example for validation is a patch antenna. As Fig. 14 shows, the size of the copper patch is 37.2 mm by 28 mm, with a thickness of 0.035 mm. The patch is located on the 10 cm × 10 cm PCB of FR4 dielectric with a thickness of 1.58 mm, and the back of the PCB is the ground. The antenna works at 2.5 GHz with a 0dBm excitation.

The simplified Huygens's surface covering the patch antenna is a 70 mm long, 70 mm wide, 5 mm high top plane and four 3 mm high side lines. Fig. 15 is the far-field comparison with the simulation for this patch antenna example.

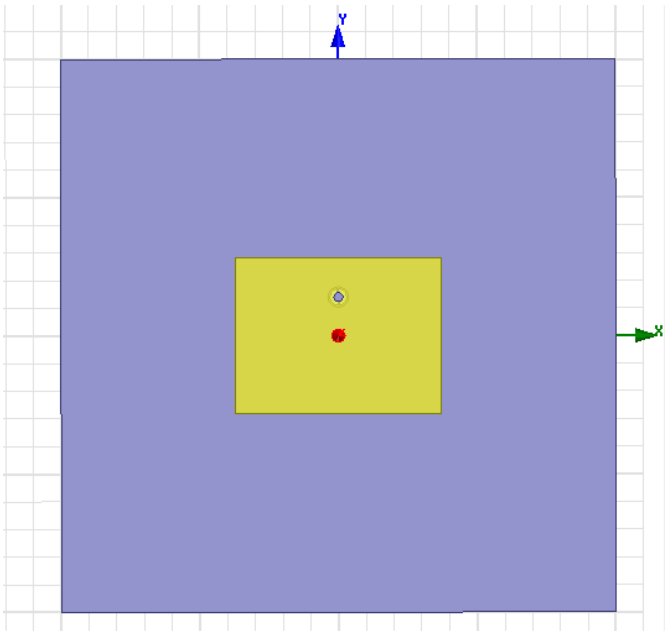

Fig. 14. The numerical model for the patch antenna in HFSS.

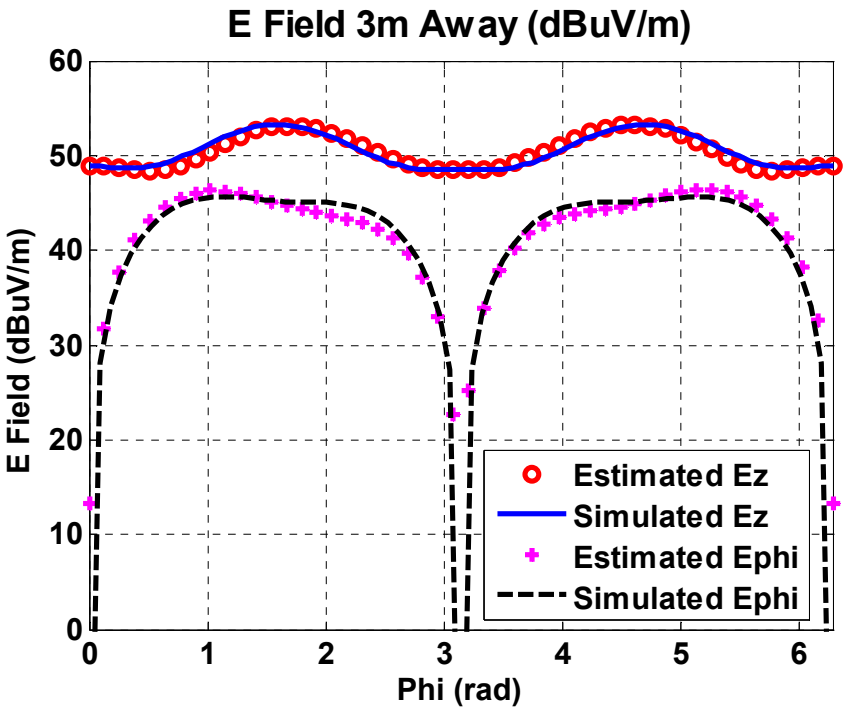

Fig. 15. Vertical and horizontal electric far-field predictions via the improved method compared to the simulation for the patch antenna.

The above numerical examples verify that the improved method using a simplified Huygens's surface can also predict the far-field radiation well from only the horizontal magnetic near fields. This approach will reduce the scanning points and complete the measurements with just one type of probe.

VI. MEASUREMENT VALIDATION OF IMPROVED METHOD

The patch antenna model described in Fig. 14 is fabricated for the measurements validation of the improved method. Fig. 16 is a picture of the fabricated PCB and S11 of the antenna. The PCB is 16 cm×16 cm with the FR4 dielectric.

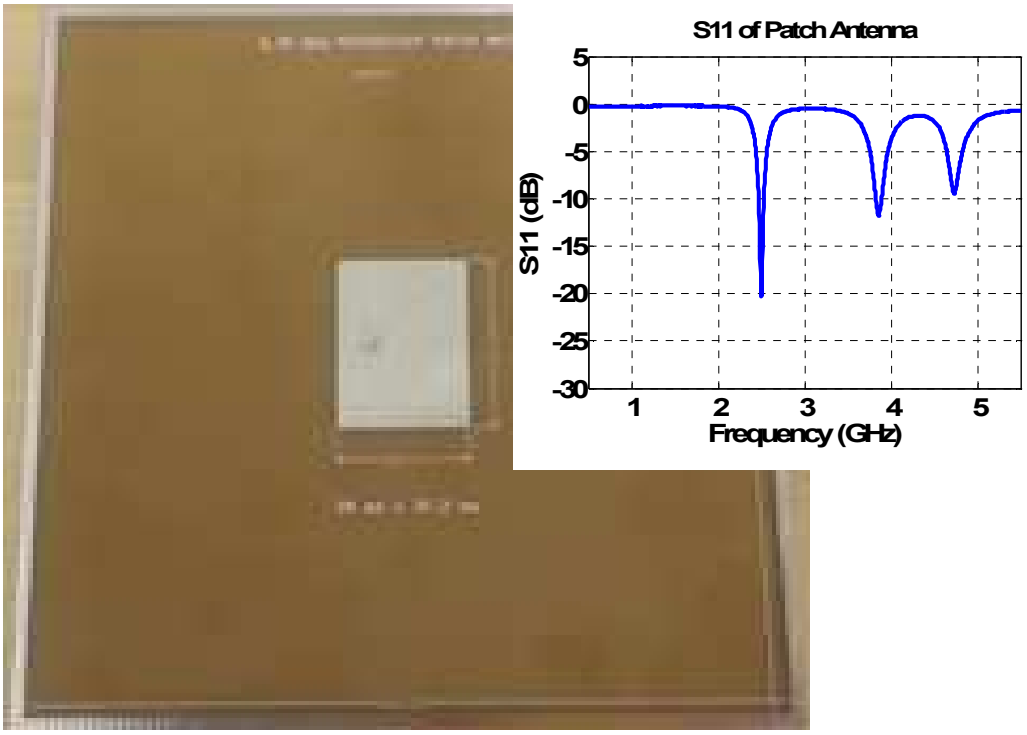

Fig. 16. Patch antenna PCB and its S11.

The simplified Huygens's surface is set as a 70 mm × 70 mm top plane with a height of 5 mm and four side lines with a height of 3 mm. The horizontal magnetic near

fields on this surface are scanned by a tangential magnetic probe based on the phase-resolved near-field scanning technique, reported in [23]. The spacing between each point is 1 mm. Fig. 17 is the near-field pattern of the top plane at 2.5 GHz when the input power is 0 dBm.

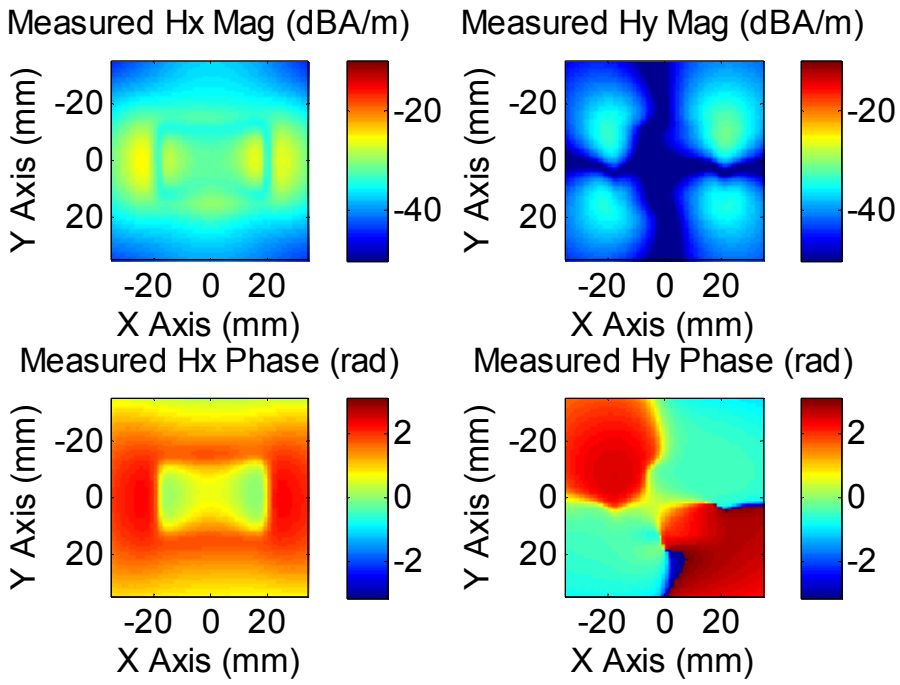

Fig. 17. Measured magnetic near-field pattern at 2.5 GHz on the top plane of the Huygens's surface.

The far-field radiation of this patch antenna is also measured in the semi-anechoic chamber. The patch antenna is grounded to the floor of the chamber so that the half-space radiation of the antenna can be measured; see Fig. 18.

The excitation power for the antenna is 0 dBm, and the radiation is recorded by a spectrum analyzer outside the chamber. The receiving antenna in the chamber is located 3 m away from the patch with a height of 1 m. The entire pattern of this circle can be

measured by rotating the patch for 360°. Fig. 19 compares the predicted far-field radiation by the improved method with the measurements in Fig. 18.

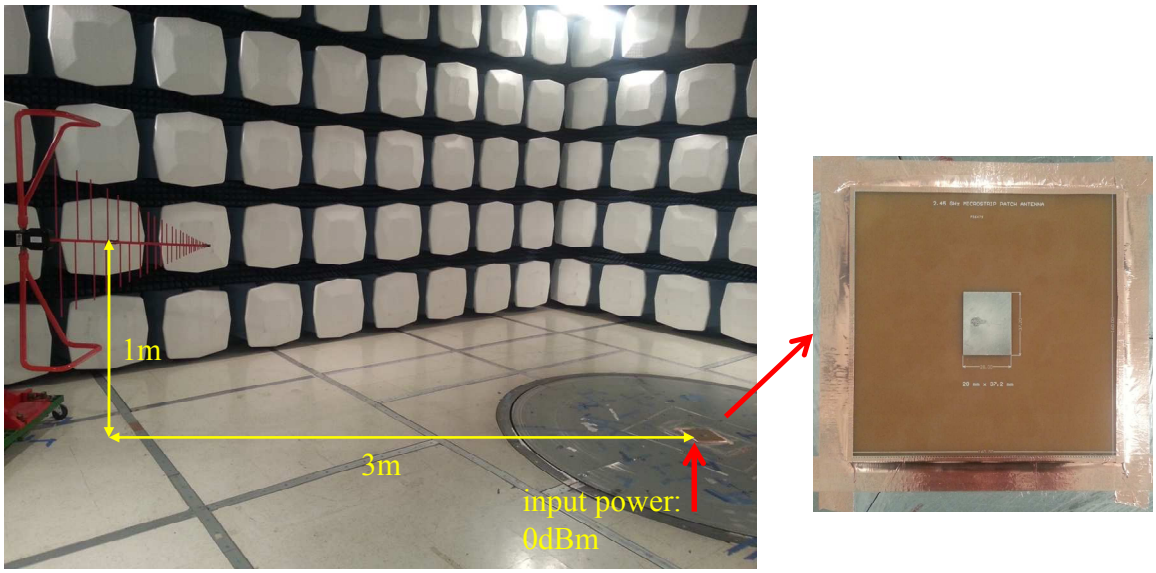

Fig. 18. Far-field measurement setup in the semi-anechoic chamber.

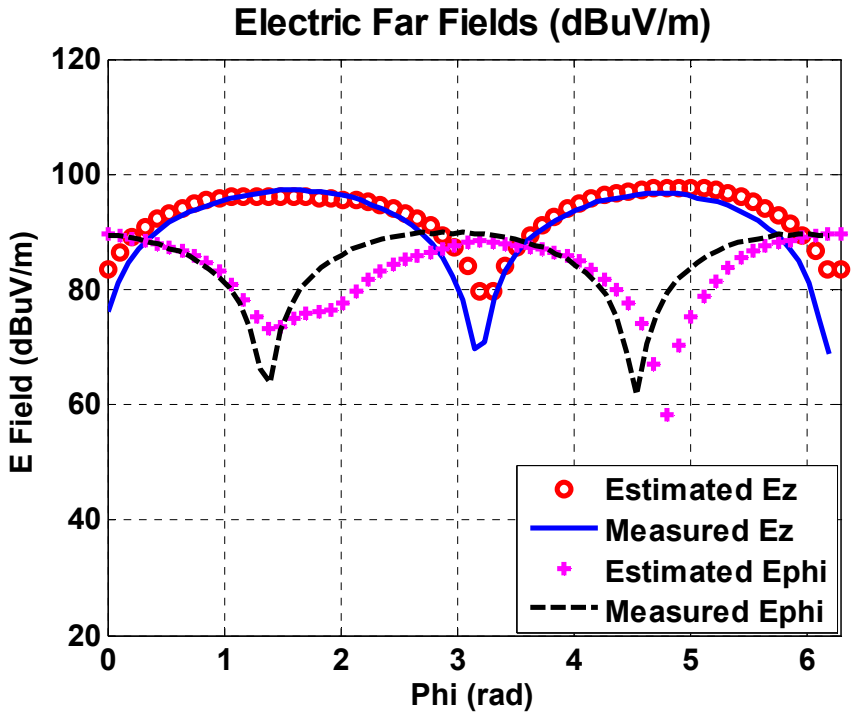

Fig. 19. Vertical and horizontal electric far-field prediction by the improved method compared to the measurements for the patch antenna.

The comparison in Fig. 19 illustrates that, with the measurement near fields on the simplified Huygens's surface, the improved method can predict the far-field pattern for both the vertical and horizontal components of the electric far fields. The maximum fields are precisely estimated. However, the minimum fields are not as good as the simulation prediction because of the lower accuracy of the measured near fields.

The performance of the proposed method for other frequencies is also studied. Similar processing is applied on the measured tangential magnetic near fields on the simplified Huygens's surface from 2 GHz to 3 GHz, with the frequency spacing of 0.1 GHz. The maximum vertical electric far fields at each frequency are calculated by the improved method and compared to the direct measurements in the chamber. Fig. 20 plots the comparison.

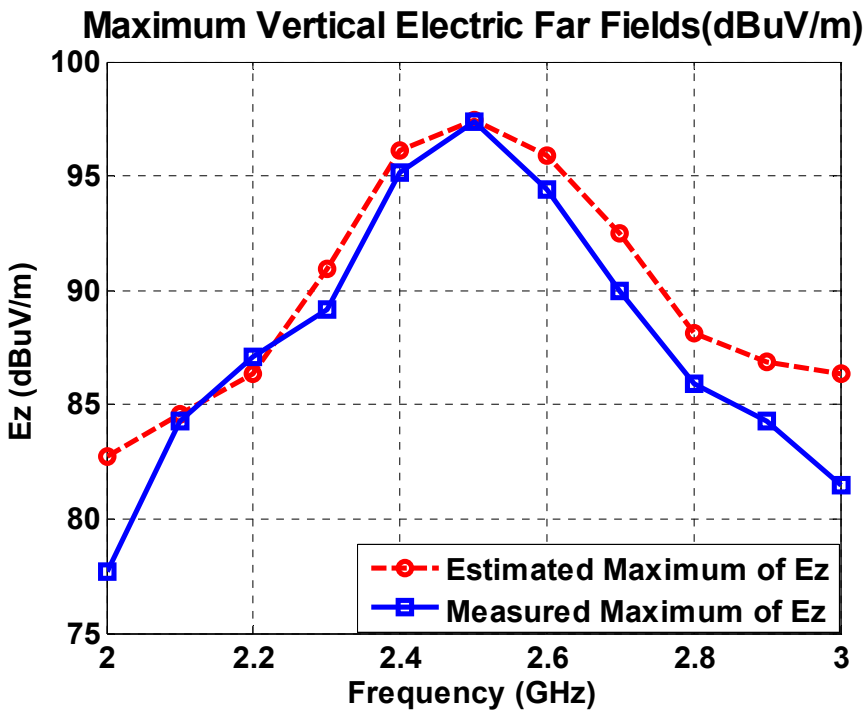

Fig. 20. Maximum vertical electric far-field prediction by the improved method compared to the measurements over 2 GHz to 3 GHz.

The results show that the improved method has successfully predicted the trend of the far-field radiation of the frequency band over 2 GHz to 3 GHz. The difference between prediction and measurement is within 5 dB. Because the antenna radiate less at the frequencies away from 2.5 GHz, the accuracy of the scanned near fields may become worse at these frequencies, corresponding to the probe limits and poor signal-to-noise ratio. This may lead to the biggest prediction error that happened at 2 GHz and 3 GHz.

One benefit of this simplified Huygens's surface is to reduce the number of scanning points while maintaining good far-field prediction accuracy. Paper [24] introduced the algorithm of the far-field estimation by the tangential electromagnetic fields on only the top plane. It is reported that, to obtain a good estimation, the size of this near-field plane should be very large. However, by the proposed method in this paper, the required scanning points on the simplified Huygens's surface can be reduced. Fig. 21 compares three cases: the far-field measurement, the 70 mm × 70 mm top plane only prediction, the prediction using a 50 mm × 50 mm simplified Huygens's surface, as well as the 50 mm × 50 mm top plane only prediction. The scanned point spacing in all cases is 1mm. It is observed that the prediction by the 50 mm × 50 mm Huygens's surface can achieve similar or even better accuracy than the 70 mm × 70 mm top plane only prediction. If we count the scanning point numbers in both cases, the 70 mm × 70 mm top plane scanned 4900 points, while the 50 mm × 50 mm Huygens's surface scanned 2900 points. Thus, 2000 scanning points are saved. This is a very considerable savings.

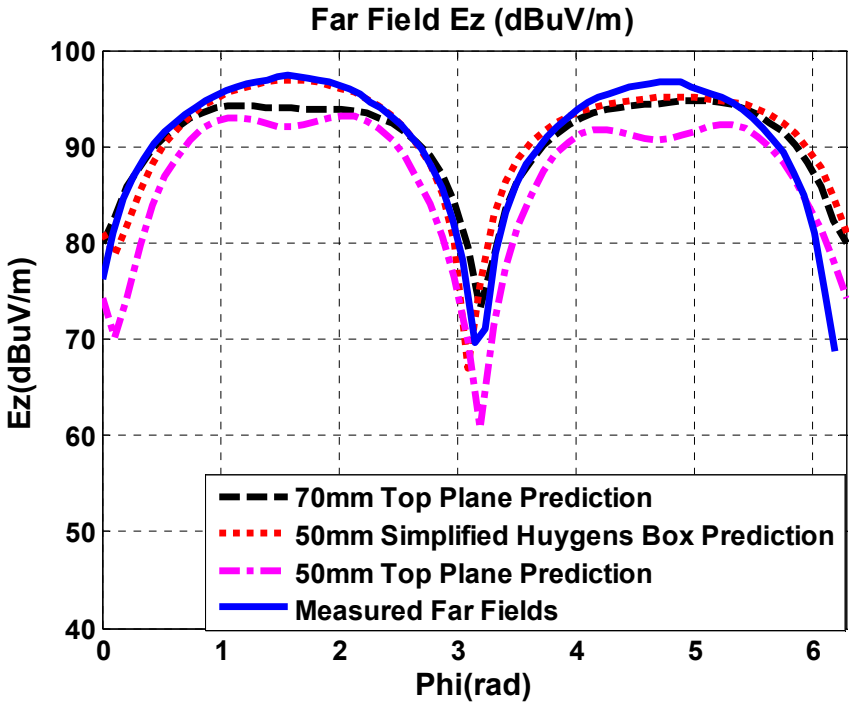

(a)

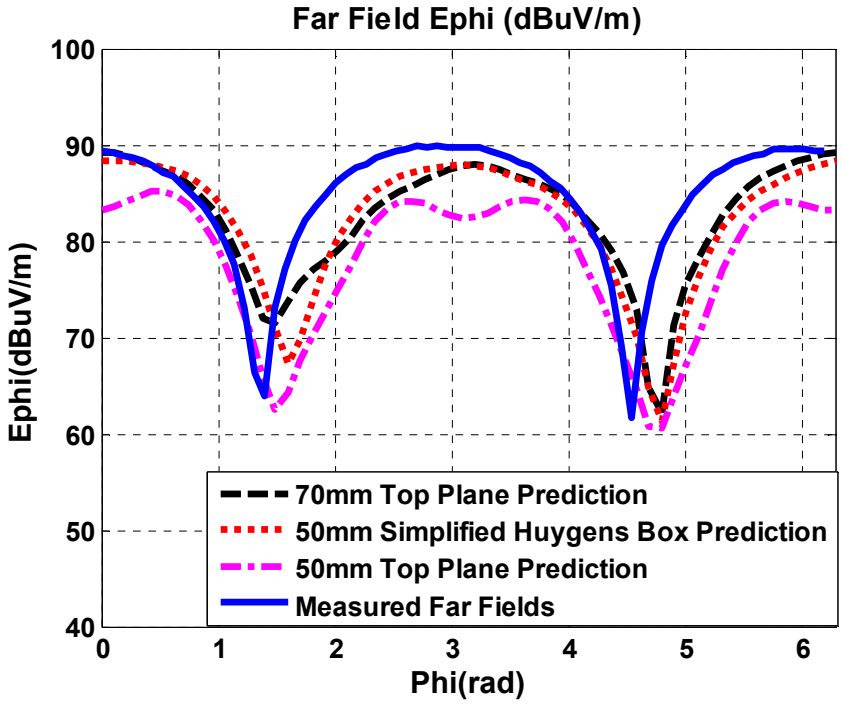

(b)

Fig. 21. Vertical (a) and horizontal (b) electric far-field prediction in three cases: 70 mm × 70 mm top plane only, 50 mm × 50 mm Huygens's surface and 50 mm × 50 mm top plane only, compared to the measurements of the patch antenna.

VII. CONCLUSION

This paper proposes a far-field prediction method that uses only the magnetic near-field for the case in which a radiation source is located on a ground plane. The near-field scanning on five sides of a Huygens's box was proposed to predict the far-field. The five-side Huygens's box, then, is further simplified into four side lines and one top plane, which greatly reduces the requirement for the near-field scanning. The proposed method was validated using both simulation and measurements. It overcomes the limitation of the electric probe design and also saves cost and scanning time for the near-field measurements. It can be used as an extension to the standard far-field measurements and may provide rough far-field estimation at the early stage of design. The proposed method, however, also has a limitation: the simplified Huygens's surface method requires that the radiation source have a low profile so that the one line measurement is enough on the side walls. Otherwise, a complete scanning on the Huygens's box (five sides) will be needed for various radiating structures with high profiles, for example, an IC with a heatsink sitting on it. For future study, the Feature Selective Validation tool based on [27] and [28] will be considered to quantitatively evaluate the validation comparisons.

REFERENCES

[1] M. Ramdani, E. Sicard, A. Boyer, S. Ben Dhia, J. J. Whalen, T. H. Hubing, M. Coenen, and O. Wada, "The electromagnetic compatibility of integrated circuits – Past, present, and future", *IEEE Trans. Electromagn. Compat*., vol. 51, no. 1, pp. 78-100, Feb. 2009.

[2] (2002). [Online]. Available: www.iec.ch, Jul. 2015.

[3] P. Wilson, "On correlating TEM cell and OATS emission measurements", *IEEE Trans. Electromagn. Compat.,* vol. 37, no. 1, pp. 1-16, Feb. 1995.

[4] B. Deutschmann, H. Pitsch, and G. Langer, "Near field measurements to predict the electromagnetic emission of integrated circuits", in *Proc. 5th Int. Workshop Electromagn. Compat. Integr. Circuits,* Munich, Germany, Nov. 2005.

[5] S. Deng, T. H. Hubing, D. G. Beetner, "Using TEM cell measurements to estimate the maximum radiation from PCBs with cables due to magnetic field coupling", *IEEE Trans. Electromagn. Compat.,* vol. 50, no. 2, pp. 419-425, May. 2008.

[6] A. D. Yaghjian, "An overview of near-field antenna measurements", *IEEE Trans. Antennas Propag*., vol.34, no.1, pp.30-45, Jan. 1986.

[7] T.K. Sarkar and A. Taaghol, "Near-field to near/far-field transformation for arbitrary near-field geometry utilizing an equivalent electric current and MoM", *IEEE Trans. Electromagn. Compat*., vol. 47, no.3, pp. 566-573, Mar. 1999.

[8] A. Taaghol and T.K. Sarkar, "Near-field to near/far-field transformation for arbitrary near-field geometry, utilizing an equivalent magnetic current", *IEEE Trans. Electromagn. Compat*., vol. 38, no. 3, pp. 536-542, Aug. 1996.

[9] L. Li, J. Pan, C. Hwang, G. Cho, H. Park, Y. Zhang and J. Fan, "Near-field coupling estimation by source reconstruction and Huygens's equivalence principle", in *Proc*. *IEEE International Symposium on Electromagnetic Compatibility.,* Santa Clara, CA, Mar. 2015.

[10] Y. Vives, C. Arcambal, A. Louis, F. de Daran, P. Eudeline, and B. Mazari, "Modeling magnetic radiations of electronic circuits using near-field scanning method", *IEEE Trans. Electromagn. Compat*., vol. 49, no. 2, pp. 391-400, May. 2007.

[11] Z. Yu, J. A. Mix, S. Sajuyigbe, K. P. Slattery, D. Pommerenke, J. Fan, "Heat-Sink Modeling and Design With Dipole Moments Representing IC Excitation", Electromagnetic Compatibility, IEEE Transactions on , vol.55, no.1, pp.168-174, Feb. 2013.

[12] J. Pan, G. Li, Y. Zhou, Y. Bai, X. Yu, Y. Zhang, and J. Fan, "Measurement validation of the dipole-moment model for IC radiated emissions", in *Proc*. *IEEE International Symposium on Electromagnetic Compatibility.,* Denver, CO, pp. 666-670, Aug. 2013.

[13] P. Fernández-López, C. Arcamba, D. Baudry, S. Verdeyme, and B. Mazari, "Radiation modeling and electromagnetic simulation of an active circuit", in *Proc. 7th Int. Workshop Electromagn. Compat. Integr. Circuits,* Toulouse, France, Nov. 2009.

[14] W. He, "Characterizing near-field circuit board radiation using crossed electric and magnetic dipoles sources", M. Eng. thesis, Missouri Univ. Sci. Technol., Rolla, MO, 2010.

[15] J. Pan, L. Li, X. Gao and J. Fan, "Application of dipole-moment model in EMI estimation", *IEEE International Symposium on Electromagnetic Compatibility and EMC Europe.,* to be published.

[16] L. Li, J. Pan, C. Hwang, G. Cho, B. Park, Y, Zhang and J. Fan, "Measurement validation for radio-frequency interference estimation by reciprocity theorem", *IEEE International Symposium on Electromagnetic Compatibility and EMC Europe.,* to be published.

[17] D. Baudry, C. Arcambal, A. Louis, B. Mazari, and P. Eudeline, "Applications of the near-field techniques in EMC investigations", *IEEE Trans. Electromagn. Compat*., vol. 49, no. 4, pp. 805-815, Nov. 2007.

[18] H. Fan and F. Schlagenhaufer, "Near-field Far-field conversion based on genetic algorithm for predicting radiation from PCBs", in *Proc*. *IEEE International Symposium on Electromagnetic Compatibility.,* Honolulu, HI, pp. 1-6, Jul. 2013.

[19] J. R. Regue, M. Ribo, J. Gomila, A. Perez, and A. Martin, "Modeling of radiating equipment by distributed dipoles using metaheuristics methods", in *Proc*. *IEEE International Symposium on Electromagnetic Compatibility.,* Chicago, IL, pp. 8-12, Aug. 2005.

[20] Y. Vives-Gilabert, C. Arcambal, A. Louis, P. Eudeline, and B. Mazari, "Modeling magnetic emissions combining image processing and an optimization algorithm", *IEEE Trans. Electromagn. Compat*., vol. 51, no. 4, pp. 909-918, Nov. 2009.

[21] X. Gao, J. Fan, Y. Zhang, D. Pommerenke, "Far-Field prediction using only magnetic near-field scanning for EMI test", *IEEE Trans. Electromagn. Compat*., vol. 56, no. 6, pp. 1335-1343, Dec. 2014.

[22] C.A. Balanis, *Advanced Engineering Electromagnetics*, Wiley, 1989.

[23] J. Zhang, K. Keong, M. Jin, V. Khilkevich, D. Pommerenke and J. Fan, "An effective method of probe calibration in phase-resolved near-field scanning for EMI application", *IEEE Trans. Instrum. Meas*., vol. 62, no. 3, pp. 648-658, Mar. 2013.

[24] J. Pan, X. Gao, Y. Zhang, J. Fan, "Far-field radiation estimation from near-field measurements and image theory", in *Proc*. *IEEE International Symposium on Electromagnetic Compatibility.,* Raleigh, NC, pp. 609-614, Aug. 2014.

[25] X. Gao, H. Zhong, Z. Zhang, Z. Feng and M. F. Iskander, "Low-profile planar tripolarization antenna for WLAN communications", *Antennas and Wireless Propagation Letters*, *IEEE*., vol. 9, pp. 83-86, Feb. 2010.

[26] Z. Zhang, X. Gao, W. Chen, Z. Feng and M. F. Iskander, "Study of conformal switchable antenna system on cylindrical surface for isotropic coverage", *IEEE Trans. Antennas and Propagation*., vol. 59, no. 3, pp. 776-783, Mar. 2011.

[27] V. Rajamani, C. F. Bunting, A. Orlandi, A. Duffy, "Introduction to feature selective validation (FSV)", *IEEE International Symposium on Antennas and Propagation*, pp. 601-604, Jul. 2006.

[28] A. Dufy, A. Martin, G. Antonini, A. Orlandi, C. Ritota, "The feature selective validation (FSV) method", *IEEE International Symposium on Electromagnetic Compatibility.,* vol.1, pp. 272-277, Aug. 2005.

II. RADIO-FREQUENCY INTERFERENCE ESTIMATION USING EQUIVALENT DIPOLE-MOMENT MODELS AND DECOMPOSITION METHOD BASED ON RECIPROCITY

Jingnan Pan, Hanfeng Wang, Xu Gao, Chulsoon Hwang, Eakhwan Song, Harkbyeong Park, Jun Fan, *Senior Member, IEEE*,
Electrical Engineering
Missouri University of Science and Technology, Missouri, U. S. A. 65409
Email: jpfz6@mst.edu, jfan@mst.edu

Abstract

In modern electronic products, the noise from high-speed digital parts is likely to interfere with nearby receivers, causing radio frequency interference (RFI) issues. In this paper, equivalent dipole-moment models and a decomposition method based on reciprocity theory are proposed being used together to estimate the coupling from the noise source to the victim antennas. The dipole-moment models are extracted from the near fields of the noise source by solving the inverse problem. The tangential electromagnetic fields on a Huygens's surface, which enclose the victim antenna, can be calculated from these equivalent dipole-moment models. Then, the victim antenna only is treated as a radiator. The tangential electromagnetic fields from the radiating antenna on the same Huygens's surface can be obtained. With these two groups of the fields on the Huygens's surface, the reciprocity theory is applied to estimate the coupling from the noise source to the victim antenna. This method is validated by full-wave simulations and measurements of a simple printed circuit board (PCB). The proposed method provides convenience to estimate RFI issues in the early design stage and saves the time of RFI simulation and measurements.

Index Terms

Equivalent dipole-moment models, Reciprocity, Decomposition, Radio frequency interference.

I. INTRODUCTION

Radio frequency interference (RFI) from the high-speed digital circuits to the radio frequency subsystem may interrupt, obstruct, or degrade the effective performance of the mixed RF/digital systems. Since many digital electronics such as clocks, high-speed I/O traces, cables, power delivery networks, and processing components are all possible noise sources for the RF receivers [1], RFI issues are becoming increasingly critical for modern electronic design. On the other hand, as it is preferable to decrease the size of the electronic product, its internal structure becomes more and more complex. Thus, the coupling mechanisms between the noise source and victim RF subsystem could be very complicated and have more possibilities. In the meanwhile, correcting RFI problems after systems are designed and ready to go into production is usually expensive and can result in program delays that adversely affect the acceptance of a new product [1]. Therefore, a method is needed to estimate RFI in complex systems during the early design and development phases.

In [2], the author proposed a decomposition method based on reciprocity theory to predict the coupling from a digital noise source to an RF antenna. Compared to the traditional Friis transmission equation, which is used to calculate the coupling in the far-field region, the decomposition method in [2] has very good performance for the coupling estimation in the near-field region, which is the common situation in mixed RF/digital systems. The method consisted of three steps illustrated by full-wave simulation examples in [2]. First, with the existence of the noise source and the victim antenna, a Huygens's box was introduced to enclose the antenna. Afterwards, the antenna was removed. In this case, the noise source was excited and the induced tangential

electromagnetic fields on the Huygens's box are obtained by the full-wave simulation tool. Second, only the victim antenna was simulated as a radiating antenna. The tangential electromagnetic fields from the antenna radiation on the same Huygens's box were also recorded. Finally, using the two groups of tangential electromagnetic fields on the Huygens's box, the coupled power from the noise source to the victim antenna could be calculated by reciprocity theory [2]. This method was applied in several numerical models and achieved decent RFI estimation.

However, to model the actual noise source, such as high-speed digital integrated circuits, LCD panels, etc., is very difficult. Sometimes the radiation interference of the victim antenna comes from multiple sources, so it is difficult to draw the real structure in the full-wave software. In addition, when the structure of the noise source is complex, the full-wave simulation could be very time-consuming. Hence, the tangential electromagnetic fields on the Huygens's box in the first step of [2] are no longer easily available by direct simulation. On the other hand, directly measuring tangential fields on the Huygens's box is limited by the 3D scanning technique. It also costs a lot of time and computer resources to scan the fields on all five surfaces. Thus, a method to model the noise source easily and calculate its radiation accurately is needed.

Much research effort has been put into the development of an equivalent model for the noise source from near-field scanning. The equivalent electric and magnetic currents were calculated from the near-field measurements by a moment method procedure to present antenna radiation in [3] and [4]. The equivalent current sources were placed over a fictitious surface that encompassed the antenna and both the synthetic and experimental results illustrated the accuracy of this method. In [5] through [8], electric

and magnetic dipoles were proposed as the equivalent model for the noise source. The magnitudes and the phases of the equivalent dipoles were determined by solving the inverse problem from near-field electromagnetic fields. The results in these publications showed that the equivalent dipole-moment models have good prediction of the radiation anywhere outside the source. Several researchers have also successfully imported these equivalent dipole-moment models into commercial full-wave simulation tools for system level simulations, such as in [9] and [10].

In this paper, the equivalent dipole-moment models and the decomposition method based on reciprocity are proposed being used together to estimate the coupling from the noise source to the victim antennas. This method can improve the coupling estimation efficiency and is feasible for real products. The equivalent dipole-moment models were extracted to model the noise source from the tangential magnetic fields on one near-field plane [7], by the least square method. Employing only magnetic near fields, this method can save almost half of the measurement time compared to the traditional method in [8], using both electric and magnetic near fields. Since there are close equations to calculate the dipole radiation, the tangential electromagnetic fields on the Huygens's box can be obtained quickly in MATLAB, rather than doing a full-wave simulation. Thus, the first step of the decomposition method was fulfilled. Then, similarly with [2], the victim antenna was modeled and excited in simulation software to export the tangential fields on the same Huygens's box. Finally, the coupling from the noise source to the victim antenna was estimated by reciprocity theory.

The proposed method prevents using complex models and time-consuming simulations for the source. Using only magnetic near fields for dipole extraction, the

scanning consistency can be kept and the scanning time is also saved significantly. With the equivalent dipole-moment models and the tangential fields from the antenna on the Huygens's box, the source and antenna can be placed in arbitrary locations. The proposed method can estimate the interference quickly and accurately for each location combination in the early design phase. The measurement validation for this kind of problem is demonstrated for the first time in this paper.

In this paper, Section II illustrates the equivalent dipole-moment models extraction algorithm and decomposition method based on reciprocity theory. Section III and Section IV contain the numerical and measurement validation of the proposed method. Finally, the discussion and conclusion are given in Section V and VI.

II. ALGORITHM

This section illustrates the algorithm of equivalent dipole-moment model and the decomposition method based on reciprocity.

A. Equivalent Dipole-Moment Model

An arbitrary electrically small source can be approximately replaced by six kinds of dipoles based on the multiple expansion of a radiation source [11]. For a lot of electronic products, the noise source is usually located closely on a large ground plane. In this situation, the radiation from tangential electric dipoles and vertical magnetic dipoles will almost be cancelled by their images. Thus, in Cartesian coordinates, just the vertical electric dipoles (P_z) and tangential magnetic dipoles (M_x, M_y) are enough to be the model for the noise source. The dipoles are located in or near the noise source and determined

by the tangential magnetic fields on a near-field plane of the source. Fig. 1 illustrates the equivalence of the dipole-moment model and the noise source.

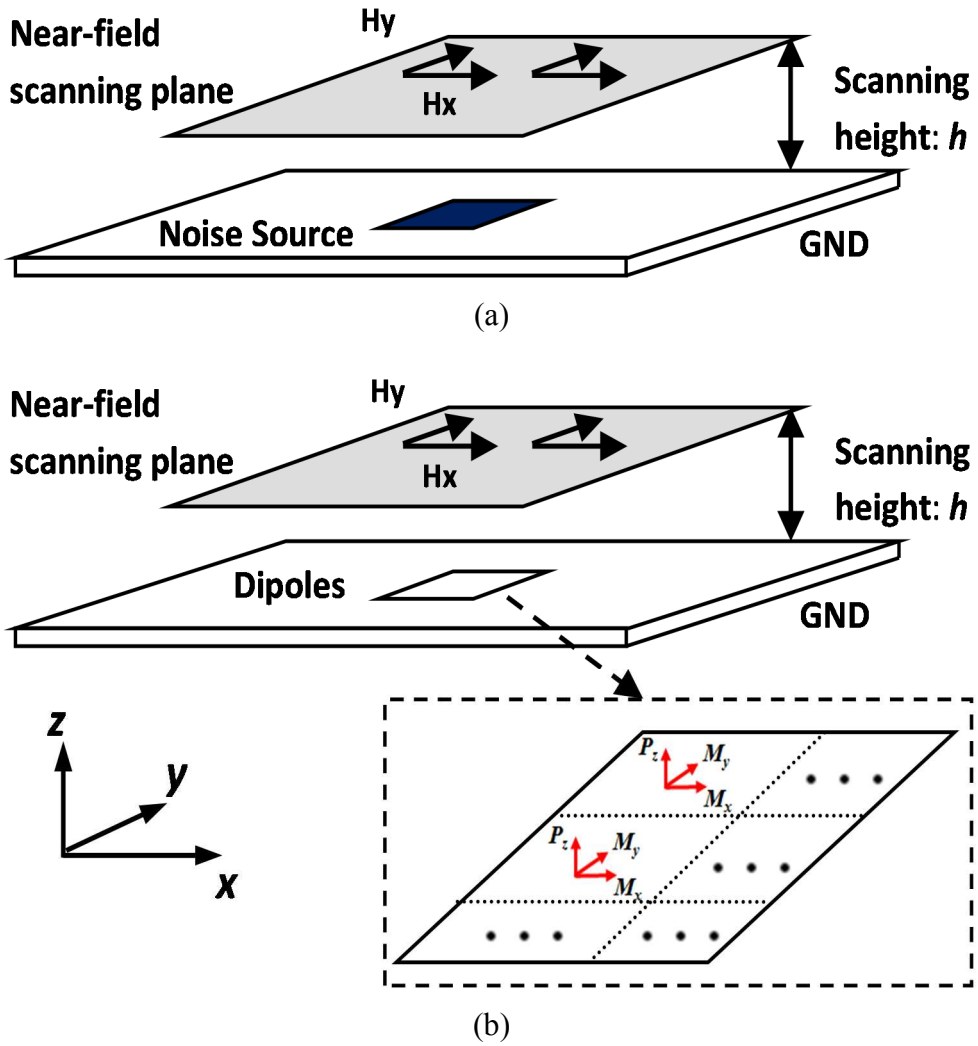

Fig. 1. Equivalent dipole-moment model for the noise source: (a) Original noise source and its near-field plane; (b) Equivalent dipole-moment model to represent the noise source.

The procedure to obtain the equivalent dipole-moment model is summarized as follows:

In Fig. 1 (a), the near-field plane was divided into $L_x \times L_y$ grids. The tangential magnetic fields in the center of each grid were scanned and organized as two $(L_x \times L_y) \times 1$

arrays, [H_x], and [H_y]. In Fig. 1 (b), the dipoles were distributed in $N_x \times N_y$ locations and each location had one P_z, one M_x, and one M_y dipole. Thus, these dipole moments in different locations were denoted as three ($N_x \times N_y$) ×1 arrays, [P_z], [M_x], and [M_y]. With the analytical radiation equations in [10], the dipole-moment model's radiation on every near-field grid was given as [H_x (D)] and [H_y (D)]. As the equivalent model, the dipole generated magnetic fields were equal to the scanned fields from the real source, as shown in the following equation:

$$\begin{pmatrix} [H_x] \\ [H_y] \end{pmatrix} = \begin{pmatrix} [H_x(D)] \\ [H_y(D)] \end{pmatrix} \tag{1}$$

Thus, the scanned [H_x] and [H_y] were used to determine the dipole moments by

$$\begin{pmatrix} [H_x]_{(L_x \times L_y)\times 1} \\ [H_y]_{(L_x \times L_y)\times 1} \end{pmatrix} = T \begin{pmatrix} [P_z]_{N_x \times N_y \times 1} \\ [M_x]_{N_x \times N_y \times 1} \\ [M_y]_{N_x \times N_y \times 1} \end{pmatrix} \tag{2}$$

where the T matrix was expressed by

$$T = \begin{pmatrix} T_{HxPz} & T_{HxMx} & T_{HxMy} \\ T_{HyPz} & T_{HyMx} & T_{HyMy} \end{pmatrix} \tag{3}$$

Each sub-matrix has the size of ($L_x \times L_y$)×($N_x \times N_y$), denoting the contribution of one type of the dipoles to one component of the magnetic fields.

Then, both the field arrays and the dipole arrays were normalized, as shown in (4) and (5). Here, k_0 is the propagation constant in the free space. $H_{\max}$ is the maximum magnitude of [H_x] and [H_y].

$$F_n = \begin{pmatrix} [H_x]_{Lx \times Ly \times 1} / H_{\max} \\ [H_y]_{Lx \times Ly \times 1} / H_{\max} \end{pmatrix} \tag{4}$$

$$X_k = \begin{pmatrix} [P_z]_{N_x \times N_y \times 1} \\ [k_0 M_x]_{N_x \times N_y \times 1} \\ [k_0 M_y]_{N_x \times N_y \times 1} \end{pmatrix} \tag{5}$$

In this case, equation (2) becomes

$$F_n = T_{nk} X_k \tag{6}$$

where

$$T_{nk} = \begin{pmatrix} T_{HxPz}/H_{\max} & T_{HxMx}/(H_{\max} k_0) & T_{HxMy}/(H_{\max} k_0) \\ T_{HyPz}/H_{\max} & T_{HyMx}/(H_{\max} k_0) & T_{HyMy}/(H_{\max} k_0) \end{pmatrix} \tag{7}$$

When the coordinates of all the near-field grids and the dipole locations were defined, the T_{nk} matrix was generated. The least-square method was applied to solve the inverse problem in (6). The solution is given by

$$X_k = [T_{nk}' T_{nk}]^{-1} T_{nk}' F_n \tag{8}$$

Then the actual dipole moments were obtained by dividing k_0 from $[M_x]$ and $[M_y]$ in X_k.

Compared to the global optimization method, the least square method to extract dipole-moment model might be more sensitive to the accuracy of the measurements, and perform worse when having too many independent variables [12]. On the other hand, global optimization methods required a lot of computing time and might lack stopping criteria in some situations. Each method has its advantages and disadvantages. This paper employed the least square method for its fast calculation and effectiveness.

B. Decomposition Method Based on Reciprocity

As described in the previous section, the decomposition method has three steps to do the RFI estimation between the noise source and the victim antenna. This section will explain the method with the equivalent dipole-moment model as the source in detail.

Step 1, Forward Problem

Based on the equivalent dipole-moment model extraction algorithm, the dipole moments were calculated from the tangential magnetic near fields to represent the real noise source first. The coupling between the source and the victim antenna, Fig. 2(a), was equal to the coupling between the dipoles and the antenna, Fig. 2(b). The coupling induced electromagnetic fields on the port of victim antenna, named as E_d^{fwd}, H_d^{fwd}.

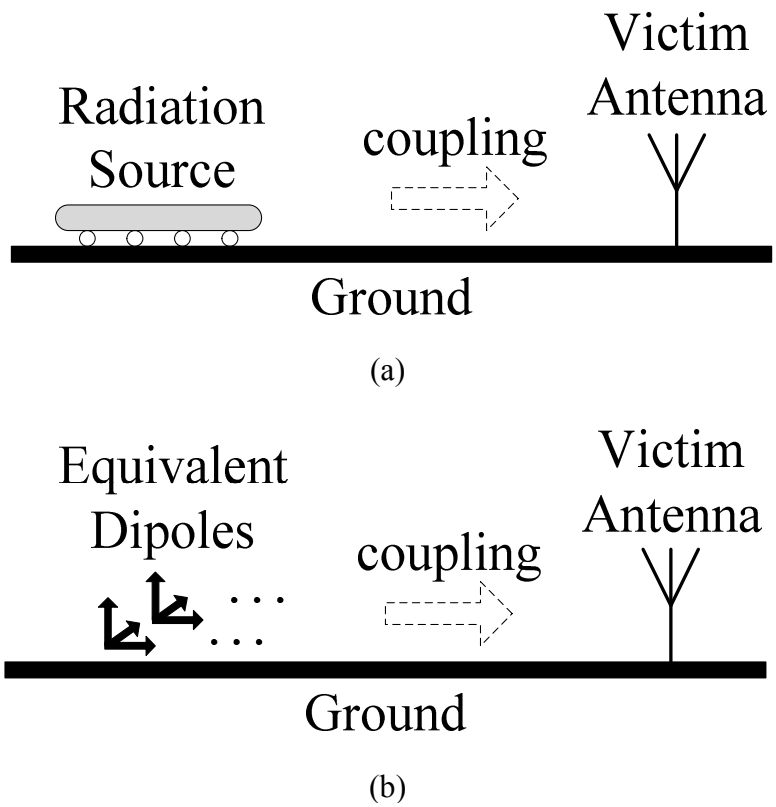

Fig. 2. Dipole-moment model representation for the noise source: (a) Original interference problem; (b) Equivalent problem using equivalent dipoles.

In Fig. 3, a Huygens's box was set up to enclose the victim antenna and then the antenna was removed. The Huygens's box was divided into many cells on which the tangential electromagnetic fields were calculated from the dipole moments. This

procedure was named “Forward Problem” and the tangential fields on the Huygens’s box were recorded as E_c^{fwd} and H_c^{fwd}.

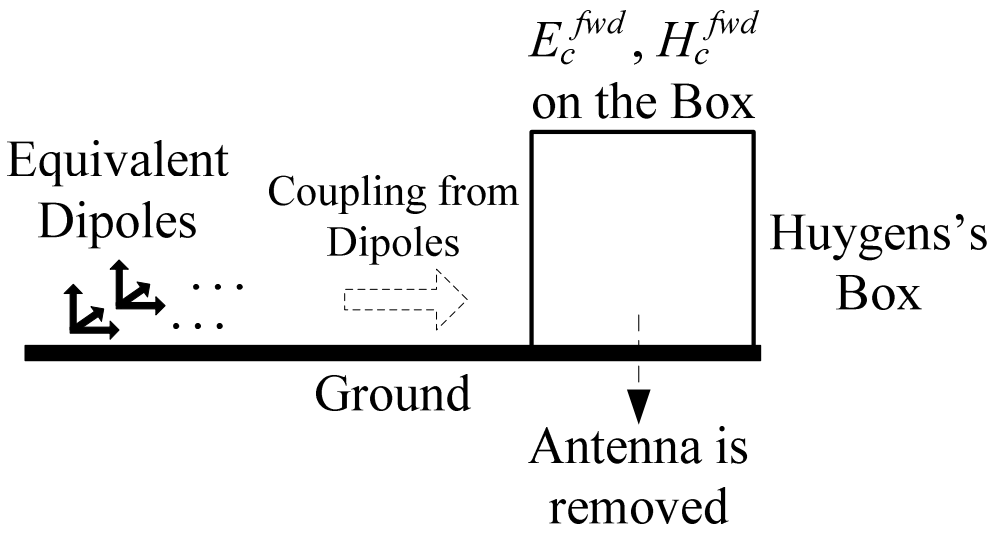

Fig. 3. “Forward Problem” obtained the tangential fields on the Huygens’s box from the dipole-moment model of the noise source.

Step 2, Reverse Problem

Corresponding to the “Forward Problem”, step 2 was named “Reverse Problem” in which the source was removed and only the victim antenna was excited. Thus, on the same Huygens’s box, the tangential electromagnetic fields generated from the excited antenna were recorded as E_c^{rev} and H_c^{rev}. On the antenna port, the fields induced by the excitation were recorded as E_a^{rev} and H_a^{rev}. This step is shown in Fig. 4.

Step 3, Interference Estimation

As we already have the E_d^{fwd}, H_d^{fwd}, E_c^{fwd}, H_c^{fwd}, E_a^{rev}, H_a^{rev}, E_c^{rev}, and H_c^{rev} from the “Forward Problem” and “Reverse Problem”, the interference was estimated based on these fields by reciprocity theory.

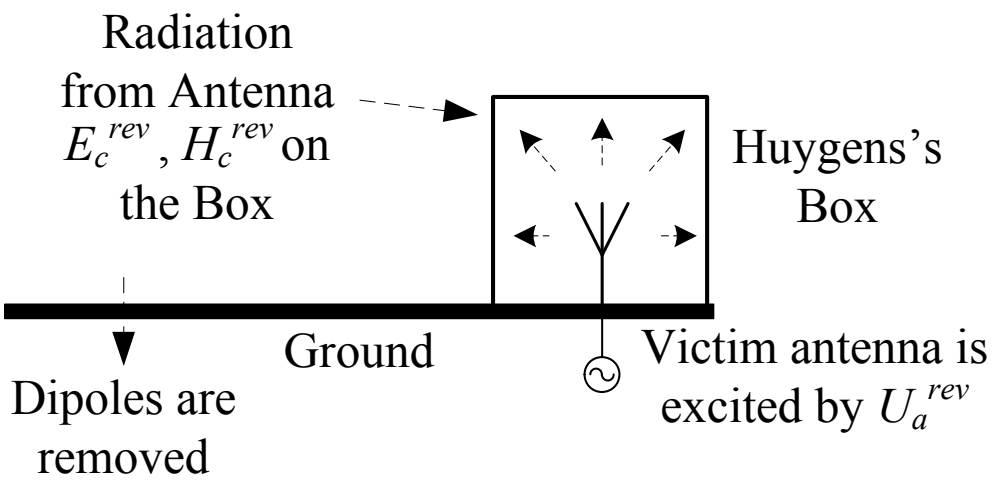

Fig. 4. "Reverse Problem" obtained the tangential fields on the Huygens's box from the excited victim antenna only.

The reciprocity theory was expressed by the fields and source quantities in the forward and reverse problem as [2]:

$$\begin{aligned} &-\int_S \left(E^{rev}\times H^{fwd} - E^{fwd}\times H^{rev}\right)\cdot ds \\ &= \int_V \left(E^{rev}\times J^{fwd} + H^{fwd}\times M^{rev}\right)dv \\ &- \int_V \left(E^{fwd}\times J^{rev} + H^{rev}\times M^{fwd}\right)dv \end{aligned} \tag{9}$$

J and M are electric current and magnetic current source, where "fwd" and "rev" denote the problem type. When the integral is over the entire space, (9) was further simplified as:

$$\begin{aligned} &\int_V \left(E_c^{rev}\cdot J_c^{fwd} - H_c^{rev}\cdot M_c^{fwd}\right)dv \\ &\qquad = \int_V \left(E_a^{fwd}\cdot J_a^{rev} - H_a^{fwd}\cdot M_a^{rev}\right)dv \end{aligned} \tag{10}$$

The subscript "c" means the corresponding fields or currents located on the Huygens's box, and similarly, "a" means the antenna port. The current sources J_c^{fwd} and M_c^{fwd} are equivalent sources resulting from the tangential electromagnetic fields on the Huygens's box.

Replacing the sources by the fields, the two terms on the left side of (10) were derived as (11) and (12).

$$\begin{aligned}&\int_V \left(E_c^{rev}\cdot J_c^{fwd}\right)dv=\int_{S_c}\left(E_c^{rev}\cdot J_c^{fwd}\right)ds\\&=\sum_{cells}E_c^{rev}\cdot J_c^{fwd}S_{cell}=\sum_{cells}E_c^{rev}\cdot\left(\hat{n}\times H_c^{fwd}\right)S_{cell}\end{aligned}\tag{11}$$

$$\begin{aligned}&\int_V \left(H_c^{rev}\cdot M_c^{fwd}\right)dv=\int_{S_c}\left(H_c^{rev}\cdot M_c^{fwd}\right)ds\\&=\sum_{cells}H_c^{rev}\cdot M_c^{fwd}S_{cell}=\sum_{cells}H_c^{rev}\cdot\left(E_c^{fwd}\times\hat{n}\right)S_{cell}\end{aligned}\tag{12}$$

Following the procedure in [12], the two terms on the right side of (10) became (13) and (14).

$$\begin{aligned}&\int_V \left(E_a^{fwd}\cdot J_a^{rev}\right)dv=-\int_{S_a}E_a^{fwd}J_a^{rev}ds\\&=-I_a^{rev}U_a^{fwd}\end{aligned}\tag{13}$$

$$\begin{aligned}&\int_V \left(H_a^{fwd}\cdot M_a^{rev}\right)dv=\int_V H_a^{fwd}\cdot\left(E_a^{rev}\times\hat{n}\right)dv\\&=\int_V E_a^{rev}\cdot\left(\hat{n}\times H_a^{fwd}\right)dv=\int_V E_a^{rev}\cdot J_a^{fwd}dv\\&=\int_{S_a}J_a^{fwd}E_a^{rev}ds=I_a^{fwd}U_a^{rev}\end{aligned}\tag{14}$$

Substituting (11)-(14) into (10) obtained:

$$\begin{aligned}&\sum_{cells}\hat{n}\times H_c^{fwd}\cdot E_c^{rev}S_{cell}+\sum_{cells}\hat{n}\times E_c^{fwd}\cdot H_c^{rev}S_{cell}\\&=-I_a^{rev}U_a^{fwd}-I_a^{fwd}U_a^{rev}=-\left(\frac{1}{Z_{in}}+\frac{1}{Z_L}\right)U_a^{fwd}U_a^{rev}\end{aligned}\tag{15}$$

In (11)-(15), S_c is the overall surface of the Huygens's box and equally meshed into small square cells with the area of S_{cell}. The fields were distributed uniformly in each cell. Thus, the integral over S_c can be expressed by the summation over all the cells. Z_{in} is the input impedance of the antenna in the "Reverse Problem" and Z_L is the load impedance at the antenna port in the "Forward Problem", 50 Ω in common usage. U_a^{rev} is the exciting voltage in the "Reverse Problem".

Finally, with the fields on the Huygens's box from the forward and reverse problems, the coupling voltage was solved by:

$$U_a^{fwd} = -\frac{Z_{in}Z_L}{U_a^{rev}\left(Z_{in}+Z_L\right)}\times \left(\sum_{cells}\hat{n}\times H_c^{fwd}\cdot E_c^{rev}S_{cell}+\sum_{cells}\hat{n}\times E_c^{fwd}\cdot H_c^{rev}S_{cell}\right) \tag{16}$$

Based on U_d^{fwd}, the scattering parameter from the victim antenna to the source was easily calculated by (17). U_{in} in (17) is the incident voltage at the source port.

$$S = \frac{U_a^{fwd}}{U_{in}} \tag{17}$$

III. NUMERICAL VALIDATION

A group of passive structures were modeled, as shown in Fig. 5, in a commercial full-wave simulation tool (HFSS) to validate the proposed method. Structures 1, 2, and 4 are three patch antennas, modeled by copper, working at 2.5 GHz. The sizes of the patches are 28 mm × 37.2 mm. Structure 3 is a shorted curving trace with the characteristic impedance of 50 Ω. The antennas and the trace are located on the printed circuit board (PCB), of which the dielectric material is FR4. The back side of this PCB is the ground modeled by copper. The distance between the centers of antennas 1 and 2 is 77.2 mm, while the distance between antennas 2 and 4 is 111 mm.

The antennas and the trace are designed to have the input impedance of 50 Ohm. Their impedances are matched with common equipment reference impedance. One end of the trace is short terminated. Ports 1, 2, 3, 4 are modeled in the full-wave simulation tool as the excitations for these passive structures.

A. Noise Source: Trace

Taken as the noise source, the trace was excited at one end and the short terminated at the other one. The three patches are victim antennas at different locations. After the full-wave simulation of the whole model, the scattering parameters between the ports of the trace and the antennas indicated the corresponding interference.

Meanwhile, the equivalent dipole-moment models for the trace were established from its simulated tangential magnetic fields on a near-field plane. Then, applying the proposed method, the coupling power on each antenna port was also estimated.

Fig. 6 (a) shows the magnetic near-field pattern at 2.5 GHz. This plane was centered at the center of the trace, with 60 mm in length, 60 mm in width and 5 mm in height. Assuming the dipoles are located at 8 × 8 arrays centered at the trace center, with 4 mm spacing in x- and y- direction, the reconstructed pattern of the same near-field plane is shown in Fig. 6 (b).

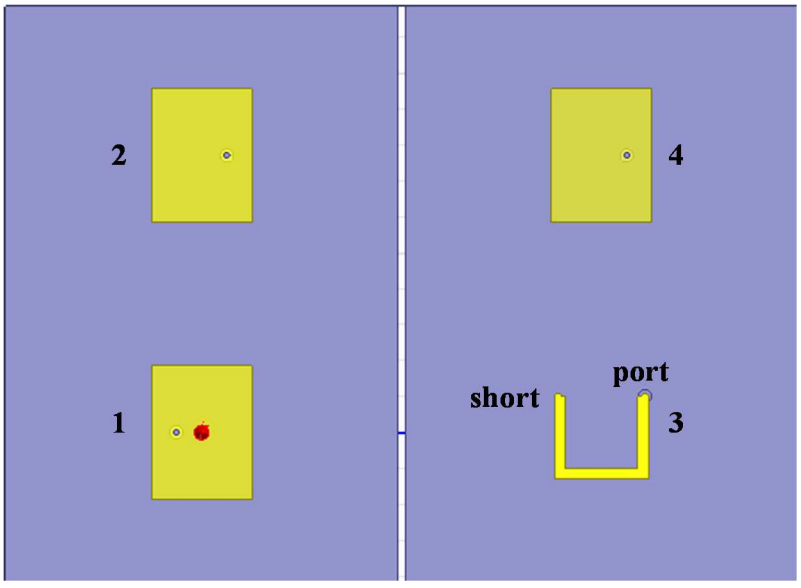

Fig. 5. Passive structures model in HFSS for the numerical validation. 1, 2, 4 are three patch antennas; 3 is the short terminated trace.

The agreement between the simulation and the dipole reconstruction validated the equivalence of the dipole-moment model.

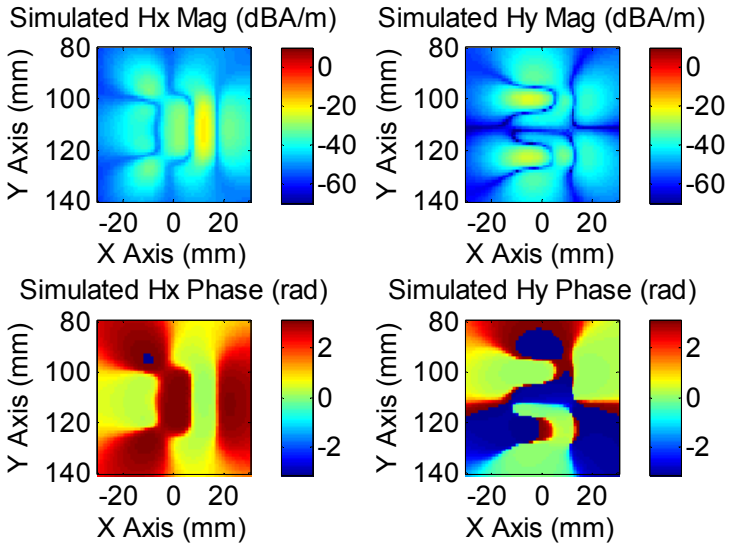

(a)

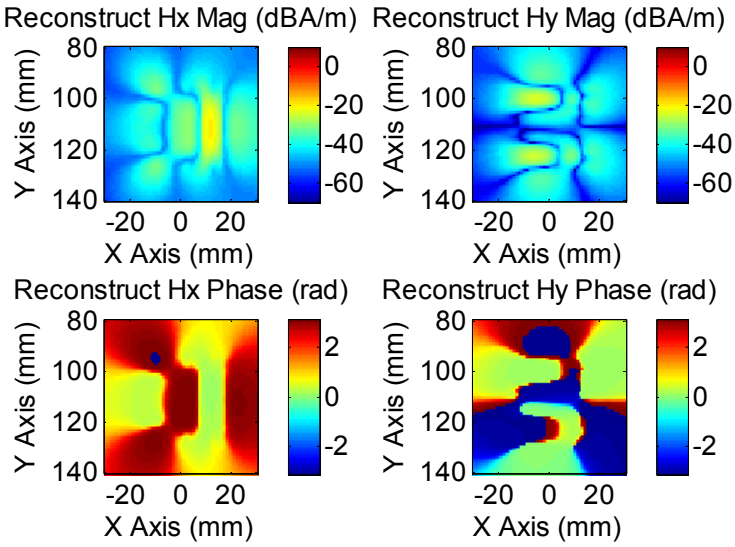

(b)

Fig. 6. Dipole-moment model reconstructed near-field pattern. (a) Simulated near fields of the trace. The near fields are used to extract dipole-moment model. (b) The reconstructed near-field pattern from the corresponding dipole moment model.

In “Forward Problem” and “Reverse Problem”, the Huygens’s box for each antenna was a 40 mm × 40 mm × 40 mm cube. Fig. 7 shows antenna 1 as an example.

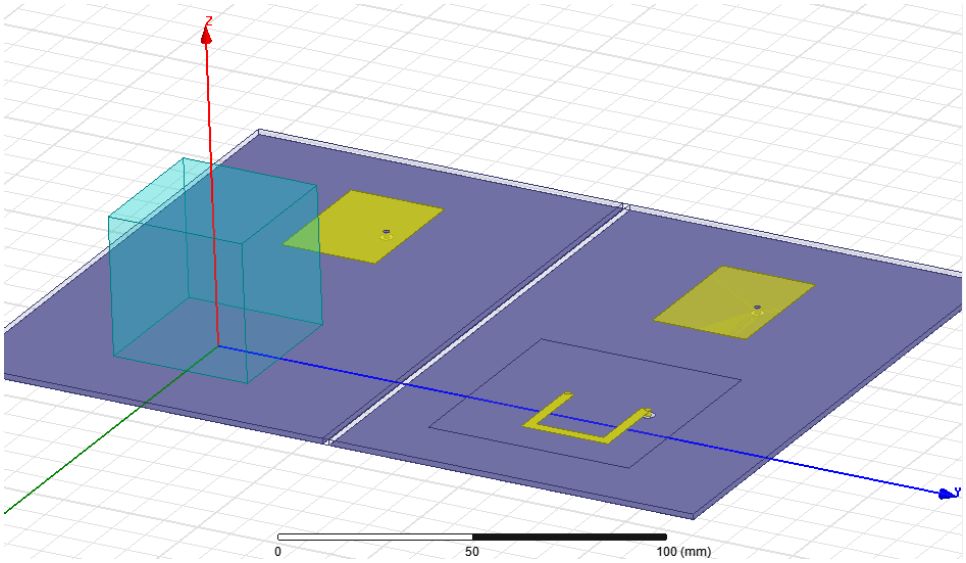

(a)

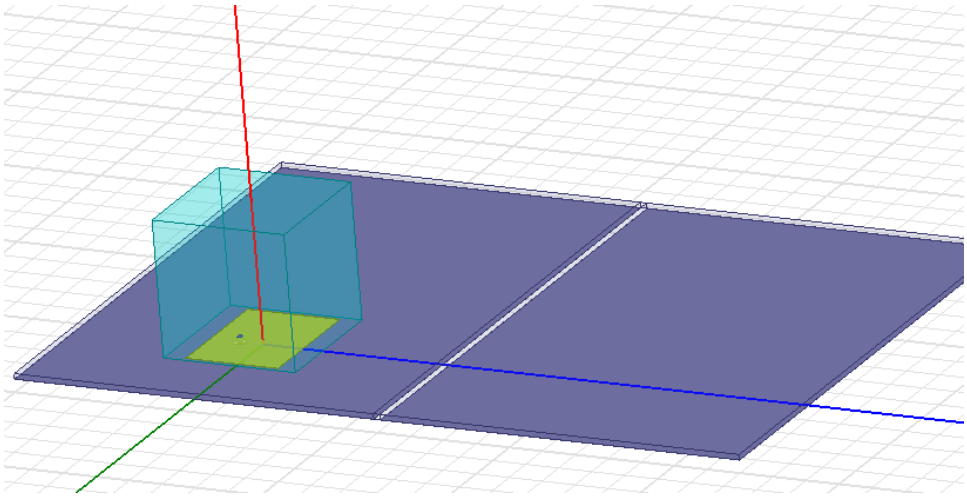

(b)

Fig. 7. Huygens’s box in “Forward Problem” (a) and “Reverse Problem” (b).

The tangential electromagnetic fields on the Huygens’s box in the “Forward Problem” (E_c^{fwd}, H_c^{fwd}), and the “Reverse Problem” (E_c^{rev}, H_c^{rev}), were obtained by the calculation from the dipoles and the simulation of the excited antenna with voltage U_a^{rev}, respectively. Then applying (16)-(17), U_d^{fwd} and the scattering parameter were calculated.

Fig. 8 shows the comparisons between the proposed method estimation and the direct simulation for each victim antenna.

The comparison illustrated that the proposed method can predict the trend of the scattering parameters well. Thus, the worst coupling frequency could be identified and the effect of the antennas' locations could also be evaluated.

B. Noise Source: Antenna

In the meanwhile, one of the antennas was also taken as the noise source to examine the method. Fig. 9 shows the magnetic near-field pattern of antenna 4 and the reconstructed fields by its dipole-moment model at 2.5 GHz.

This near-field plane size was 70 mm × 70 mm with the height of 5 mm. The dipoles also had 8 × 8 locations and 4 mm spacing.

Similarly, the Huygens's box was setup to cover antennas 1, 2 and the shorted trace. With the tangential fields on the Huygens's box in the "Forward Problem" and "Reverse Problem", the scattering parameters between antenna 4 and the other structures were estimated by the proposed method. Fig. 10 shows the comparisons between the estimation and direct simulation in HFSS.

The comparisons in Fig. 8 and Fig. 10 show that the proposed method worked for different kinds of noise sources and antennas. The trends of the scattering parameters are well predicted in both cases. The differences for most frequencies were within 3 dB.

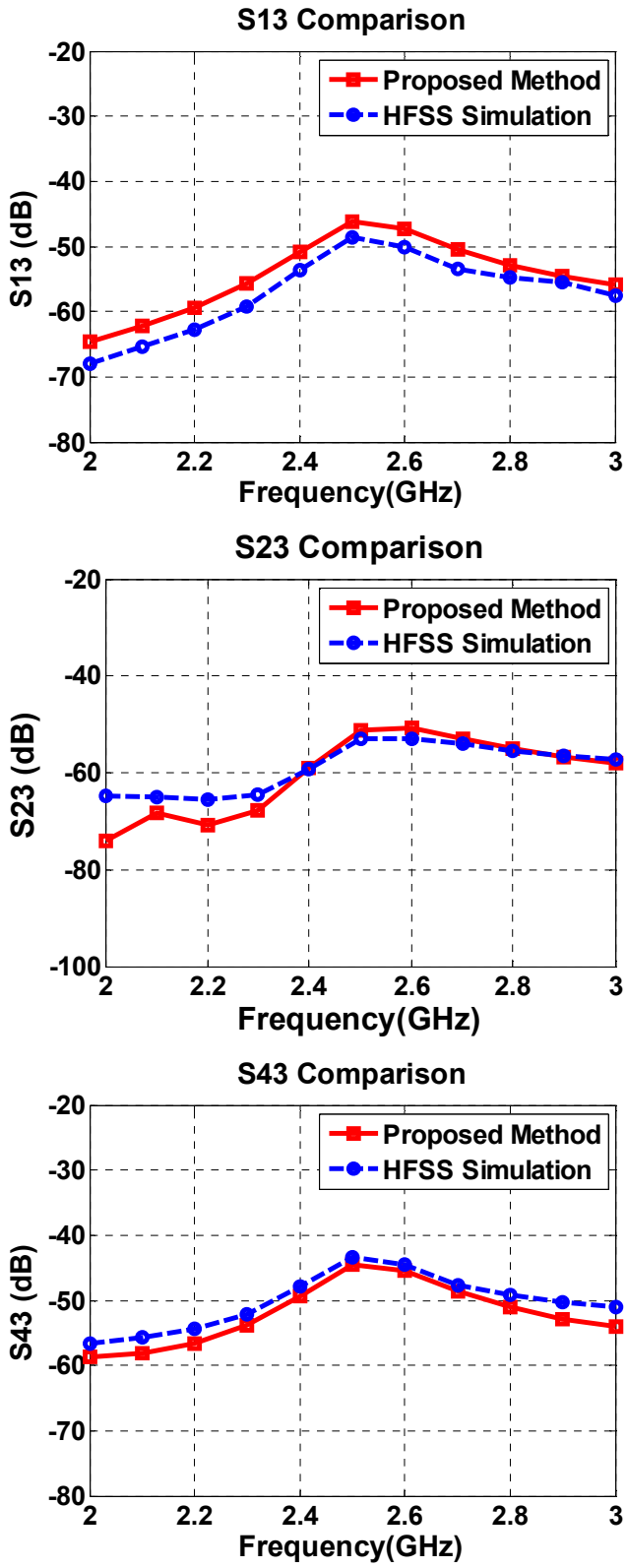

Fig. 8. Prediction of the scattering parameters between each antenna and the trace, compared to the direct HFSS simulation.

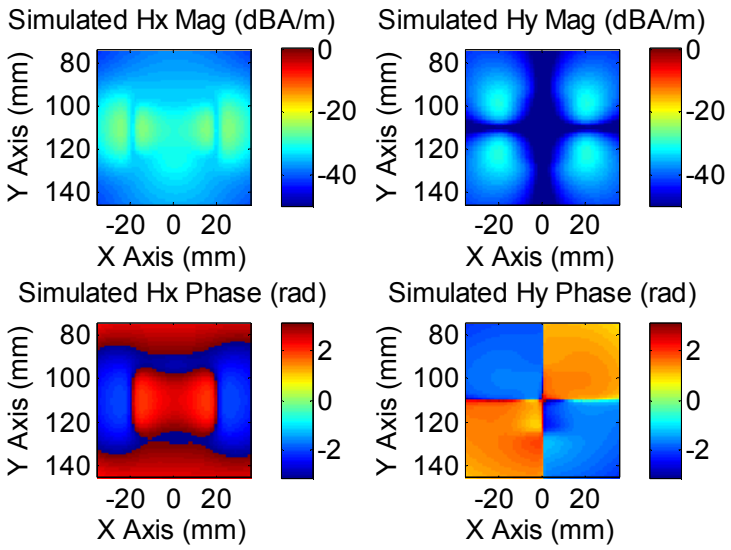

(a)

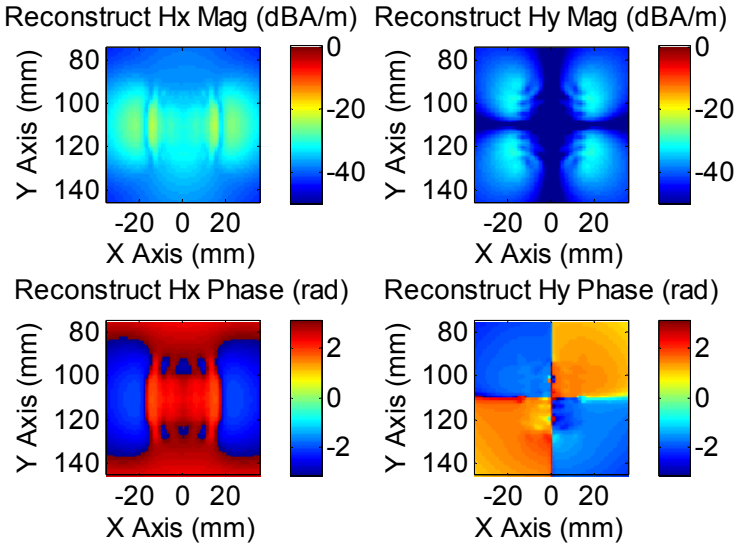

(b)

Fig. 9. Dipole-moment model reconstructed near-field pattern. (a) Simulated near fields of antenna 4. The near fields are used to extract dipole-moment model. (b) The reconstructed near-field pattern from the corresponding dipole moment model.

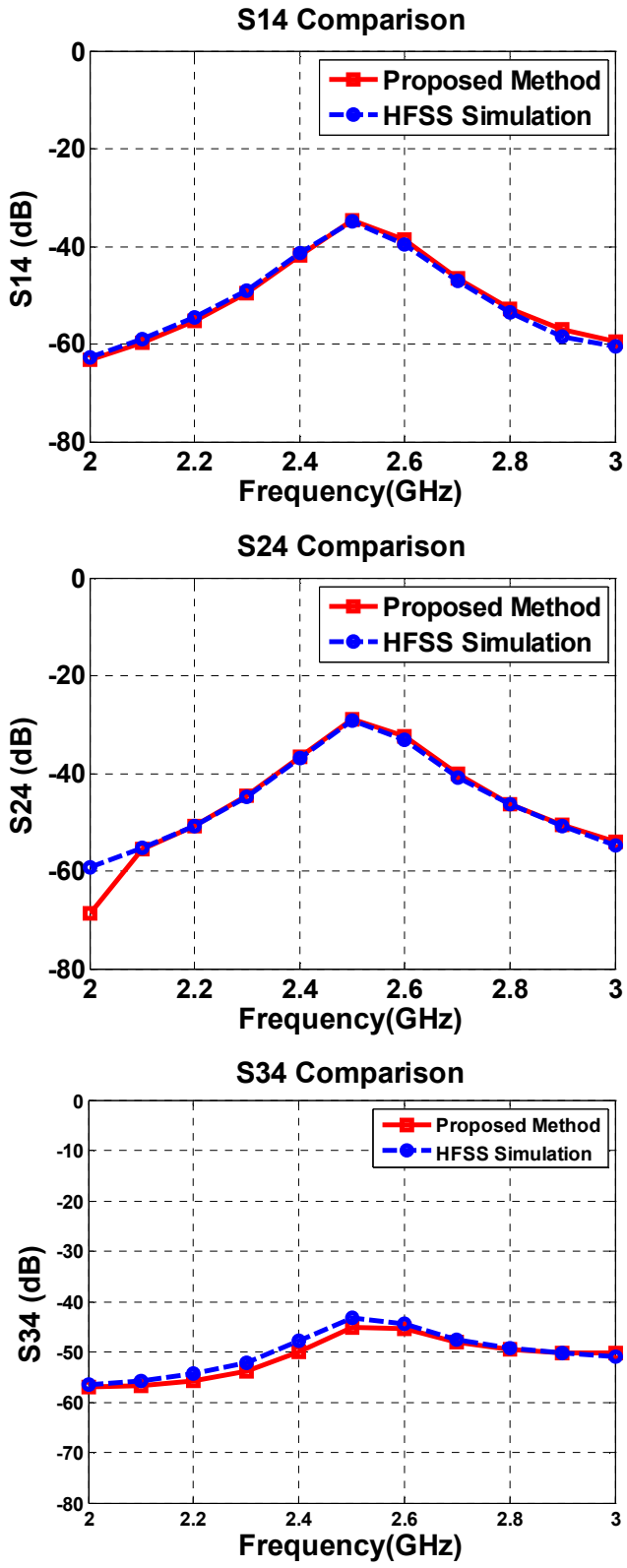

Fig. 10. Scattering parameters prediction of the other structures to antenna 4, compared to the direct simulation.

IV. MEASUREMENTS VALIDATION

A PCB board of the passive structures in Fig. 5 was also fabricated, as shown in Fig. 11. Similar to Section III, the shorted trace and one of the antennas were taken as the noise sources, respectively. Their tangential magnetic near fields were measured by the phase-resolved near-field scanning technique, reported in [13], to extract the dipole-moment model. The measurements instrument and its setup were described in Fig. 12.

In measurements, the sources (trace and one antenna) were excited by the signal from port 1 of the vector network analyzer (VNA). After defining the scanning area above the source, the probe moved from point to point. At each scanning point, the probing signal was amplified and received by port 2 of the VNA. Thus, the magnitudes of received S_{21} reflected the fields' magnitudes, as well as the S_{21} phase reflected the phase of the scanned fields. Given the probe factor by the method in [13], the real value of the scanned fields can be obtained by multiplying S_{21} by the probe factor at each frequency. Then, the dipole-moment model was extracted from the measured near fields as Section II. Finally, the coupling from the source to the other structures in measurement was studied by the proposed method.

A. Noise Source: Trace

Using the shorted trace as the noise source, the same near-field plane as Section III was set up. Fig. 13 displays the measured near-field pattern at 2.5 GHz as an example. The reconstructed pattern was from the same 8 × 8 dipole-moment arrays.

Considering the noise, imbalance of the probe and the inaccuracy of the probe calibration, the near-field pattern reconstruction from the real measurements was not as

good as the simulation. But the main distribution of the magnitudes and phases was restored.

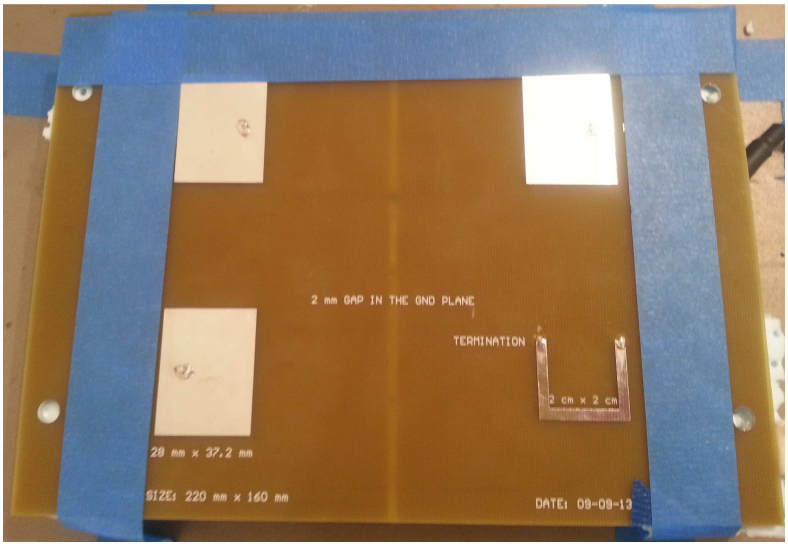

Fig. 11. Passive structures PCB board for the measurements validation.

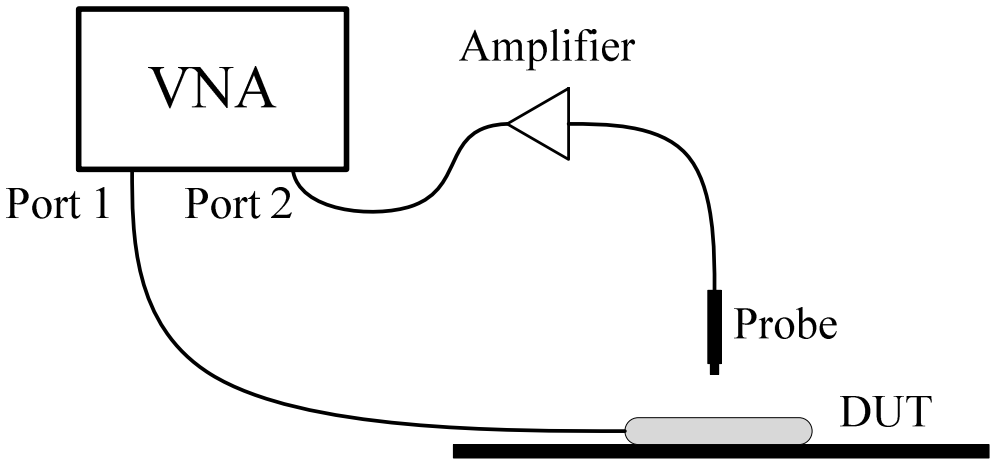

Fig. 12. Diagram of the phase-resolved near-field scanning measurement.

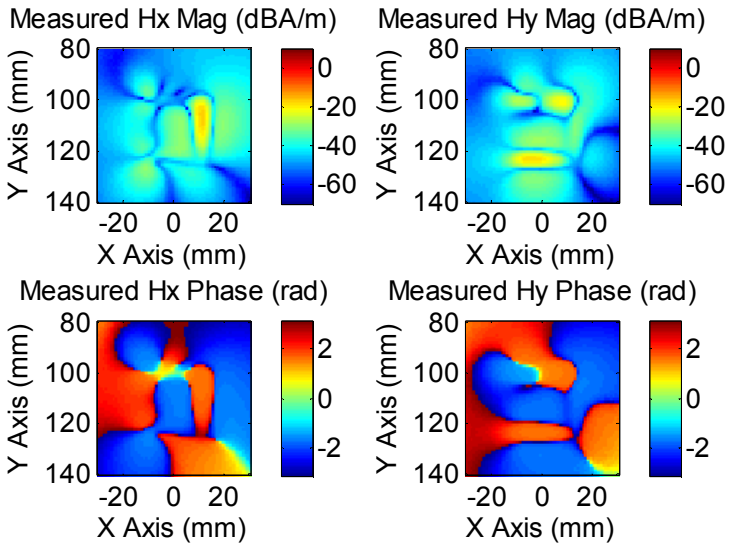

(a)

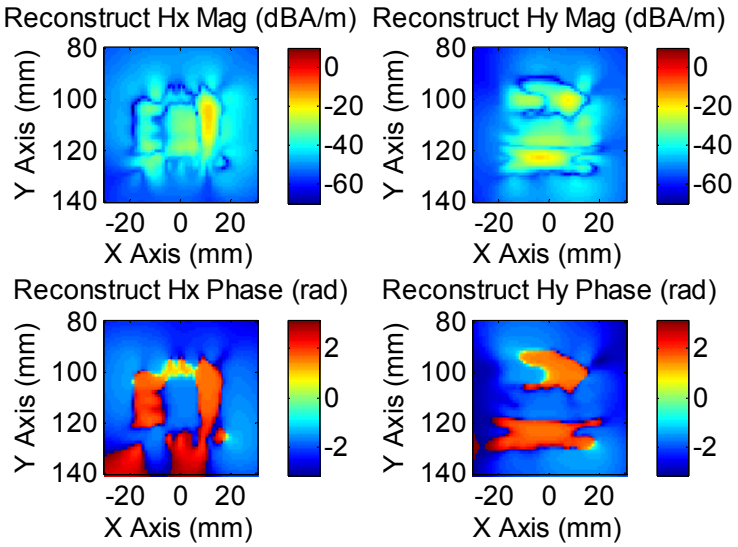

(b)

Fig. 13. Dipole-moment model reconstructed near-field pattern. (a) Measured near fields of the trace. The near fields are used to extract dipole-moment model. (b) The reconstructed near-field pattern from the corresponding dipole moment model.

Similar to Fig. 7, the Huygens's boxes were set up as 40 mm × 40 mm × 40 mm cubes enclosed a victim antenna. In "Forward Problem", the dipole-moment model calculated the tangential fields over the Huygens's box. And in "Reverse Problem", the

tangential fields over the Huygens's box were obtained by the simulation when exciting the corresponding antenna only. In Fig. 14, the proposed method gives the estimation of the scattering parameters and compares to the direct measurements by vector network analyzer (VAN). The agreement between the estimation and the measured scattering parameters indicates that the proposed method can closely predict the interference from the source to the antennas at different locations.

B. Noise Source: Antenna

Consistent with the simulation, the same near-field pattern of antenna 4 was measured and used to extract the dipole moment models. Fig. 15 shows the comparison between the measurements and the dipole reconstructed one.

Applying the same Huygens's box and getting the tangential magnetic fields on it in both "Forward Problem" and "Reverse Problem", the scattering parameters between the victim structures and antenna 4 were compared to the VNA measurements in Fig. 16. The results validated that the proposed method has very good RFI estimation.

V. APPLICATION AND DISCUSSION

The performance of the proposed method for RFI estimation was verified in the previous sections. With this method, the interference between the noise source and the victim antenna can be estimated in the early design stage. This method provides advantages for engineers to evaluate the location influence, the frequency effect and other issues in RFI problems before the product fabrication. With the dipole moment models, this method also works for complex noise sources. The model can be extracted from the measurements of the real source, instead of modeling the structure in a simulation tool.

This makes the RFI estimation possible for the real products. Furthermore, the concept of "RF Library" can be introduced by applying the proposed method. The dipole models for different noise sources can be extracted and saved in the "Source Library". Likewise, different kinds of antennas can also be modeled and simulated with a known excitation. The tangential fields on a defined Huygens's box can be obtained and saved in the "Antenna Library". Thus, engineers are able to play with different noise sources and different antennas from the "RF Library" in various locations to find out the best solution.

For the equivalent dipole-moment extraction algorithm, it was observed that the near-field pattern reconstructed from the simulation was usually better than the one reconstructed from the real measurements. Previous experience showed that the accuracy of the measured near fields was limited by the probe sensitivity, environment noise, probe calibration error, and other measurement errors. While the least square method is a simple and fast method to solve the inverse problem, its accuracy relates to how good the measurements are. For example, in both simulation and measurements, the coupling prediction between two antennas was always better than the one between the trance and antenna. The possible reason might include that the radiation from the trace was weaker than the antenna at the studied frequencies. As a result, the scanned near fields of the trace suffered more from the worse signal-to-noise ratio so that the solved dipole-moment model had more inaccuracy compared to taking antenna as the source. Another possible reason was the dipoles were placed as an 8×8 array for both cases. This distribution matched better for the patch antenna, the shape of which was also a rectangle. Thus, the approaches to improve the measurements will benefit the overall method.

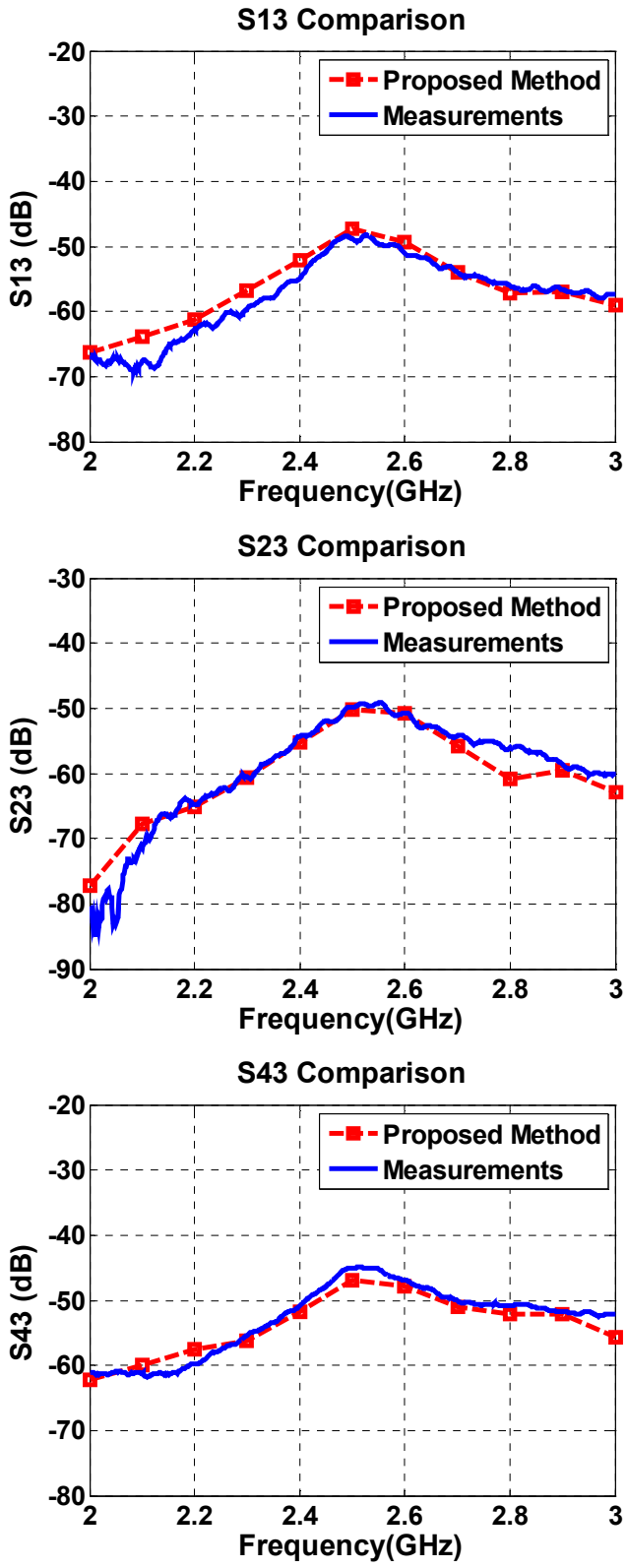

Fig. 14. Prediction of the scattering parameters between each antenna and the trace, compared to the direct VNA measurements.

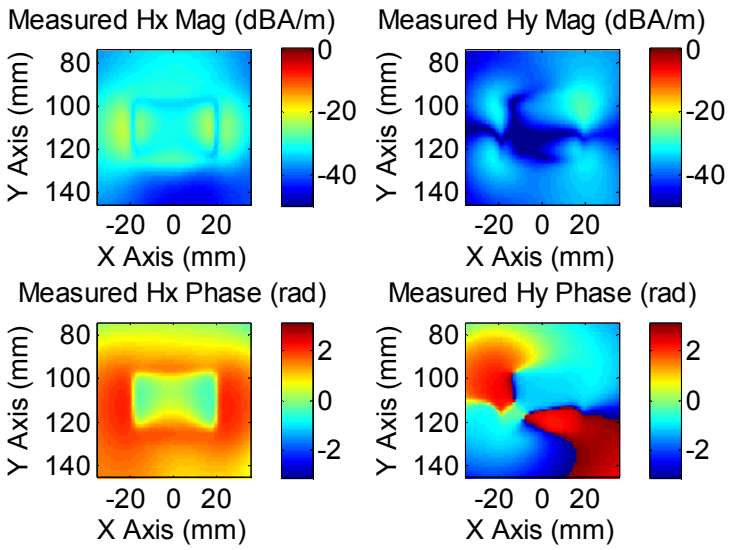

(a)

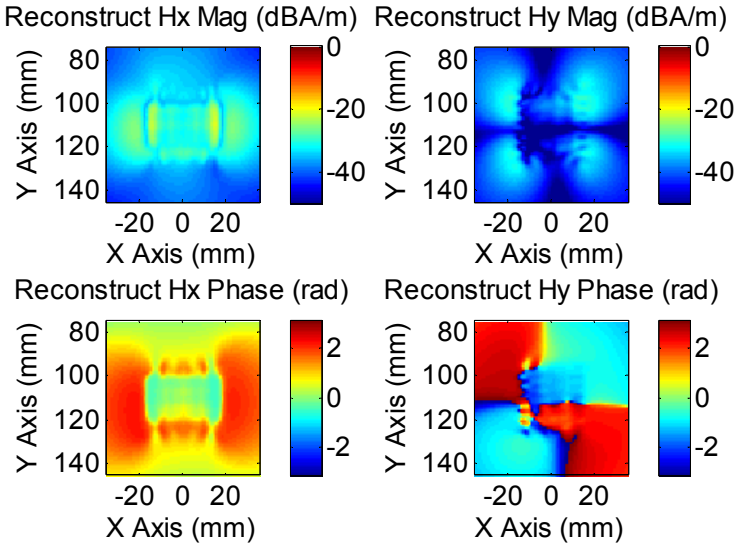

(b)

Fig. 15. Dipole-moment model reconstructed near-field pattern. (a) Measured near fields of antenna 4. The near fields are used to extract dipole-moment model. (b) The reconstructed near-field pattern from the corresponding dipole-moment model.

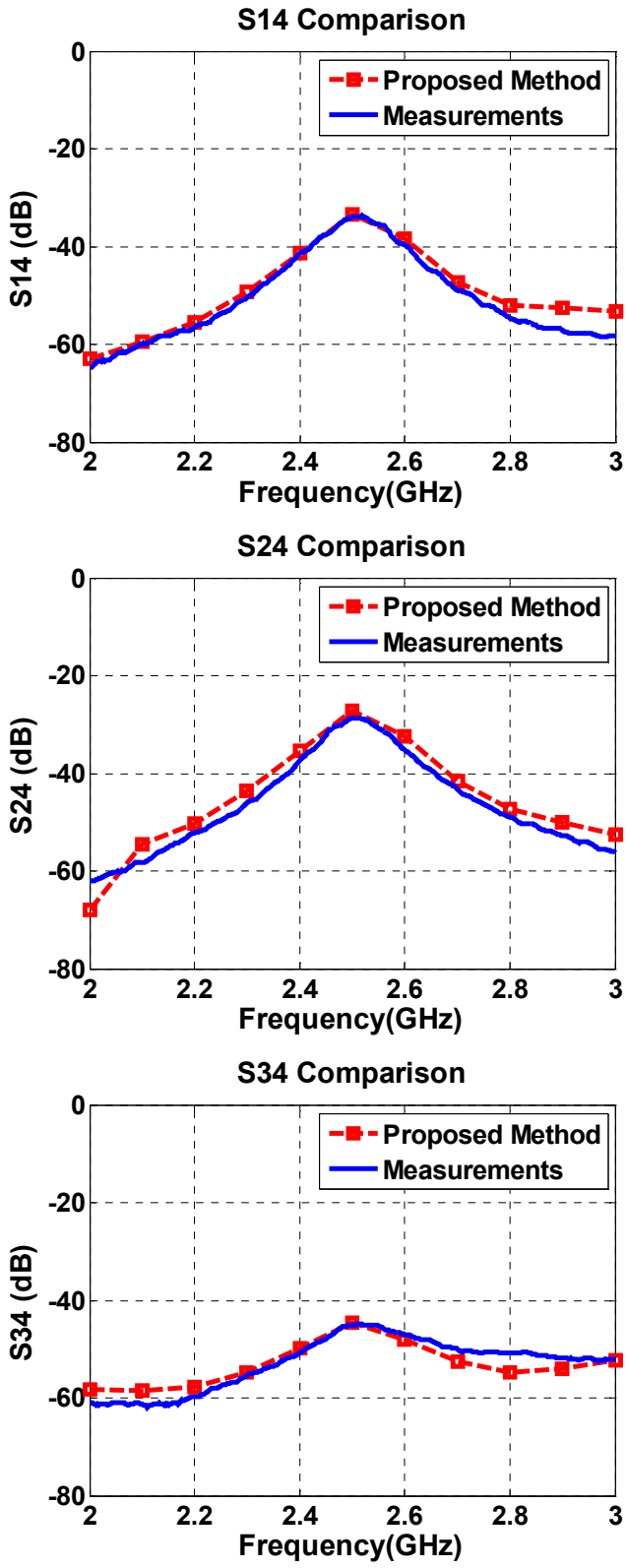

Fig. 16. Prediction of the scattering parameters between other structures and antenna 4, compared to the direct VNA measurements.

VI. CONCLUSIONS

This paper proposed an RFI estimation method by using equivalent dipole-moment models and the decomposition method based on reciprocity. This method allows engineers to model the complicated noise source, which may be very difficult to draw in the simulation tool, by dipole-moment models. By applying the decomposition method based on reciprocity, the RFI between the modeled source and the victim antenna can be reasonably estimated. With this method, the interference for any locations of the source and the victim antenna can be calculated fast in MATLAB, instead of the time-consuming simulation of the whole structure. Thus, engineers would be able to efficiently assess RFI issues of the product in the early design stage. The proposed method has been validated by a PCB example numerically and experimentally for the first time.

REFERENCES

[1] K. Slattery and H. Skinner, *Platform Interference in Wireless Systems: Models, Measurement, and Mitigation.* Burlington, MA, USA: Newnes, 2008, pp. 5-6.

[2] H. Wang, V. Khilkevich, Y. Zhang and J. Fan, "Estimating radio-frequency interference to an antenna due to near-field Coupling using decomposition method based on reciprocity", *IEEE Trans. Electromagn. Compat*., vol. 55, no. 6, pp. 1125-1131, Dec. 2013.

[3] T.K. Sarkar and A. Taaghol, "Near-field to near/far-field transformation for arbitrary near-field geometry utilizing an equivalent electric current and MoM", *IEEE Trans. Electromagn. Compat*., vol. 47, no.3, pp. 566-573, Mar. 1999.

[4] A. Taaghol and T.K. Sarkar, "Near-field to near/far-field transformation for arbitrary near-field geometry, utilizing an equivalent magnetic current", *IEEE Trans. Electromagn. Compat*., vol. 38, no. 3, pp. 536-542, Aug. 1996.

[5] Y. Vives, C. Arcambal, A. Louis, F. de Daran, P. Eudeline, and B. Mazari, "Modeling magnetic radiations of electronic circuits using near-field scanning method", *IEEE Trans. Electromagn. Compat*., vol. 49, no. 2, pp. 391-400, May. 2007.

[6] D. Baudry, C. Arcambal, A. Louis, B. Mazari, and P. Eudeline, "Applications of the near-field techniques in EMC investigations", *IEEE Trans. Electromagn. Compat*., vol. 49, no. 4, pp. 805-815, Nov. 2007.

[7] J. Pan, L. Li, X. Gao, and J. Fan, "Application of dipole-moment model in EMI estimation", *IEEE International Symposium on Electromagnetic Compatibility and EMC Europe*, 2015, accepted.

[8] L. Li, J. Pan, C. Hwang, G. Cho, H. Park, Y. Zhang and J. Fan, "Near-field coupling estimation by source reconstruction and Huygens's equivalence principle", in *Proc*. *IEEE International Symposium on Electromagnetic Compatibility.,* Santa Clara, CA, pp. 324-329. Mar. 2015.

[9] P. Fernandez Lopez, C. Arcambal, D. Baudry, S. Verdeyme, and B. Mazari, "Simple electromagnetic modeling procedure: From near-field measurements to commercial electromagnetic simulation tool", *IEEE Trans. Instrum. Meas*., vol. 59, no. 12, Dec. 2010.

[10] D. Baudry, C. Arcambal, A. Louis, B. Mazari, and P. Eudeline, "Applications of the near-field techniques in EMC investigations", *IEEE Trans. Electromagn. Compat*., vol. 49, no. 4, pp. 805-815, Nov. 2007.

[11] P. Wilson, "On correlating TEM cell and OATS emission measurements", *IEEE Trans. Electromagn. Compat.,* vol. 37, no. 1, pp. 1-16, Feb. 1995.

[12] M. Burger and J. Repisky, "Problems of linear least square regression and approaches to handle them", *The 1st Virtual International Conference on Advanced Research in Scientific Areas*, pp. 3-7, Dec. 2012.

[13] J. H. Richmond, "A reaction theorem and its applications to antenna impedance calculations", *IRE Trans. Antennas Propag*., vol. 9, no. 6, pp. 515-520, Nov. 1961.

[14] J. Zhang, K. Keong, M. Jin, V. Khilkevich, D. Pommerenke and J. Fan, "An effective method of probe calibration in phase-resolved near-field scanning for EMI application", *IEEE Trans. Instrum. Meas*., vol. 62, no. 3, pp. 648-658, Mar. 2013.

III. IDENTIFY THE INTERFERENCE FROM MULTIPLE NOISE SOURCES BY MAGNETIC NEAR FIELDS ONLY

Jingnan Pan, Xu Gao, Jun Fan, *Senior Member, IEEE*,
Electrical Engineering
Missouri University of Science and Technology, Missouri, U. S. A. 65409
Email: jpfz6@mst.edu, jfan@mst.edu

Abstract

As electronic products are becoming more and more complicated, the radio frequency (RF) receiver in a system is very likely to be interfered by multiple noise sources simultaneously. This paper proposes a method to identify the interference from different noise sources separately, even when they are radiating at the same time. This method converts magnetic fields to electric fields by finite element method (FEM) and employs the decomposition method based on reciprocity. In the proposed method, firstly, a Huygens's surface will be set up for each source. The tangential magnetic near fields on each Huygens's surface are used to solve tangential electric fields correspondingly by FEM. Then, the sources are removed, but their Huygens's surfaces are kept. The victim structure is excited in this case to get the tangential magnetic fields on the Huygens's surfaces. A creative FEM processing procedure is applied to obtain tangential electric fields in this situation. Finally, with these two groups of the fields, the interference from each noise source can be estimated separately based on reciprocity theory. This method is validated by a numerical example. It is very helpful for engineers to identify the contribution of the coupling from different sources and further solve the electromagnetic interference issues efficiently.

Index Terms

Electromagnetic interference, Finite element method, Reciprocity theory

I. INTRODUCTION

Most electronic systems have radio frequency interference (RFI) problems. The most common sources include components such as switching power supplies, repays, high-speed I/O traces and processing components. As the size of the overall size of the products is decreasing year by year, the RFI issue is becoming increasingly considerable. However, usually in one system, the radiation source is not unique. It is likely several sources radiating simultaneously, and all of them will contribute some coupling to the victim structure. In this situation, how to identify the corresponding contribution of the interference from each source is critical. It helps engineers to find out the dominant radiator easily and quickly so that the action to overcome the RFI issues can be completed efficiently.

In the early days, engineers identified the EM noise source mainly based on their experience or by using a spectrum analyzer to differentiate their operating frequencies. Since a decade ago, artificial neural networks (ANN) have also been widely applied to identify electromagnetic (EM) radiated noise source types based on their different frequencies [1]-[3]. In [1], the authors utilized a multilayer perception architecture neural network to identify different types of the source devices. The shielding effectiveness of an enclosure was also investigated by ANN method in [2], and in [3], the authors further evaluated the direction of arrival based on phase difference. However, all of the above applications cannot handle the sources radiating at the same or close frequency. Due to in modern electronic products, different sources often have overlapped radiation frequencies. A method to discriminate the interference from different sources as the same frequency is in great request.

Paper [4] proposed a decomposition method based on reciprocity and got good estimation results in some numerical cases. In paper [5], this method was further developed and well predicted the coupling from one source to victim antenna in different locations so as to evaluate the placement of the victim. The essential approach of this method is the tangential fields on the Huygens's surface which covered victim antenna in "Forward Problem" and "Reverse Problem" of [4]. In this paper, these Huygens's surfaces are proposed to move to the locations of the sources. By doing this, the fundamental theory still works and the coupling from different sources to the same antenna can be obtained. It not only makes it possible to discriminate the coupling contribution from each source at the same frequency, but also overcomes the difficulty when the setup of the antenna is not suitable to place the Huygens's surface.

Moreover, as paper [6] has discussed, for the radiator located close to the ground plane of printed circuit board (PCB), its five-faced Huygens's surface can be further simplified as the top plane and four side lines. This paper uses this simplified Huygens's surface instead of the ones in [4]. They make the near-field scanning to be implemented as close as possible to the specific radiator, so that the radiation from other sources will not be involved. Also, as the simplified Huygens's surface is smaller than the five-faced one, the scanning procedure is less likely to be interrupted by the nearby structures in the complex system. Based on the analysis in [6], the vertical components on the side lines can be neglected so that all the measurements can be finished by one probe and the measurements' consistency is also kept.

Another contribution of this paper is using magnetic fields only in the measurements. The corresponding electric fields will be converted from scanned

magnetic fields by the finite element method (FEM). The conversion procedure was first introduced in [7]. Then paper [8] improved this procedure to make it usable for the "Forward Problem" in the decomposition method of [5]. In this paper, a novel and creative FEM processing procedure is proposed for the first time to solve the electric fields from the magnetic fields in the "Reverse Problem" of [5]. Thus, the decomposition method can be fulfilled by only the magnetic fields from measurements. This approach prevents using an electric probe, which usually performed worse in accuracy compared to magnetic probe, and also saved half of the scanning time and the cost of related resources.

In sum, this paper employs the decomposition method based on reciprocity to identify the interference contribution from different sources at their overlapped frequencies. Compared to the methods in [1]-[3] and [9], the proposed method is more practical for intersystem sources in complex products. Also by using simplified Huygens's surface and conversion of electric fields from magnetic fields, time and cost of the measurements are saved while accuracy increases.

II. DECOMPOSITION METHOD WITH HUYGENS'S SURFACE ON THE SOURCE

In this section, the decomposition method based on reciprocity will be explained. As in modern complex electronic products, sometimes it is more difficult to set the Huygens's surface above the victim antenna. In this situation, the Huygens's surface is set up above the radiation source. The validation of this method is also given in Part B of this section.

A. Methodology

As described in [4] and [5], the decomposition method has three steps, "Forward Problem", "Reverse Problem", and "Interference Estimation", to estimate the coupling from the radiation source to the victim antenna. Choosing the Huygens's surface on the radiation source, the method is illustrated in Fig. 1.

One typical RFI problem is described in Fig. 1(a); the radiation source and the victim antenna are located on the ground of the printed circuit board (PCB). When the radiation source is excited, its radiation will be coupled to the nearby victim antenna.

In "Forward Problem" shown in Fig. 1(b), a Huygens's surface is set up to enclose the radiation source. This Huygens's surface can be divided into many cells on which the tangential electromagnetic fields are denoted as E_c^{fwd} and H_c^{fwd}. The coupling induces electromagnetic fields on the port of victim antenna, which is in receiving mode, named as E_d^{fwd}, H_d^{fwd}.

In "Reverse Problem" shown in Fig. 1(c), the source is removed and the victim antenna is excited with a known voltage, U_a^{rev}. The tangential electromagnetic induced by this excitation on the antenna port are E_a^{rev} and H_a^{rev}. Thus, the tangential fields on the same Huygens's surface with "Forward Problem" are from the radiation of the victim antenna. They are recorded as E_c^{rev} and H_c^{rev}.

Furthermore, similar with [6], when the five-faced Huygens's surface is very close to the PCB ground, the four side walls can be simplified as four side lines and the vertical components of magnetic fields. Horizontal components of electric fields can be neglected.

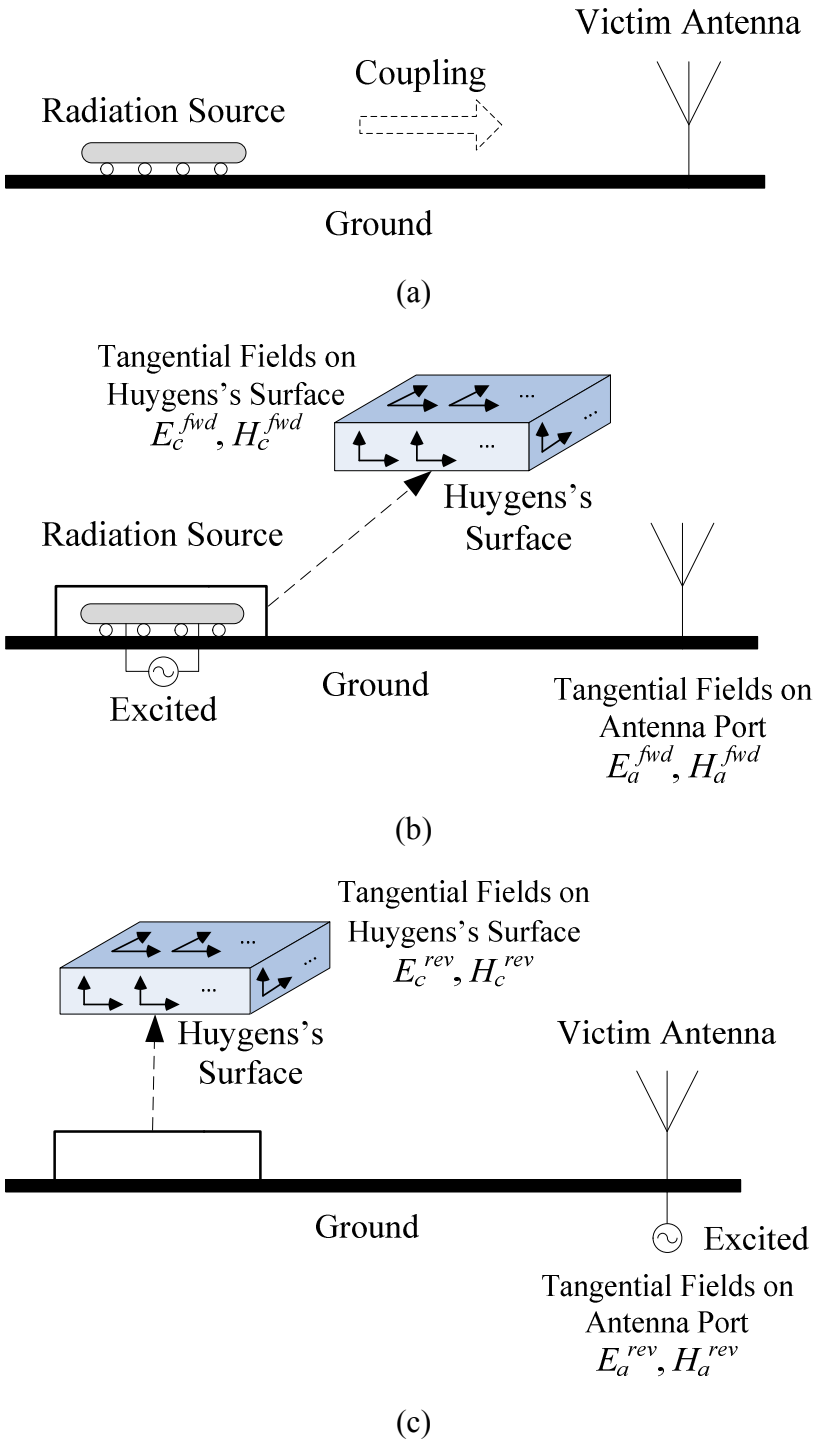

Fig. 1. Decomposition method based on reciprocity: (a) Original RFI problem; (b) "Forward Problem"; (c) "Reverse Problem".

Based on reciprocity theorem, the electric current J and magnetic current and M in "Forward Problem" and "Reverse Problem" satisfy:

$$\begin{aligned}&\int_V \left(E_c^{rev}\cdot J_c^{fwd} - H_c^{rev}\cdot M_c^{fwd}\right)dv \\ &\qquad = \int_V \left(E_a^{fwd}\cdot J_a^{rev} - H_a^{fwd}\cdot M_a^{rev}\right)dv\end{aligned} \tag{1}$$

where "fwd" and "rev" denote the problem type, the subscript "c" means the corresponding fields or currents located on the Huygens's box, and similarly, "a" means the antenna port.

The current sources J_c^{fwd} and M_c^{fwd} are equivalent sources resulting from the tangential electromagnetic fields on the Huygens's surface, which can be replaced by the tangential fields on the box. On the other hand, following the procedure in [10], the two terms on the right side of (1) can be expressed by the current and voltage on the antenna port. Thus, (1) becomes:

$$\begin{aligned}&\sum_{cells}\hat{n}\times H_c^{fwd}\cdot E_c^{rev}S_{cell} + \sum_{cells}\hat{n}\times E_c^{fwd}\cdot H_c^{rev}S_{cell} \\ &= -I_a^{rev}U_a^{fwd} - I_a^{fwd}U_a^{rev} = -\left(\frac{1}{Z_{in}}+\frac{1}{Z_L}\right)U_a^{fwd}U_a^{rev}\end{aligned} \tag{2}$$

where the Huygens's surface and equally meshed into small square cells with the area of S_{cell}; Z_{in} is the input impedance of the antenna and Z_L is the load impedance at the antenna port in "Forward Problem", 50 Ω in common usage; U_a^{rev} is the exciting voltage of antenna in "Reverse Problem".

By solving (2), the coupling voltage is obtained in (3).

$$\begin{aligned}U_a^{fwd} &= -\frac{Z_{in}Z_L}{U_a^{rev}\left(Z_{in}+Z_L\right)}\times \\ &\left(\sum_{cells}\hat{n}\times H_c^{fwd}\cdot E_c^{rev}S_{cell} + \sum_{cells}\hat{n}\times E_c^{fwd}\cdot H_c^{rev}S_{cell}\right)\end{aligned} \tag{3}$$

B. Validation

To validate the decomposition method based on reciprocity, one simple passive structure is taken as an example in Fig. 2.

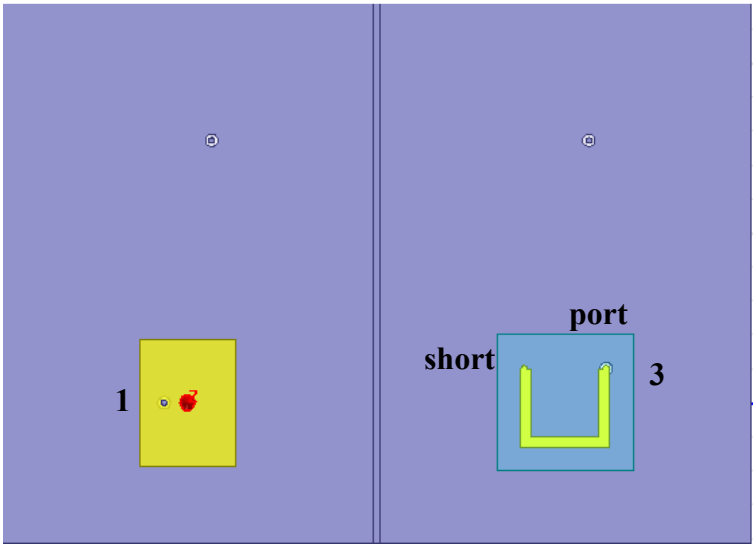

Fig. 2. Passive structure model in HFSS for validation. 1 is the victim antenna; 3 is the radiation source.

Structure 1 is a patch antenna working at 2.5GHz as well as a curved 50 Ω trace, structure 3, plays the role of radiation source. The trace is shorted at one end and excited at the other one. The Huygens's surface is the blue box above the trace. It is a 40mm by 40mm box with a height of 5mm. Four lines just below the edges of the top plane with a height of 3mm are taken as the side lines of the Huygens's surface. Applying the decomposition method based on reciprocity, the S-parameter between the victim antenna and the source could be estimated. The results are compared with direct simulation in HFSS in Fig. 3.

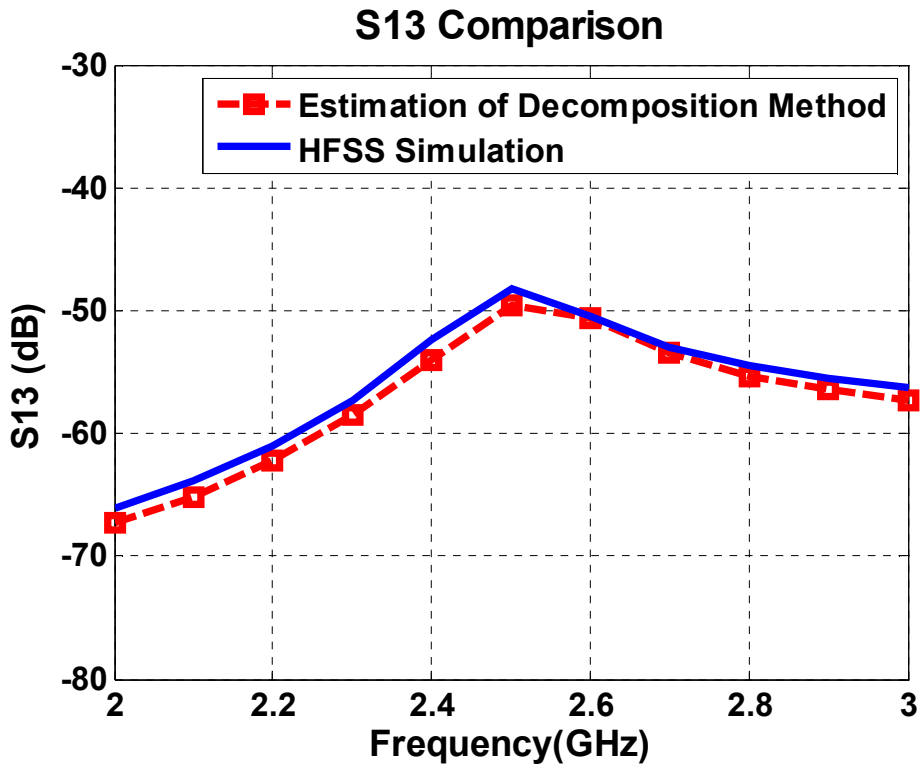

Fig. 3. Estimation of the S parameters between the victim antenna and the radiation source, compared to direct simulation in HFSS.

The good agreement of the comparison validates that the decomposition method based on reciprocity can well predict the interference between the victim antenna and the noise source.

III. H FIELDS TO E FIELDS CONVERSION IN FORWARD PROBLEM

In Section II, the procedure of how to estimate the interference between the radiation source and the victim antenna by decomposition method is demonstrated. In both "Forward Problem" and "Reverse Problem", the tangential electromagnetic fields are employed to do the calculation. However, in practical applications, electric fields probe is much more difficult to design and calibrate. It is very propitious to obtain the E

fields from the measured H fields instead of directly measuring E fields. This section will introduce a method to convert H fields to E fields in "Forward Problem" by the Huygens's principle and the finite element method (FEM).

A. Methodology

In "Forward Problem", the tangential electromagnetic fields on the Huygens's surface are from the radiation source inside the surface. Thus, some specific boundaries are set up based on Huygens's principle [11] and the FEM processing is applied to solve E fields from H fields as in [8]. This procedure is illustrated in Fig. 4.

The original situation in "Forward Problem" is described in Fig. 4(a). The ground plane of PCB is assumed as PEC boundary. Based on Huygens's principle, the fields outside Huygens's surface S_1 can be reproduced by the equivalent current sources converted from the tangential electromagnetic fields on S_1. By filling PMC boundary inside S_1, all the radiation outside is coming from the equivalent electric current sources (J in Fig. 4(b)) [8]. Therefore, the E fields on S_1 can be solved by the FEM processing set up in Fig. 4(b). The absorbing boundary condition (ABC) is applied on the five-faced box S_2, which is located proper distance away from the Huygens's surface. Meshing the area between S_2 and S_1, the electric fields everywhere in the mesh space can be calculated by equation (4).

$$\nabla \times \left(\frac{1}{\mu_r} \nabla \times \overline{E} \right) - k_0^2 \varepsilon_r \overline{E} = -jk_0 Z_0 \overline{J} \tag{4}$$

Equation (4) is derived from Maxwell functions and can be used to solve the electric fields everywhere with the knowledge of the electric currents, which are converted from the tangential magnetic fields on the Huygens's surface.

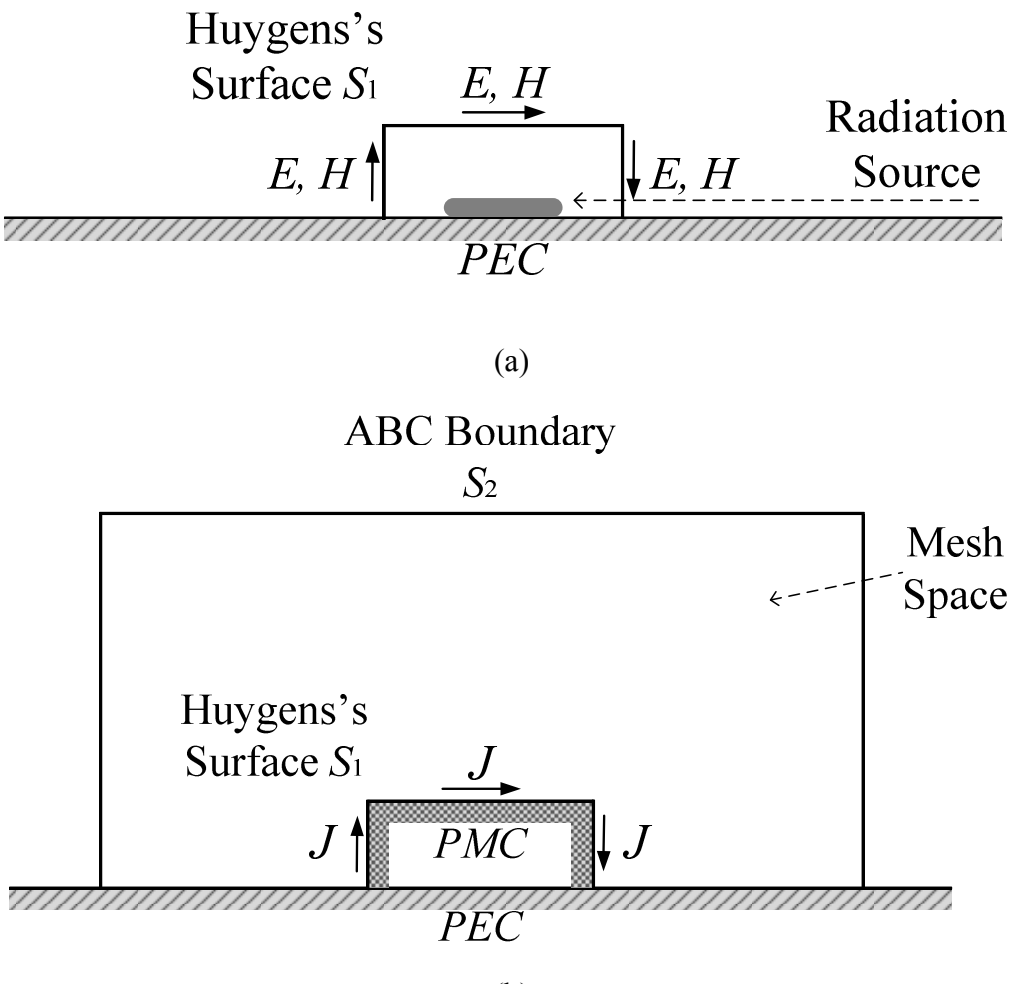

Fig. 4. Convert H fields to E fields in "Forward Problem": (a) Original situation; (b) FEM processing to solve the E fields by the equivalent electric current sources from H fields.

Consequently, the tangential electromagnetic fields, E_t^{fwd} and H_t^{fwd}, on the Huygens's surface in "Forward Problem" are obtained. This approach prevents using problematic electric probes to improve the accuracy of the measurements.

B. Validation

A dipole is taken as the radiation source inside the Huygens's surface in this part to validate the above-mentioned H fields to E fields conversion method. Its full-wave model in HFSS is plotted in Fig. 5.

An electric dipole directing to z-axis is located in the center of Huygens's surface with the size of 60 mm × 60 mm × 60 mm. The bottom of the Huygens's surface is an infinitely large PEC boundary. The excitation of the dipole is 1 μA·m at 1GHz. The solved electric fields by the method in Part A are compared to the simulation on the top plane of the Huygens's surface in Fig. 6.

From Fig. 6, it is observed that although the E fields converted from H fields has suffered a little bit by the numerical error on the Huygens's surface, the average fields distribution and strength are still reconstructed by the proposed method.

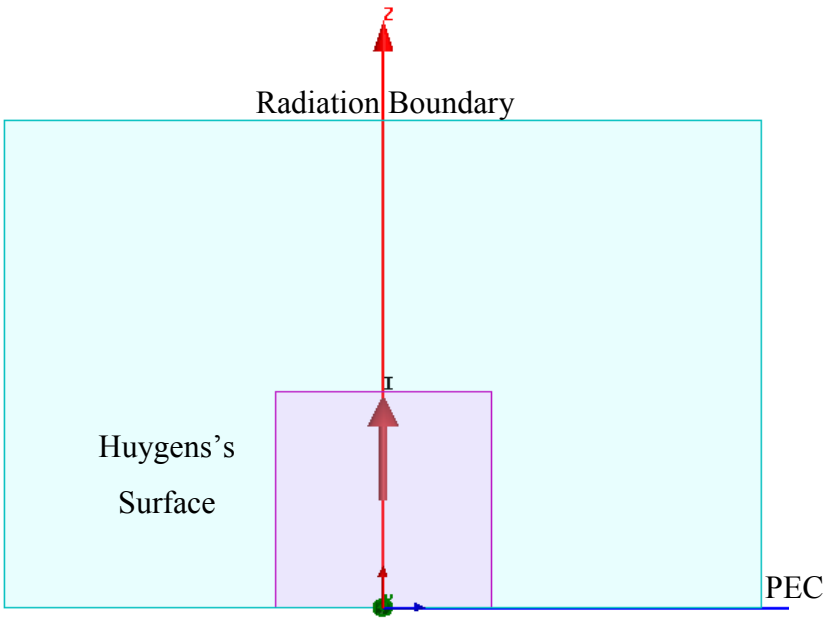

Fig. 5. HFSS model of one dipole to validate the H fields to E fields conversion method in "Forward Problem".

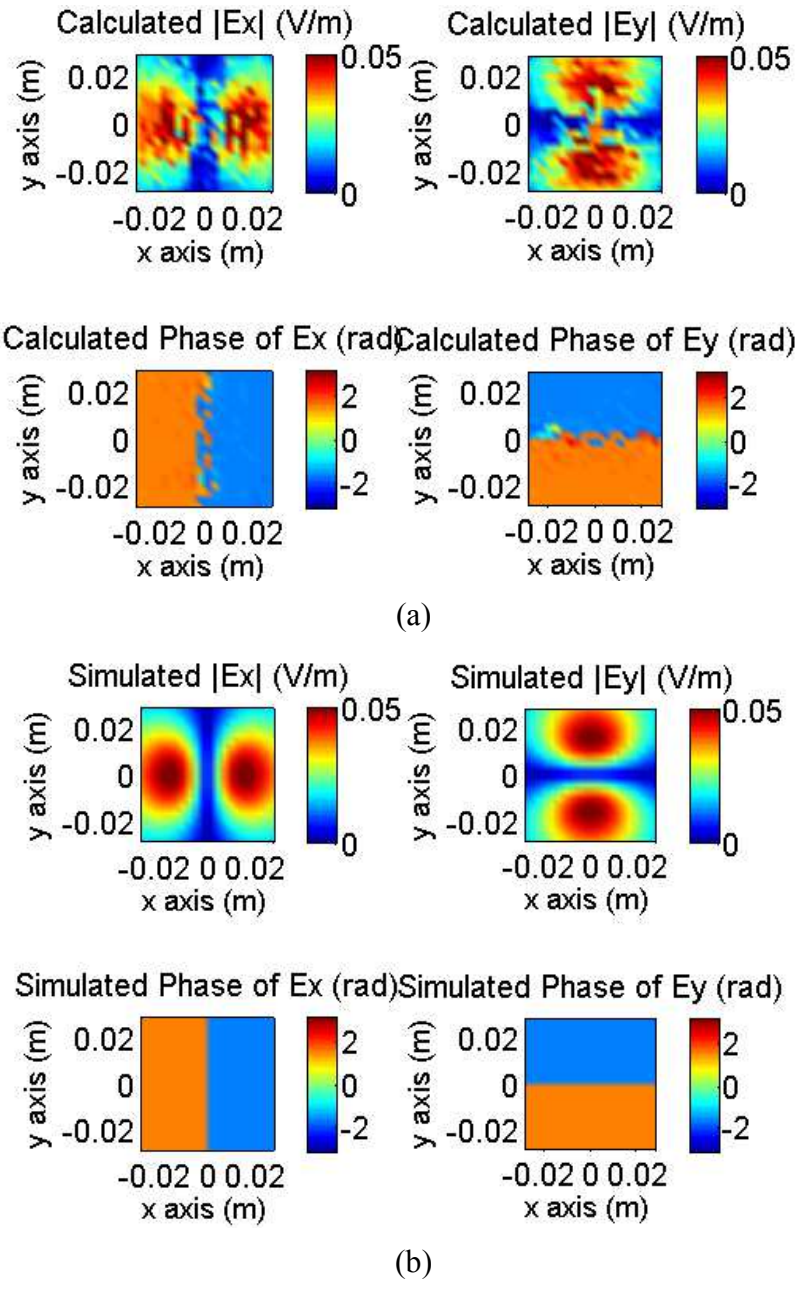

Fig. 6. E fields comparison on the top plane of the Huygens's surface in "Forward Problem": (a) E fields converted from H fields by proposed method; (b) Simulated E fields.

IV. H FIELDS TO E FIELDS CONVERSION IN REVERSE PROBLEM

On the other hand, in "Reverse Problem", electric fields are also preferred to be solved from the measured magnetic fields. However, different with "Forward Problem", the excited source is the victim antenna, located outside the Huygens's surface in this case. For this situation, an innovative FEM processing procedure is proposed to fulfill H fields to E fields conversion in this section.

A. Methodology

As described in Fig. 7(a), the radiation source is removed and the victim antenna is excited by a known voltage. Under this circumstance, the electromagnetic fields on the same Huygens's surface with the "Forward Problem" are all from the radiation of the victim antenna. Then filling PMC boundary on and outside the Huygens's surface, the fields inside it can be reproduced by the equivalent electric current sources, converted from magnetic fields, on the surface. It is a similar FEM procedure but uses the interior of the Huygens's box as the mesh and calculation region, shown in Fig. 7(b). The region for FEM processing has five faces of PMC boundary and one face of PEC boundary so that the fields in it can be solved by (4). Thus, E_c^{rev} on the Huygens's surface are obtained from the measured H_c^{rev} in the "Reverse Problem".

B. Validation

The validation of H fields to E fields conversion in "Reverse Problem" also uses a 1 μA·m electric dipole at 1GHz. However, this time, the dipole is outside the Huygens's surface, drawn in Fig. 8. The distance between the dipole and the center of the 60 mm side-length box is 60 mm. The simulated magnetic fields on the Huygens's surface are

exported, and the proposed method is applied to get the electric fields on it. The solved electric fields are compared to the simulated fields in Fig. 9.

The comparison in Fig. 9 indicates similar results with Section III. The H fields to E fields conversion method for "Reverse Problem" also has good performance to solve the electric fields. Both the pattern and the strength are well predicted.

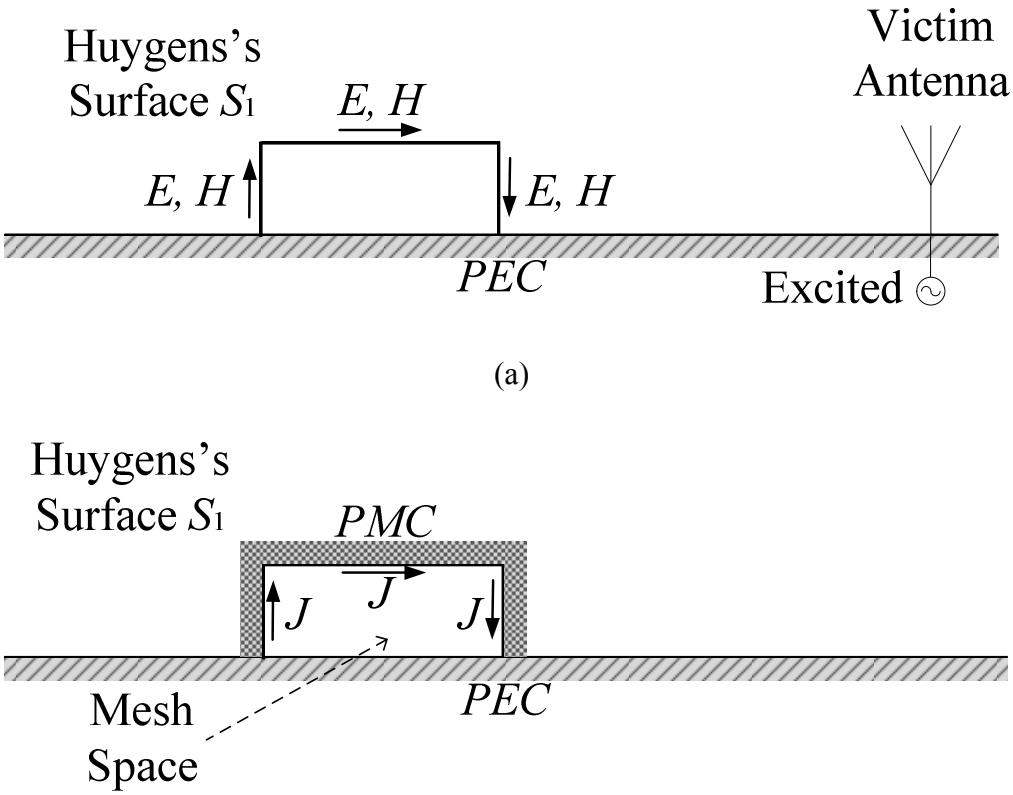

Fig. 7. Convert H fields to E fields in "Reverse Problem": (a) Original situation; (b) FEM processing to solve the E fields by the equivalent electric current sources from H fields.

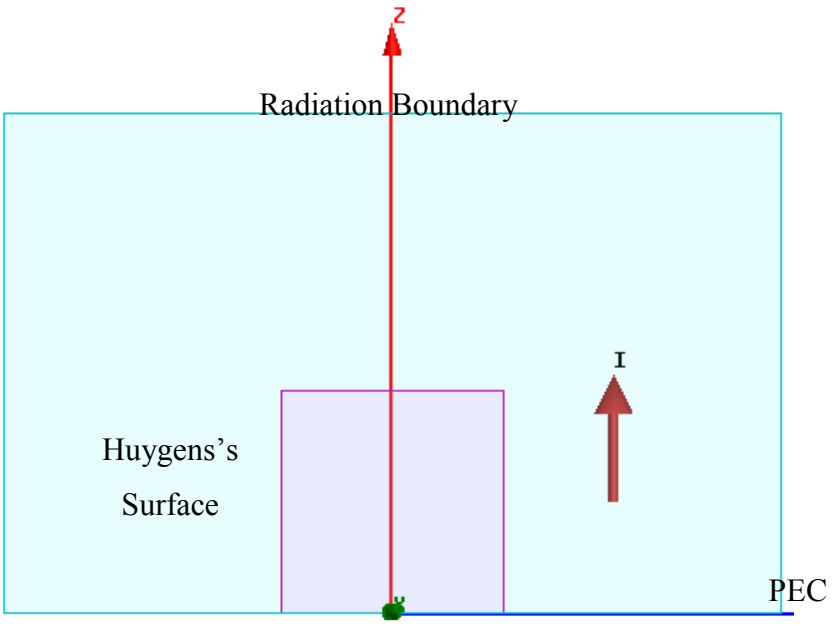

Fig. 8. HFSS model of one dipole to validate the H fields to E fields conversion method in "Reverse Problem".

V. IDENTIFY MULTIPLE NOISE SOURCES

Previous sections have illustrated three algorithms: decomposition method based on reciprocity shows how to predict the interference between the radiation source and the victim antenna; and in both "Forward Problem" and "Reverse Problem", the electric fields on Huygens's surface can be obtained from magnetic fields, which are more accurate in measurement. Combining the three methods above, the interference can be estimated by the magnetic fields only.

Furthermore, in the situation of multiple sources, it is likely that at the very close region of each source, the radiation is mainly from this specific source itself. Thus, although the radiation from multiple sources cannot be distinguished from each other at the victim antenna, the radiation at the close region to the source are non-interfering.

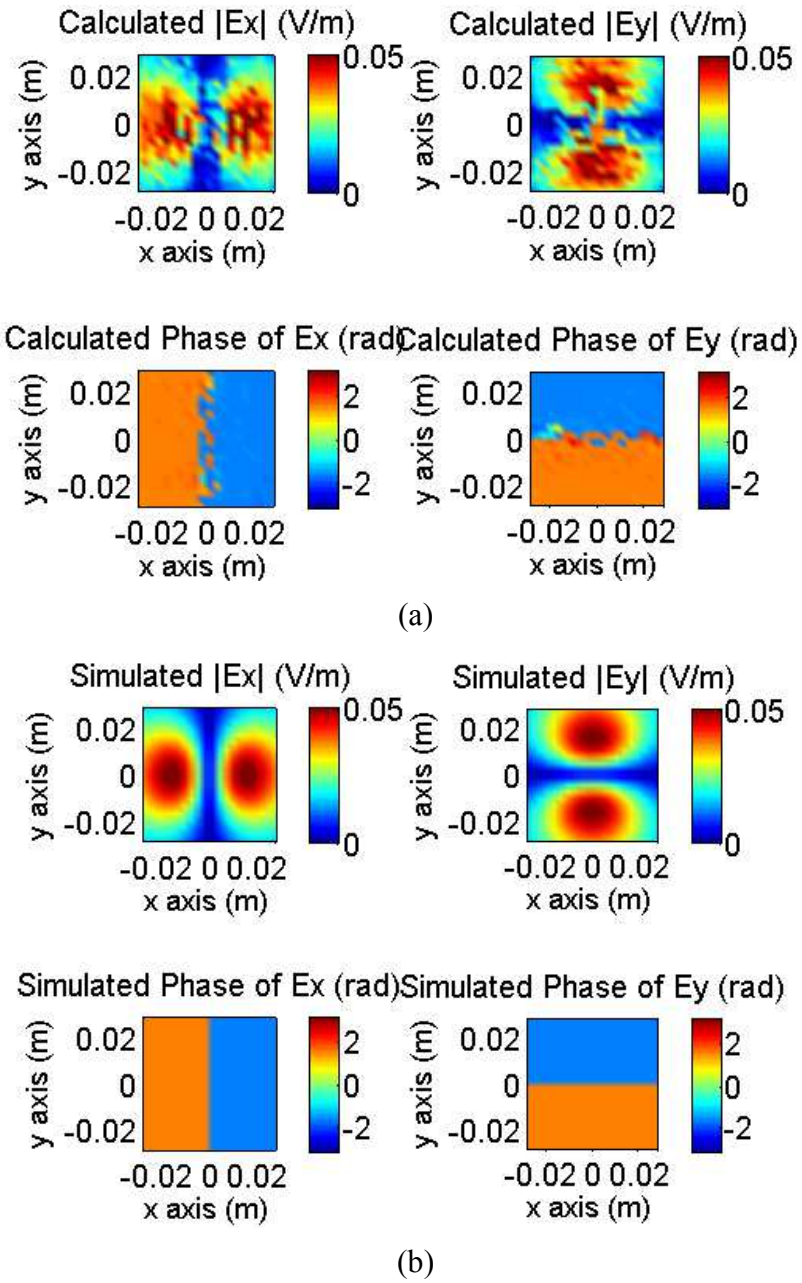

Fig. 9. E fields comparison on the top plane of the Huygens's surface in "Reverse Problem": (a) E fields converted from H fields by proposed method; (b) Simulated E fields.

Hence, when the Huygens's surface is set above one radiation source, the decomposition method could give the interference from this specific source, having nothing to do with any other one. By calculating the interference using different

Huygens's surface on different sources, the interference contribution from different sources are identified.

The diagrams for identifying the interference from different sources are plotted in Fig. 10 and Fig. 11.

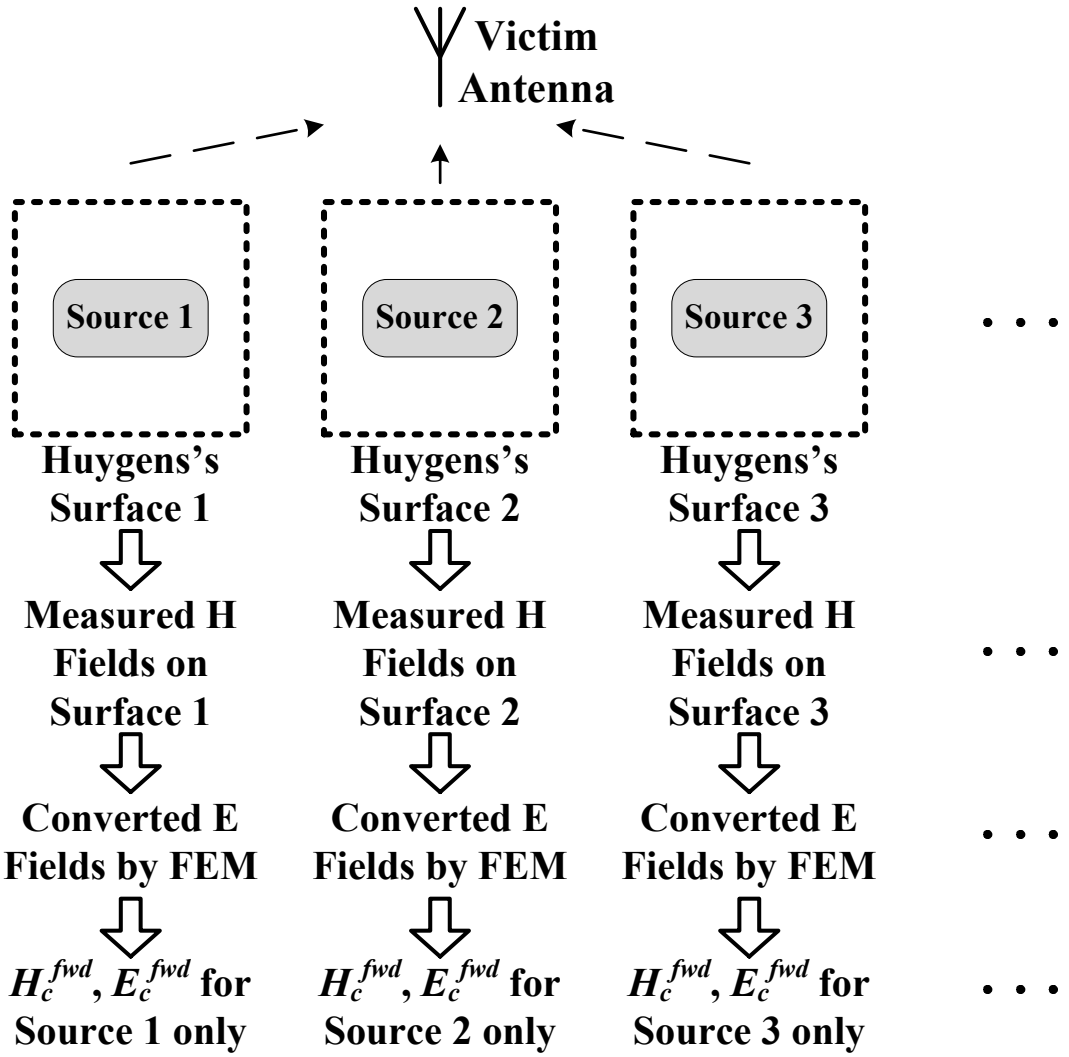

Fig. 10. Flow chart of "Forward Problem" to identify the interference from different sources.

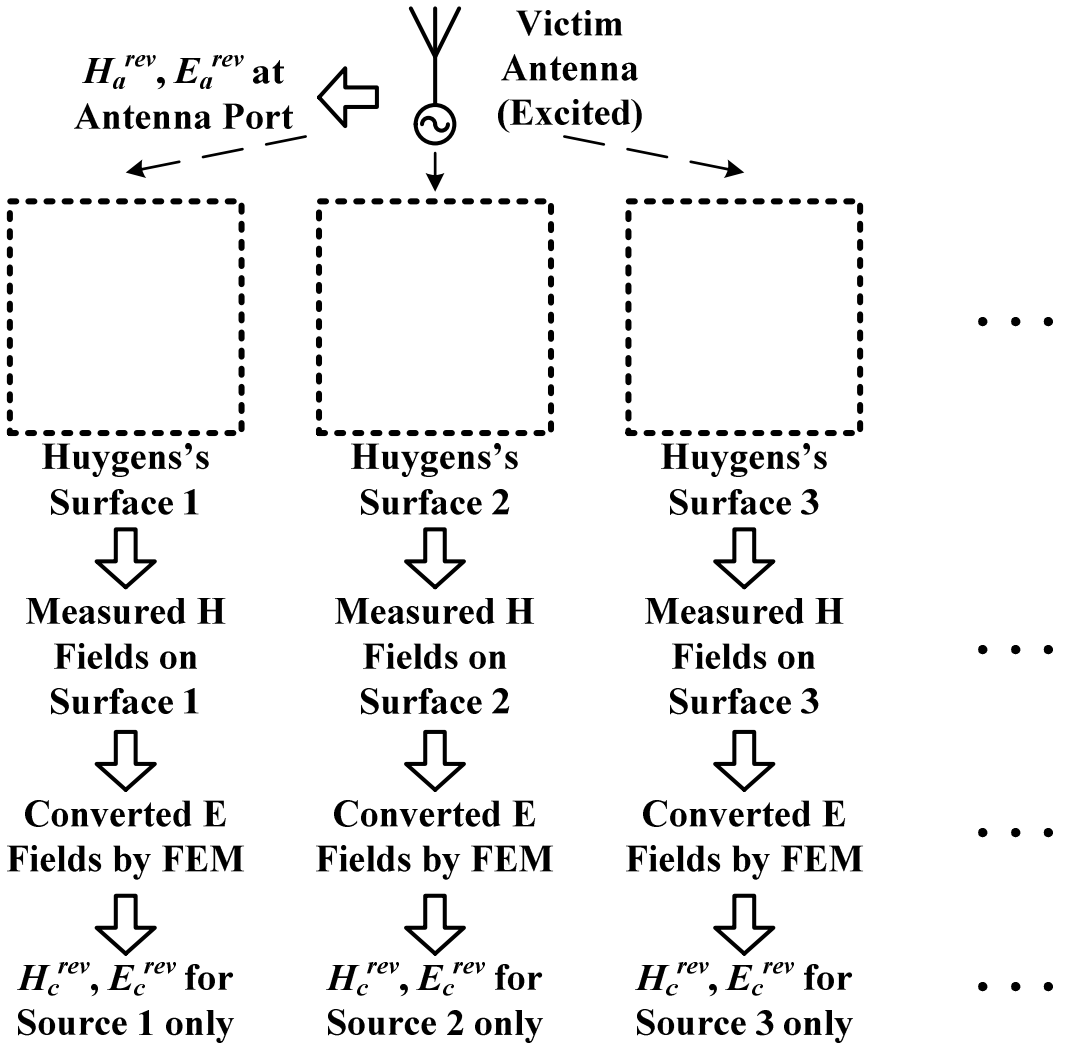

Fig. 11. Flow chart of "Reverse Problem" to identify the interference from different sources.

A simple PCB with several structures is taken to present the procedure and the performance of the proposed method to identify the coupling from different sources. Fig. 12 gives the full-wave model of this PCB.

On this PCB, a patch antenna with the size of 28 mm × 37.2 mm is the victim antenna. Its excitation port is numbered as 1. There are two sources. Source A is also a patch antenna with the same size and located 77.2 mm away from the victim. The port of Source A is numbered as 2. The other source, Source B, is a curved trace shorted at one

end, and excited by port 3 at the other end. The two blue squares on two sources are their Huygens's surfaces. Source A is 60 mm × 60 mm × 5 mm. Source B is 40 mm × 40 mm × 5 mm.

In "Forward Problem", the excitation for Source A is 0.1 V and the excitation for Source B is 0.3162 V. The two sources are excited simultaneously. The victim antenna is not excited. The magnetic fields on two Huygens's surfaces are exported from simulation. The electric fields are calculated from magnetic fields by the methods in Section III.

For "Reverse Problem", the model is changed as Fig. 13. The sources are removed as well as an excitation of 1V is applied on the victim antenna. Similarly, the magnetic fields on two Huygens's surfaces are simulated and the electric fields can be converted by the method in Section IV.

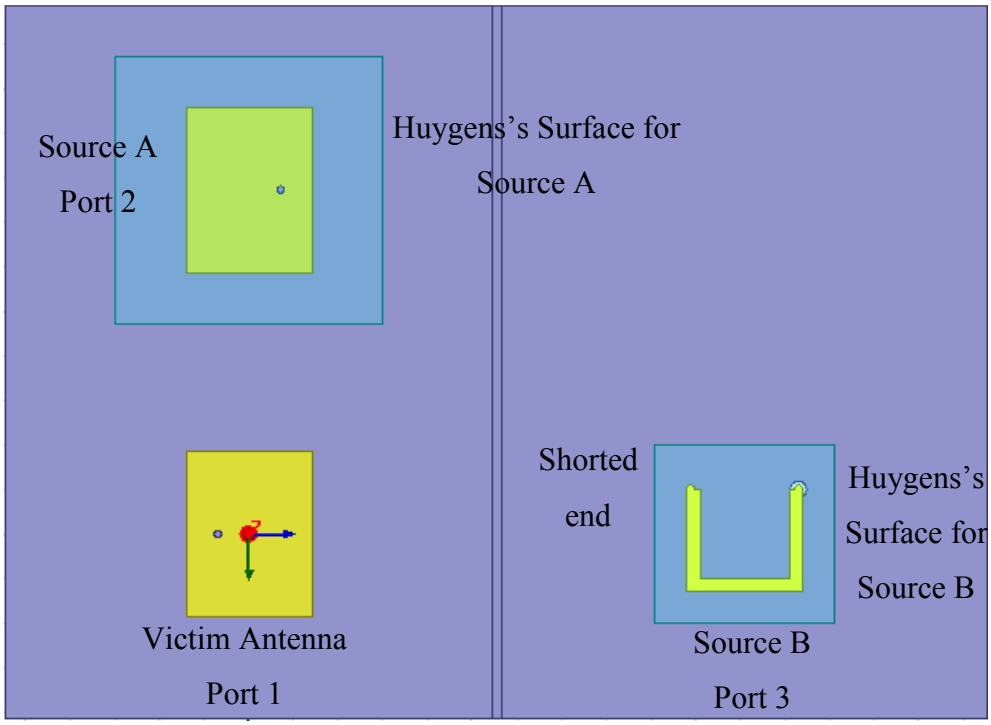

Fig. 12. Passive structures model in HFSS for identifying different sources in "Forward Problem".

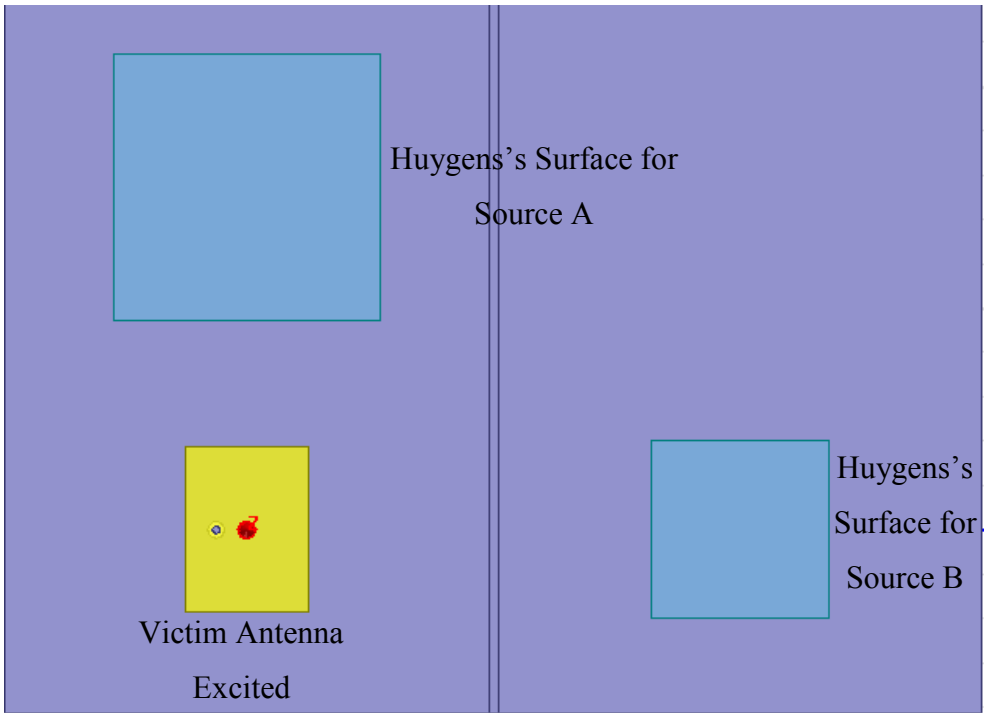

Fig. 13. Passive structures model in HFSS for identifying different sources in "Reverse Problem".

With the fields obtained in "Forward Problem" and "Reverse Problem" and the load impedance and input impedance of the victim antenna, the coupled voltages from different sources are given by (4) separately. Since all the ports are designed as 50 Ω, the S parameters and the coupled power between each source and the victim antenna can be easily calculated from the coupled voltage. Fig. 14 plots these two S parameters.

The good agreement of the S parameters of both sources validates that the proposed method can well estimate the coupled voltage from different sources separately over a frequency band. Thus, the coupled power from each source at different frequencies can also be predicted, as shown in Fig. 15.

From the estimation in Fig. 15, although two sources are radiating in the overlapped frequencies at the same time, the coupled power from each source can still be

predicted by putting the Huygens's surface on each source in the proposed method. It makes the evaluation of the interference problem easier. Engineers can conveniently find out the major noise source at different frequencies and observe the interference trend of different sources by reading the estimation in Fig. 15.

VI. CONCLUSIONS

In this paper, a method to identify the interference from multiple noise sources by magnetic near fields only is proposed. This method sets the Huygens's surfaces on each noise source in the decomposition method based on reciprocity. By doing this, the coupled power from each source to the victim antenna can be differentiated separately, even though the sources are radiating simultaneously at the overlapped frequencies. Another contribution of the proposed method is that two FEM processing procedures are introduced to solve the electric fields from the magnetic fields on the Huygens's surfaces. This approach prevents the using of the electric probes, which are less precise than the magnetic probe. As a result, the overall accuracy of the interference estimation could be improved. The proposed method has been validated step by step in this paper and provides convenience for engineers to better evaluate the RFI problems when there are multiple sources.

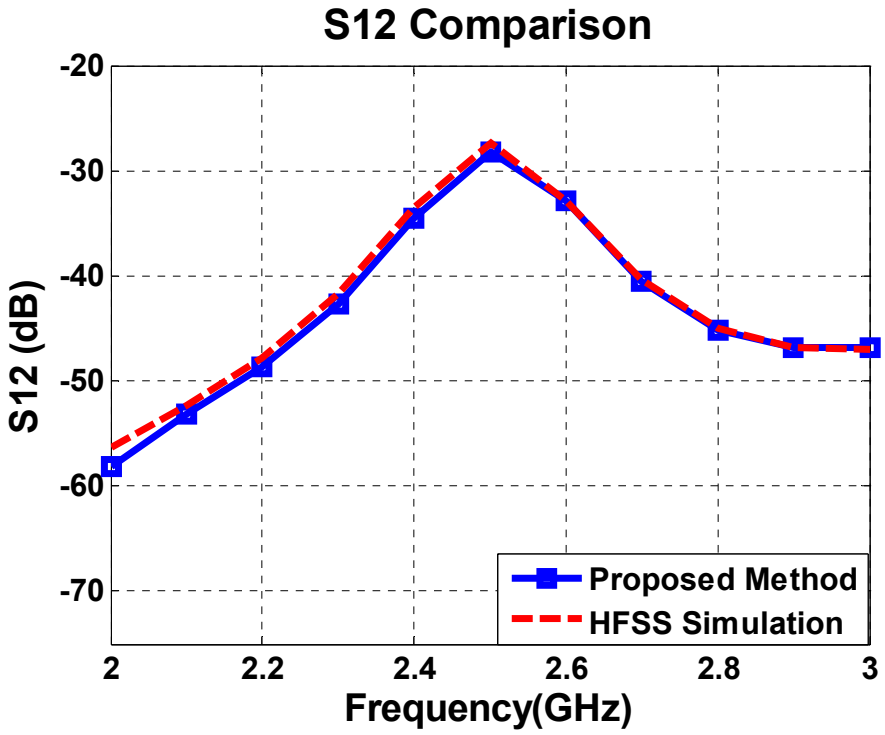

(a)

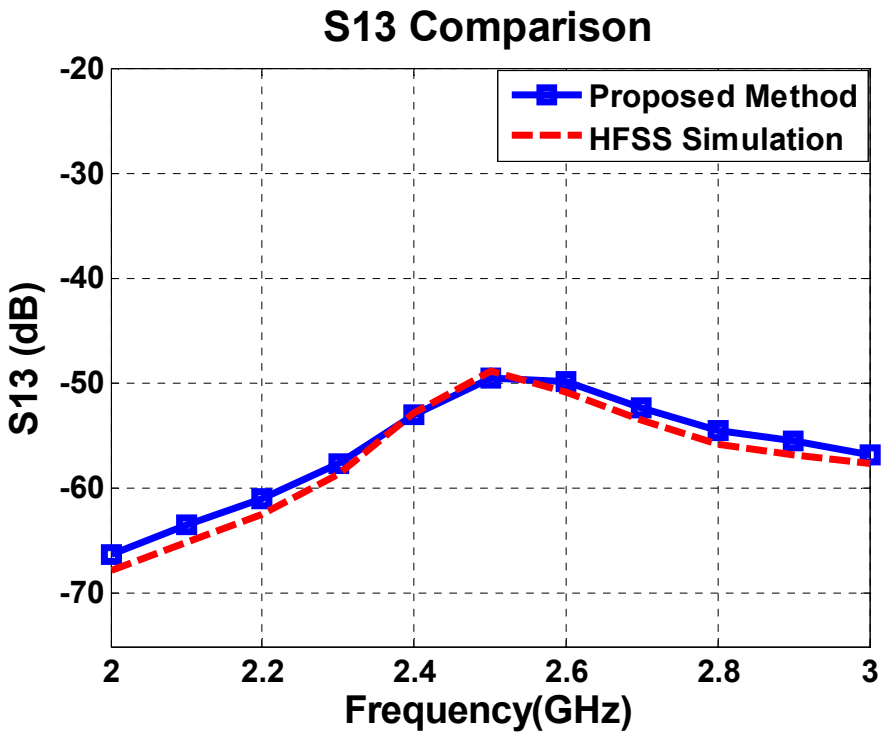

(b)

Fig. 14. Estimation of the S parameters between the victim antenna and (a) Source A (S12); (b) Source B (S13).

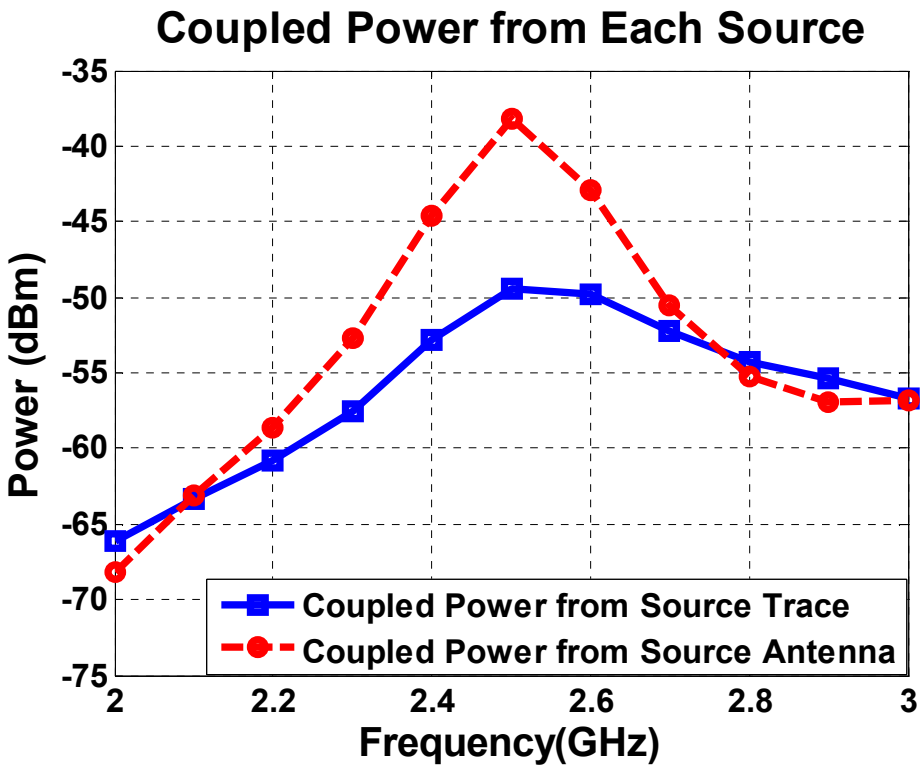

Fig. 15. Estimation of the coupled power from each source.

REFERENCES

[1] H.Weng, X. Dong, X. Hu, D. G. Beetner, T. Hubing, and D. Wunsch, "Neural network detection and identification of electronic devices based on their unintended emissions", in *Proc. IEEE International Symposium on Electromagnetic Compatibility,* vol. 1, pp. 245-249, 2005.

[2] F. T. Belkacem, M. Bensetti, M. Laour, A. Boutar, M. Djennah, D. Moussaoui, and B. Mazari, "The analytical, numerical and neural network evaluation versus experimental of electromagnetic shielding effectiveness of a rectangular enclosure with apertures", in *Proc. IEEE 9th Int. Conf. Cybern. Intell. Syst.,* pp. 1-6, 2010.

[3] C. S. Shieh and C. T. Lin, "Direction of arrival estimation based on phase differences using neural fuzzy network", *IEEE Trans. Antennas Propag*., vol. 48, no. 7, pp. 1115-1124, Jul. 2000.

[4] H. Wang, V. Khilkevich, Y. Zhang and J. Fan, "Estimating radio-frequency interference to an antenna due to near-field coupling using decomposition method based on reciprocity", *IEEE Trans. Electromagn. Compat*., vol. 55, no. 6, pp. 1125-1131, Dec. 2013.

[5] J. Pan, H. Wang, X. Gao, C. Hwang, E. Song, H. Park and J. Fan, "Radio-frequency interference estimation using equivalent dipole-moment models and decomposition method based on reciprocity", submitted to *IEEE Trans. Electromagn. Compat*.

[6] J. Pan, X. Gao, Y. Zhang and J. Fan, "Far-field radiation estimation from near-field measurements and image theory", in *Proc. IEEE International Symposium on Electromagnetic Compatibility,* vol. 1, pp. 609-614, 2014.

[7] X. Gao, J. Fan, Y. Zhang and D. Pommerenke, "Far-field prediction using only magnetic near-field scanning for EMI test", *IEEE Trans. Electromagn. Compat*., vol. 56, no. 6, pp. 1335-1343, Dec. 2014.

[8] J. Pan, X. Gao and J. Fan, "Far-field prediction by only magnetic near fields on a simplified Huygens's surface", accepted by *IEEE Trans. Electromagn. Compat*.

[9] D. Shi and Y. Gao, "A new method for identifying electromagnetic radiation sources using backpropagation neural network", *IEEE Trans. Electromagn. Compat*., vol. 55, no. 5, pp. 842-848, Oct. 2013.

[10] J. H. Richmond, "A reaction theorem and its applications to antenna impedance calculations", *IRE Trans. Antennas Propag*., vol. 9, no. 6, pp. 515-520, Nov. 1961.

[11] C. A. Balanis, *Advanced Engineering Electromagnetics*. New York, NY, USA: Wiley, 1989.

SECTION

2. CONCLUSIONS

The first topic of this dissertation proposed a far-field prediction method that used only the magnetic near-field for the case in which a radiation source is located on a ground plane. The near-field scanning on five sides of a Huygens's box was proposed to predict the far-field. The five-side Huygens's box, then, was further simplified into four side lines and one top plane, which greatly reduced the requirement for the near-field scanning. The proposed method was validated using both simulation and measurements. It overcame the limitation of the electric probe design, and also saves cost and scanning time for the near-field measurements. It can be used as an extension to the standard far-field measurements and may provide roughly far-field estimation at the early stage of design.

The second topic proposed an RFI estimation method by using equivalent dipole-moment models and the decomposition method based on reciprocity. This method allows engineers to model the complicated noise source, which may be very difficult to draw in the simulation tool, by dipole-moment models. By applying the decomposition method based on reciprocity, the RFI between the modeled source and the victim antenna can be reasonably estimated. With this method, the interference for any locations of the source and the victim antenna can be calculated fast in MATLAB, instead of the time-consuming simulation of the whole structure. Thus, engineers would be able to efficiently assess RFI issues of the product in the early design stage.

The third topic proposed a method to identify the interference from multiple noise sources by magnetic near fields only. This method set the Huygens's surfaces on each noise source in the decomposition method based on reciprocity. By doing this, the coupled power from each source to the victim antenna differentiated separately, even though the sources were radiating simultaneously at the overlapped frequencies. Another contribution of the proposed method was that two FEM processing procedures were introduced to solve the electric fields from the magnetic fields on the Huygens's surfaces. This approach prevents the using of the electric probes, which are less precise than the magnetic probe. As a result, the overall accuracy of the interference estimation was improved. The proposed method has been validated step by step in this paper and provides convenience for engineers to better evaluate the RFI problems when there are multiple sources.

VITA

Jingnan Pan was born in Luoyang, Henan, China. She received the Bachelor of Engineering in Electronic Information Science and Technology from Zhejiang University, Hangzhou, Zhejiang, China in 2008 and received the Master of Engineering in Electronic Science and Technology from Zhejiang University, Hangzhou, Zhejiang, China in 2011.

In August, 2011, she enrolled in the Ph. D. program within the Electrical Engineering Department of Missouri University of Science and Technology. She joined the Electromagnetic Compatibility research group there and received the Doctor of Philosophy in Electrical Engineering in December 2015.